

CMMT(C)-2007-xxx

## FIELD STUDIES OF ROCK ART APPEARANCE

FINAL REPORT: FUMIGATION & DUST  
DEPOSITION

PROGRESS REPORT: COLOUR CHANGE &  
SPECTRAL MINERALOGY

Deborah Lau  
Erick Ramanaidou\*  
Scott Furman  
Ivan Cole  
Tony Hughes  
Pam Hoobin

This document is to be used only within CSIRO Manufacturing  
and Materials Technology.

March 2007

© CSIRO 2007

To the extent permitted by law, all rights are reserved and no  
part of this publication covered by copyright may be  
reproduced or copied in any form or by any means except with  
the written permission of CSIRO.

\* CSIRO Division of Exploration and Mining, WA

## **DISTRIBUTION**

WA Burrup Rock Art Committee

D Lau

E Ramanaidou

S Furman

I Cole

T Hughes

P Hoobin

CMMT Registry

# Contents

Contents.....	2
Executive Summary .....	3
List of Acronyms.....	5
Project Introduction and Overview.....	6
Part 1: Fumigation.....	10
1.1 Introduction.....	10
1.1.1 Definition of Test Conditions.....	10
1.1.2 Fumigation Exposures.....	15
<i>Artificial Fumigation Studies of Rock Surface Changes.....</i>	16
<i>Preparation of rock material for fumigation exposure.....</i>	17
1.1.3 Extreme Condition Exposures.....	18
1.1.4 Analysis.....	18
1.2 Experimental.....	24
1.2.2 SEM and Microprobe Cross-Sections.....	24
1.2.3 Fourier Transform Infrared Spectroscopy.....	28
1.2.1 Environmental Scanning Electron Microscopy/Energy Dispersive Spectroscopy (ESEM/EDS) of Rock Surfaces.....	35
1.2.4 Surface Colour Measurements.....	39
1.3 Results and Discussion.....	40
1.3.1 Extreme pollutant exposure response colour measurements.....	40
Part 2: Dust Deposition.....	43
2.1 Introduction.....	43
2.1.1 Considerations for Particulate Deposition.....	43
2.1.2 Rock Washing in the Field.....	44
2.2 Experimental Methodology.....	45
2.2.1 Tile Construction and Installation.....	45
2.3 Results and Discussion.....	45
2.3.1 Comparative Dust Analysis.....	45
2.3.2 Iron Ore Dust Elemental Composition.....	46
2.3.3 Dust Collection.....	48
2.4 Results and Discussion.....	55
Part 3: Colour Measurement.....	57
3.1 Introduction.....	57
3.2 Experimental Methodology.....	57
3.2.1 Measurement Principles.....	57
3.2.2 Sampling Protocol.....	59
3.3 Results and Discussion.....	60
3.3.1 Reflectance Spectra.....	68
3.4 Conclusions and Future Work.....	70
Part 4: Spectral Mineralogy.....	72
4.1 Introduction.....	72
4.2 Experimental.....	73
4.3 Results and Discussion.....	74
4.4 Conclusions and Future Work.....	91
Concluding Remarks.....	92
References.....	93

# Executive Summary

---

In 2004, the West Australian (WA) Burrup Rock Art Monitoring Management Committee commissioned a number of independent scientific studies to evaluate the condition of rock art in the Pilbara region in the Dampier Archipelago. These studies set about evaluating the physico-chemical aspects of the effect of environmental modification on the visible appearance of the rock art.

CSIRO Manufacturing and Materials Technology (CMMT, Clayton) (formerly CSIRO Manufacturing and Infrastructure Technology) performed components of the study relating to fumigation, dust deposition and colour change, and are working in collaboration with CSIRO Exploration and Mining (CEM) who are performing spectral mineralogy. This work is also associated with the Burrup Peninsula air pollution study performed by CSIRO Marine and Atmospheric Research (CMAR) and microbiological studies performed by Murdoch University (WA).

Due to the cultural significance of the study sites, the research approach has been to employ non-destructive testing strategies. Together with the ethics and principles of the heritage conservation profession, work in the field has progressed with respect for the importance of the area.

This is a combined document covering the period to March 2007. Included is a final report for the studies:

1. Fumigation.
2. Dust deposition.

And a progress report for the studies:

1. Colour change.
2. Spectral mineralogy.

## ***Fumigation***

Assessment of physical, chemical and mineralogical changes was undertaken with an emphasis on determining early indicators of damage. Fumigation chamber studies on typical rock samples from the Burrup Peninsula were carried out on current, future and at 5–10 times the future pollutant estimates. The final report will assess the relevance of results to the predicted air quality scenario for the Burrup Peninsula and the rock art in the area.

In order to evaluate the role that dust may play in rock surface modification, duplicate experiments were run involving the addition of dust to rock surfaces. The results of the fumigation experiments and exposure studies involving extreme exposure scenarios with concentrated pollutants (organic solvents and acids) applied to rock minerals have resulted in surprisingly few mineralogical phase changes.

## ***Dust Deposition***

Current understanding of rock interface chemistry suggests that dust deposition may play a role in rock surface weathering mechanisms. The deposition processes and composition of deposited dust in the region was monitored through the use of micro-topographically replicated surfaces used to collect airborne dust.

The studies presented here are designed to characterise the dust that actually settles on rock surfaces rather than all airborne dust available for settling. Studies performed by CMAR have found that dust deposition rates are extremely low, and CMMT work shows additionally that in the long term (over annual cycles), the natural environment leaves levels of dust on unsheltered rock surfaces that are at the limits of detection. Dust collected from protected surfaces at the southern sites (closer to industrial activity) is consistent with that of iron ore dust, and dust collected from protected surfaces at the northern sites (far from industrial activity) is consistent with that of local soil-derived dust and sea salt.

### ***Colour Change***

A key issue of concern is the potential for colour change on petroglyphs that may occur with environmental modification, and to establish whether evidence of changes in the colour and contrast of images is measurable. Selected petroglyphs were identified by the WA Burrup Rock Art Monitoring Management Committee, and these are being monitored annually over four years with microspectrophotometry. This is providing a numerical, objective record of the colour at points within selected petroglyphs and the background rock surface, which may be referred to at any stage in the future and evaluated for any evidence of colour change. After examining three successive years of measurement (comprising nearly two and a half thousand individual colour measurements), a colour change is not evident in the colour measurement data.

### ***Spectral Mineralogy***

Each of the measurement points being evaluated for colour change is also characterised with spectral mineralogy to evaluate whether changes in mineralogy are observed on rock surfaces. Reflectance spectroscopy is a non-destructive, in situ materials characterisation technique that provides information about the chemistry of a mineral from its reflected light. Current results indicate that the surface mineralogy of the rocks has not changed over the three years of measurements. In 2006 the absorption features were similar to those found in 2004. The minerals include hematite, poorly ordered kaolinite, chlorite, minor goethite and minor manganese oxides.

This report documents the completion of two components of the study – dust deposition and fumigation. The evaluation of colour change and spectral mineralogy will continue, with a fourth and final annual measurement in 2007.

## List of Acronyms

---

AES	Absorption electron spectroscopy
ASD	Analytical spectra device
BSE	Back Scattered Electron
EDS	Energy dispersive spectroscopy
ESEM	Environmental scanning electron microscopy
FTIR	Fourier Transform infra-red (spectroscopy)
CEM	CSIRO Exploration and Mining
CMAR	CSIRO Marine and Atmospheric Research
CMMT	CSIRO Manufacturing and Materials Technology (formerly CSIRO Manufacturing and Infrastructure Technology)
CSIRO	Commonwealth Scientific and Industrial Research Organisation
ICP	Inductively coupled plasma (emission spectroscopy)
OM	Optical microscopy
RH	Relative humidity
SE	Secondary Electron
SEM	Scanning electron microscopy
WA DoIR	Western Australian Department of Industry and Resources
XPS	X-ray photoelectron spectroscopy
XRD	X-ray diffraction

## Project Introduction and Overview

---

The Burrup Peninsula is the location of a major industrial centre in Western Australia. The largest industrial developments are North West Shelf Joint Venture, with the main LNG, domestic gas and LPG treatment plant and processing facility; Hamersley Iron with an iron ore export port; and the Dampier Salt solar salt fields and export port. Additionally, Burrup Fertilisers has constructed an ammonia plant, and there is a range of other gas processing proposals awaiting consideration. An agreement has been reached with the three native title claimant groups to allow for development of industrial land while establishing management of non-industrial land, which occupies some 60% of the Peninsula north of Burrup Road.

The Burrup Peninsula is the largest land mass in the broader Dampier Archipelago, characterised by virtually treeless steep ridges and hills comprised of boulders and smaller rocks. The entire region is well recognised as the location of a remarkable number of indigenous petroglyphs. The images have been created by pecking and/or engraving into the surface-weathered coat of boulders and faces of gabbro and granophyre. These petroglyphs have cultural significance for the local indigenous people, as well as being archaeologically important at a national and international level.

The area has high summer maximum temperatures with a tropical semi-desert climate. Rainfall averages between 250 and 300 mm annually, although this is extremely variable from year to year. Tropical cyclones with rainfall in excess of 100 mm in 24 hours can occur during the period from January to April. Outside of the cyclone season, longer periods of low to moderate rainfall commonly occur during May and June.

In 2004, the WA Burrup Rock Art Monitoring Management Committee commissioned a number of independent scientific studies to assess whether emissions from industry on the Burrup Peninsula are affecting, or whether cumulative emissions from proposed industries could in the future affect indigenous rock engravings located on and adjacent to the Peninsula.

Eight sites were selected for the purposes of this study (Table 1 and Figure 1). Sites 1–3 are also referred to as the northern sites, and sites 4–8 are also referred to as the southern sites. Monitoring site locations were determined by the Rock Art Management Committee, and the final decision for a representative petroglyph at each site was determined in consultation with the Committee's Technical Advisor and nominated representatives from the local indigenous communities. Petroglyphs at each site were firstly evaluated for their suitability for scientific study in order to respect the cultural laws of the traditional owners for the entitlement of access. The second consideration, from a scientific perspective, were aspects including elevation and direction of exposure.

**Table 1: Locations of study sites**

<b>Site</b>	<b>Location</b>
1	Dolphin Island
2	Gidley Island
3	Northern Burrup
4	Woodside
5	Burrup Rd
6	Water Tanks
7	Deep Gorge
8	King Bay South



**Figure 1: Landsat image depicting the location of the rock art monitoring sites.**

CMMT have been engaged to undertake the studies of fumigation (tender number 35 DIR0603), dry dust deposition (relating to tender number 39DIR0603) and colour change (tender number 34DIR0603), in accordance with the specifications outlined in the tender documents. CEM have been engaged to undertake the measurements of the spectral mineralogy. Fumigation studies are designed to address the question of whether airborne emissions from industrial activities will affect the petroglyphs' images. Dust deposition studies are designed to address the question of the character and source of dust depositing on the petroglyphs, and whether airborne dust from industrial activities will affect the petroglyphs' images. Colour change studies are being used to monitor the colour of the images and background rock surfaces over time (four years). Spectral mineralogical studies are being used to monitor the surface mineralogy of the images and background rock surfaces over time (four years).

Within the same timeframe, CMAR has been engaged to undertake a pollution study to measure air quality (temperature, humidity, dust deposition rates and specific chemical pollutants), and Murdoch University have been evaluating the microbial flora present on rock surfaces.

As depicted in Figure 2, the six individual study components are greatly interconnected, as together they contribute to an overall understanding of Burrup rock surface chemistry and mineralogy, thereby facilitating a detailed knowledge of potential degradation processes for rock art in the region. The pollution study provides baseline data of the environmental character in the region, also enabling predictions of future emissions to be validated and, together with data for current conditions, provides the number of condensation events for rock surfaces used in designing the fumigation cycles. Colour change may be affected by dust deposition and/or spectral mineralogy, and together inform the conditions for and interpretation of the fumigation component of the study. Although it is acknowledged that microbial factors may play a significant role in the surface chemistry, their exact role in the study has not been isolated, in order to focus specifically on the individual and combined effects of gaseous airborne emissions and industrially generated dust.

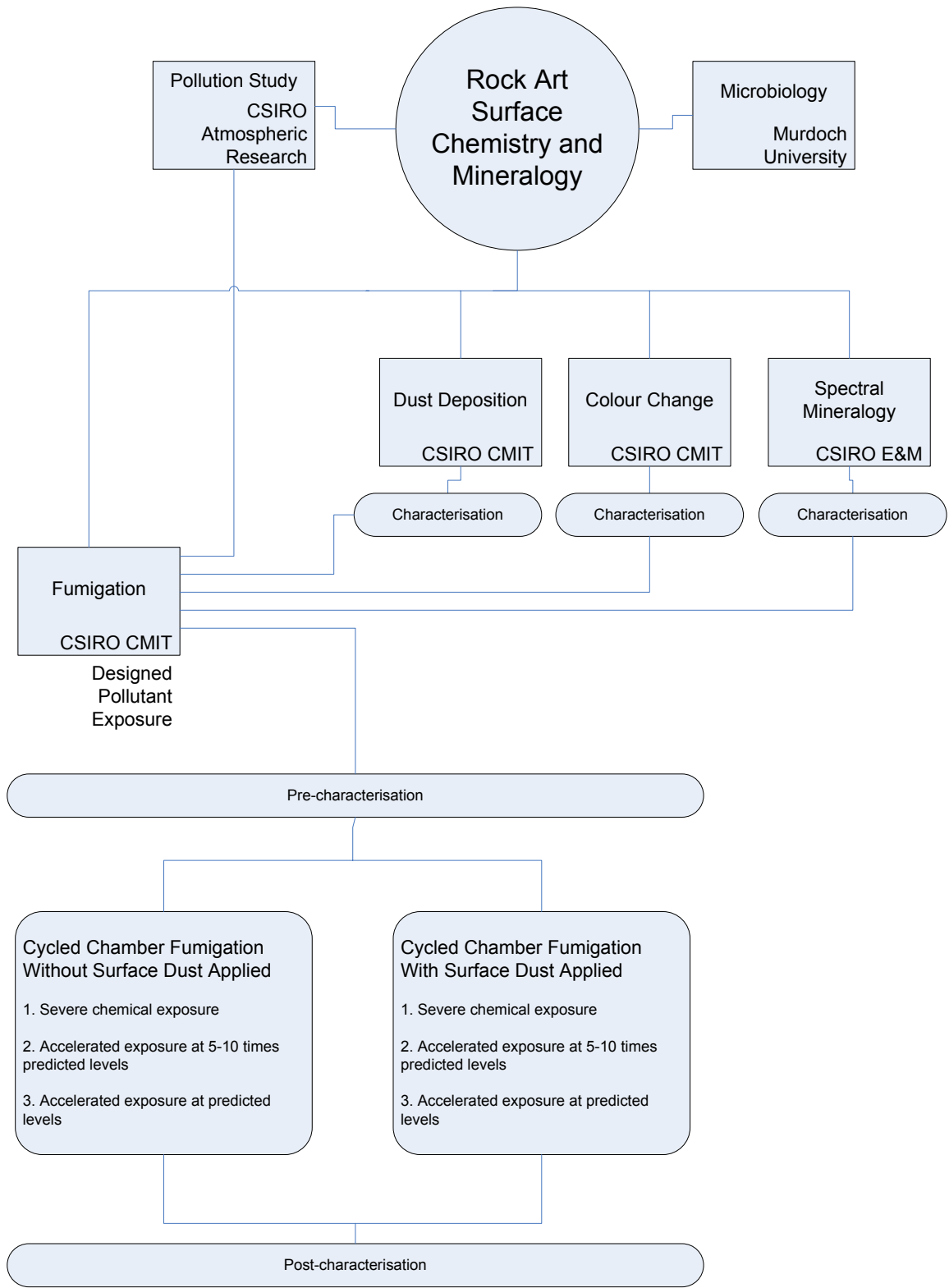


**Figure 2: Outline of study components and their associations.**

# Part 1: Fumigation

---

## 1.1 Introduction

This document reports on a systematic study that has at its core the activities outlined in the specification requirements, but which introduces a number of additional research elements necessary to ensure that the core activity is carried out and interpreted in a rigorous manner that addresses the fundamental issue of predicting risk to rock art from the combined microclimate/pollutant regimes that may arise on the Burrup Peninsula.

The study has the following elements:

- (a) A definition of test conditions – necessary to ensure that test cycles reflect the appropriate combination of microclimate cycles and pollutant levels that occur at Burrup.
- (b) Fumigation exposures – rock samples will be exposed to the climatic cycles defined in (a) with pollutant levels as in ‘response to specification’ with one adjustment. Additional tests will be undertaken with adjusted pollutants that induce the most extreme pH levels possible, given the pollutant levels.
- (c) Extreme exposures – in order to understand how early indicators of damage may progress to more profound damage, a limited number of extreme exposures will be required.
- (d) Analysis – a range of analyses (rock surface pre- and post-exposure characterisation and dust characterisation) will be undertaken with the aim of defining early damage indicators, and through (c) assess the relevance of early indicators to possible progression of damage under predicted air quality scenarios.
- (e) Elements (b)–(d) will be performed with the additional condition of dust (provided by Pilbara Iron) to establish the effect of its presence on rock surfaces.

### 1.1.1 Definition of Test Conditions

To establish an appropriate cyclic test procedure that duplicates possible damage mechanisms in the minimum possible time, the test procedure will include induced wet/dry cycles based on the diurnal cycle that occurs at Burrup. However, the investigation would determine:

- (a) Conditions required to induce moisture layers on rock samples (with and without the presence of marine salts).
- (b) The pH that is developed in moisture films as a function of time and pollutant dosage.
- (c) The relationship between a cycle period and damage for a susceptible rock.

This test program would establish the frequency of test cycles, and the relative humidity (RH), rock surface temperature and ambient temperature to be used during the cycles.

### *Wetness cycle design*

From a review of the relevant literature, we have reinforced our belief in the importance of determining the interfacial conditions existing at the rock face. Linkage between real-world and laboratory studies relies most importantly on the accurate characterisation of materials and conditions used for weathering activity.

The condition of wetting and drying at the surface is considered critical to pollutant interaction with the rock surface. The chamber experiments rely on the controlled dosing of low levels of gaseous pollutants, and considerable time has been required to design a method for achieving surface wetness of rock surfaces in the chamber. The increase and decrease of humidity required by the accelerated cycles cannot be achieved by introducing wet or dry air, as this would upset the pollutant concentration balance, so an alternative scheme has been designed using a Peltier temperature-controlled pad to heat and cool the rock samples and introduce undercooling to achieve surface wetness through condensation.

The chamber cycle conditions were designed to induce the formation of condensation on the surface of the rocks through maintaining a high humidity and inducing temperature change in the rock. The samples were arranged on a Peltier pad in a 21-litre stainless steel environmental chamber fitted with a transparent polycarbonate faceplate. The chamber underwent a full air change every hour during the entire test period.

The Peltier heating stage had a surface area of 40 x 40 mm. The humidity within the chamber was kept at about  $86\% \pm 3\%$ . The Peltier cycled between  $18^{\circ}\text{C}$  and  $63^{\circ}\text{C}$  and the rock temperature cycled between  $21^{\circ}$  and about  $49^{\circ}\text{C}$  as measured on the top of the rock (surface temperature only). There was no measurement of temperature inside the rocks.

Cycle: The total cycle length was 1 hour and each test ran for 720 cycles.

1. The chamber temperature was around  $27^{\circ}\text{C} \pm 1^{\circ}\text{C}$
2. The chamber was cooled for 10 minutes during which time the temperature dropped to around  $18^{\circ}\text{C}$ .
3. The next cycle was of 15 minutes duration. The Peltier heats rapidly so that the rocks effectively sit at the maximum temperature of the chamber ( $63^{\circ}\text{C}$ ) for the full 15 minutes. The rock temperature reaches maximum (about  $49^{\circ}\text{C}$ ) near the end of this cycle time.
4. The heating was turned off and the temperature of the chamber dropped back to about  $27^{\circ}\text{C}$  over the next 35 minutes. The humidity within the chamber also drops due to moisture up-take by the rocks.
5. The cycling process starts again from step 1 for 720 cycles.

The air, Peltier and rock temperatures and RH for the cycle are shown in Figure 3.

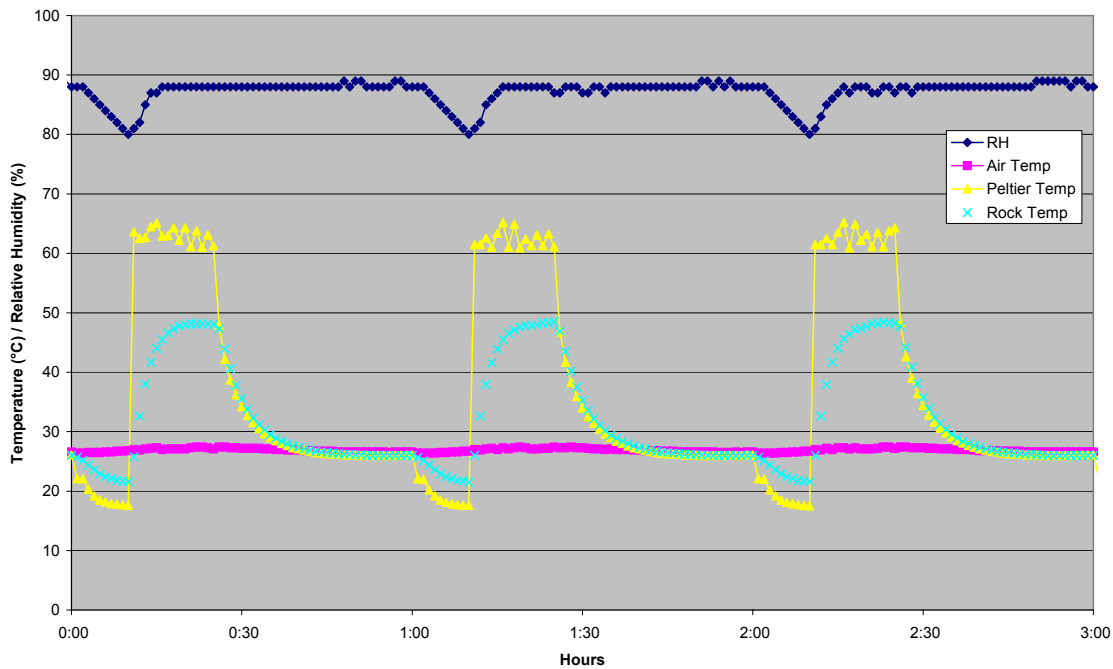


**Figure 3: Chamber cycle conditions.**

Each test exposed six (6) rock samples (three background samples plus three engraved rocks) to the prescribed range of pollutants; Benzene, Toluene, Xylene, NO<sub>2</sub>, SO<sub>2</sub> and NH<sub>3</sub>, further described in 1.1.2 Fumigation Exposures.

### ***Rock/air interface conditions***

The artificial aging and fumigation cycles rely on accelerated cycles of wetting and drying, based on naturally occurring cycles. However, there is little reliable information available regarding the parameters involved, such as the periods of wetness experienced by rock surfaces and the surface temperatures of the rocks.

Monitoring stations erected at independent locations and at the sites selected for the Burrup rock art monitoring program, indicate ambient temperature and RH conditions. Ambient air temperature and wetness can be vastly different to the conditions on the face of a rock because of surface chemistry, porosity, physical structure (microtopography), thermal lag associated with the rock pile and similar factors. Early assumptions regarding the duration and extent of wetness were re-examined, as there was a need to verify these parameters more accurately before proceeding with cycling processes for the fumigation program. This was performed through the installation of surface temperature probes and specially designed surface wetness sensors.

### ***Surface wetness – questions to be addressed***

The standard method of measuring surface wetness is to use a surface wetness probe. This method for environmental evaluation derives from equipment designed for use in forests and natural environments, and indeed, the probe itself is called a ‘leaf wetness’ sensor. The leaf wetness sensor (pictured in Figure 4) is an interdigitated gold grid on an epoxy backing, which

enables the measurement of surface resistance. Changes in moisture levels on the surface result in measurable changes in resistivity, which are recorded through a datalogger.

A preliminary investigation using this type of sensor was begun in the months preceding our visit to the area in July 2004. The results of these measurements are presented in CMIT Report 2004-090, and they indicate surface moisture for extended periods of up to 10–12 hours a day, far beyond what would be anticipated.

However, some discrepancy exists between what has been instrumentally recorded in this study using wetness sensors and anecdotal evidence. Bill Carr (Rock Art Management Committee Technical Advisor) has visited a monitoring site and reported no sign of visual wetness in the early morning, during the period when the wetness sensor was measuring and reporting surface wetness. There are two possibilities to account for the two contradictory observations:

- (a) The leaf wetness sensor has a different surface structure (chemical and physical) and as a consequence has differential wettability. As discussed above, traditional leaf wetness sensors are impervious to water and any available moisture on the surface results in both visual and electrically conductive (electronically detectable) wetness.
- (b) The porosity and surface texture of the rock surface ‘disguises’ its wetness. Although the rock surface may appear dry visually, there may be a thin moisture layer dispersed over the surface within micropores and in the near-surface substructure. Therefore the rock, while appearing dry, may have available water that can facilitate chemical mobility, with critical implications for degradative chemical processes or phase modification.



**Figure 4: Gold grid leaf wetness sensor.**

These findings have indicated that a more thorough understanding of the rock surface structure is imperative for understanding wettability, and the consequences it will have for wetting and drying cycles and the overall design of the experimental protocol, and this has meant some time has been spent designing and testing a suitable rock wetness sensor system.

### ***Rock surface wetness***

In response to the specific requirements of the Burrup rock art monitoring project, CMMT have developed a new type of surface wetness sensor, specifically designed to address the unique problem of understanding rock surface wetness. It employs the principle of wetness translatability, meaning that the surface wetness of a rock face is measured through the adaptation of another representative rock surface.

Using a completely novel design and process, pure gold tracks have been applied to the surface of a small rock (see Figure 4) and attached to a datalogger. Testing has shown this prototype device to record rock surface wetness reproducibly and in a range of wetness contexts (rain, running water, mist and dew).

The following examples show the response from water flowing over the surface (Figure 6) and from exposure to rain (Figure 7). One of the most interesting observations was that the surface did not appear visually wet below measurements of about 30% wetness.

From the evidence gathered so far, it is apparent that establishing the porosity and wettability will influence the penetration of pollutants and the reactivity of pollutant products applied during fumigation testing regimens. Together with realistic estimates of wetness events collected in a more accurately representative manner using the new wetness sensor technology, we can better measure rock surface wetness in situ.

### ***Rock surface temperature***

Rock surface temperature plays a critical role in wetness and thereby the overall chemical response of the surface to environmental effects. Ambient conditions of air temperature, RH and rainfall are being monitored at stations erected by CMAR. However, due to the thermal mass of the large rock features on the Burrup Peninsula, the temperature at a rock face can be expected to vary significantly from air temperature, and temperature needs to be recorded at the point where the study is being undertaken – on exposed rock face surfaces. For example, the surface temperature of limestone was observed to be 15–19°C less than the temperature simultaneously recorded at 50 mm above the surface [1]. This occurred over the hours of 11:00 to 15:00 and would be expected to be reversed during the cooler exposure of the evening.

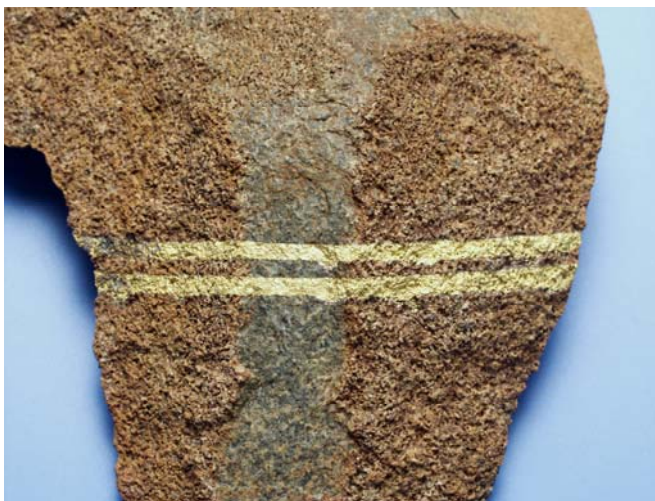


**Figure 5: Rock wetness sensor (gold tracks).**

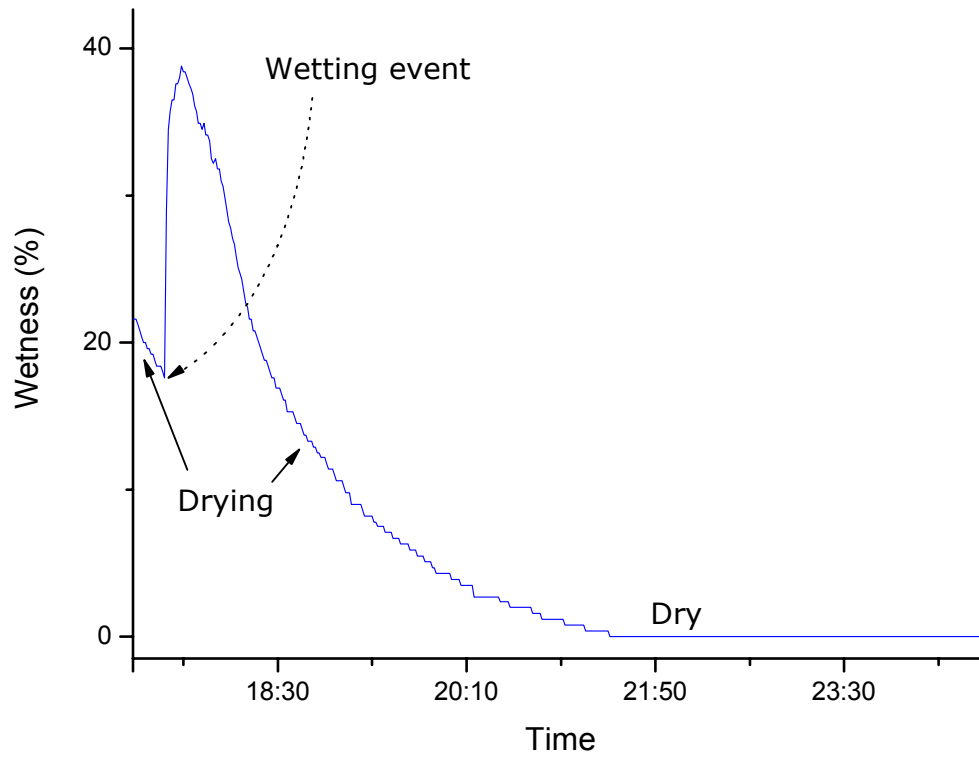


Figure 6: Response of rock wetness sensor to surface water.

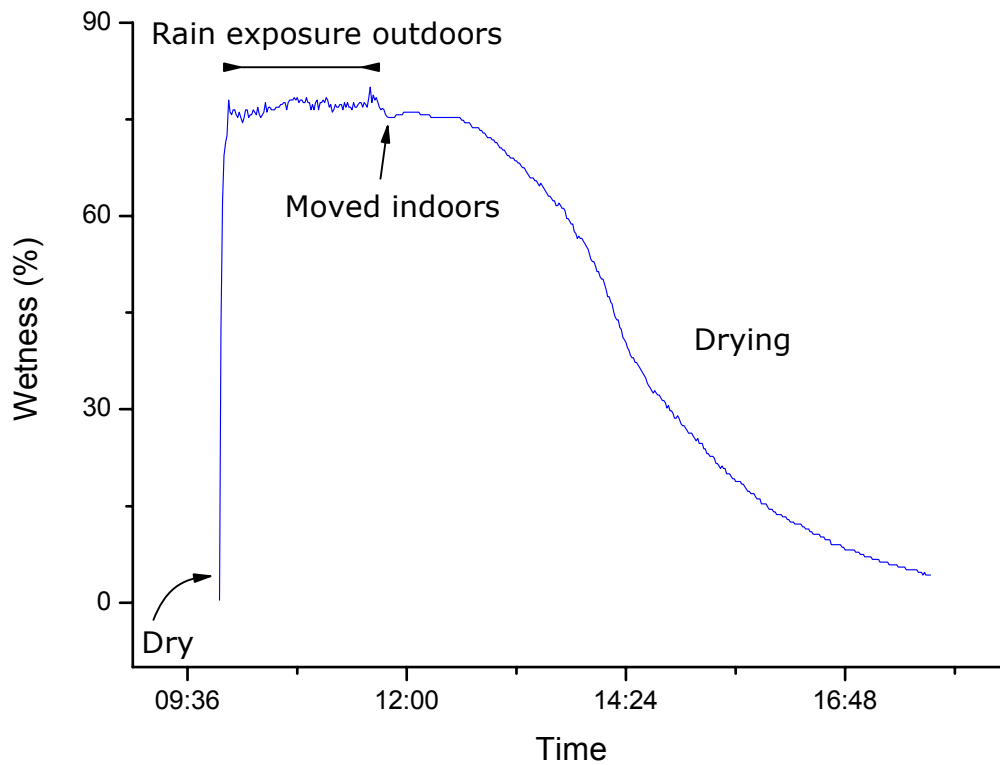


Figure 7: Response of rock wetness sensor to rain.

### 1.1.2 Fumigation Exposures

It is well established that combinations of gases may have very significantly different effects than the sum of the individual elements. For instance, it is reported that NO<sub>2</sub> and SO<sub>2</sub> may be synergistic in promoting the corrosion of metals. This may be related to chemical interactions that can occur either in atmospheric moisture (cloud droplets, wet aerosols) or on metal surfaces and, in the example above, may arise due to the ability of NO<sub>2</sub> to oxidise to S(IV). In contrast, while the absorption and oxidation of SO<sub>2</sub> in aqueous phases results in acidification of the same phases, the absorption of NH<sub>3</sub> would tend to render the phases alkaline. The presence of marine salts may also induce reactions that not only change the pH of moisture films, but also lead to the formation of aggressive species. Figure 8 outlines the experimental protocol for the fumigation experiments.

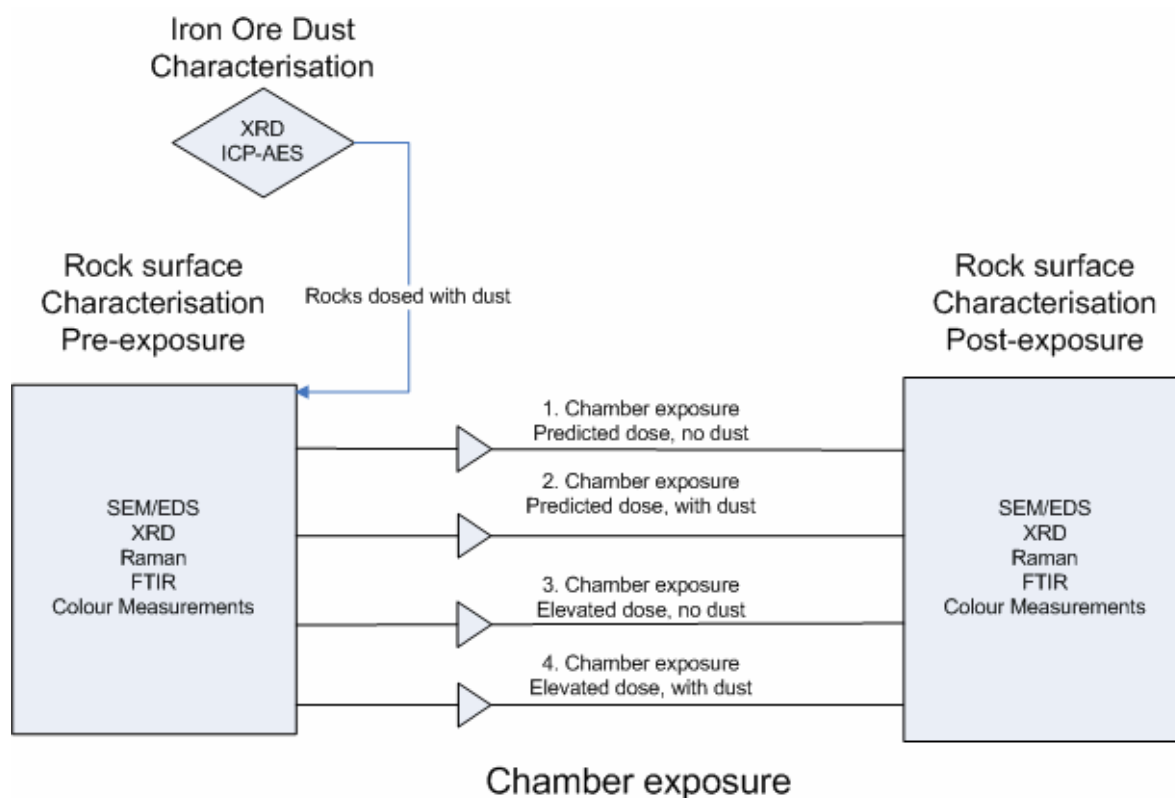


Figure 8: Schema for chamber fumigation exposures.

#### Artificial Fumigation Studies of Rock Surface Changes

Modelled maximum ground level concentrations without background are taken from studies of fumigation tender number 35 DIR0603 specifications (Part 4) and are as follows:

	<u>Current</u>	<u>Future Industry</u>	<u>Background</u>
NO <sub>2</sub>	2.4 ppb (annual)	4.5 ppb (annual)	0.8ppb
SO <sub>2</sub>	0.5 ppb (annual)	1.6 ppb (annual)	<0.1ppb
Benzene	1.2 ppb (annual)	1.9 ppb (annual)	---
Toluene	6.7 ppb (weekly)	7.7 ppb (weekly)	---
Xylene	6.9 ppb (24 hr)	7.4 ppb (24 hr)---	---
NH <sub>3</sub>		4.0 ppb (annual)	---

Accelerated ageing was performed at two exposure levels; the future industry and 10 x the future industry levels. These pollutants were supplied to the chamber as a pre-mixed gas and air flow and exchange rates used to control the pollutant dose for the 1 x and 10 x doses. The concentration delivered to the chamber was verified by active sampling of the chamber air onto an activated carbon tube that was analysed with method MA-10.AIR.01 for mono-aromatic hydrocarbons.

**Table 2: Prescribed In-Chamber Concentration.**

Exposure Level	1x	10x
	ppb	ppb
Benzene	2	20
m-Xylene	7	70
Toluene	8	80
NO <sub>2</sub>	5	50
SO <sub>2</sub>	2	20
NH <sub>3</sub>	4	40

The concentration of gases calculated from the above data was compared with the concentration supplied on the gas cylinder. These values are presented in Table 3.

**Table 3: Supplied chamber gas concentration.**

	Combined gas mix					
	Benzene	Toluene	Xylene	NO <sub>2</sub>	SO <sub>2</sub>	NH <sub>3</sub>
<b>Supplied concentration in gas cylinder (ppm)</b>	1.9	9.2	7.6	4.3	1.6	4.7

The prescribed concentrations listed in Table 2 are in ppb concentration units, while the supplied concentration in the gas cylinder was in ppm concentration units. For the fumigation exposures at x1 predicted dose and x10 (elevated dose), concentrations were supplied in the correct concentrations within the chamber using input flow control to dilute the dose to the appropriate level.

*Preparation of rock material for fumigation exposure*

It was necessary to sub-sample the rocks used in the fumigation experiments as some of the analytical instrumentation was limited in the sample size that could be accommodated. Size constraints also meant that it was not possible to expose entire rocks in the fumigation chamber.

Small pieces of rock surface were cleaved into approximately 10 mm pieces, taking care not to contaminate the surface (Figure 19). Use of a cutting wheel or any other abrasive technique to

produce small samples was considered inappropriate due to the likelihood of surface contamination.

Samples of background and engraved type rock surface were prepared in this manner.

### **1.1.3 Extreme Condition Exposures**

In order to understand how early indicators of how damage may progress to more profound damage; a limited number of extreme exposures were performed. They were performed by the application of concentrated solutions of the pollutants to the rock surface.

### **1.1.4 Analysis**

Before and after exposure, the rock samples were analysed for physical, mineralogical and chemical changes. Analytical tools included optical microscopy (OM) and scanning electron microscopy (SEM) to determine physical and mineralogical changes. A petrographic analysis was undertaken using both OM and SEM to characterise the mineralogy and texture of the weathered surface profile. The studies looked at both changes in the weathered surface (covered with ‘desert varnish’) and the engraved surface that defines the image. Particular attention was paid to the change of properties observed on the exposed surface (desert varnish) compared to the unweathered zone at depth.

#### ***Pre-fumigation rock characterisation***

Fundamental characterisation studies are being performed on representative rock surfaces before and after exposure to the fumigation program. In an effort to obtain material that was unlikely to have been contaminated by any industrial or other means, the rock material was collected from the west side of Gidley Island, approximately 200 m from the colour measurement site (Site 2). Pieces with surfaces representative of the carved and background areas of petroglyphs were collected.

Rock samples were mechanically broken to avoid the possibility of contamination, with the consideration that dry cutting would have produced dust, thereby contaminating the clean surface, while wet cutting would have produced slurry over the rock surface. Pieces were successfully cleaved with a bolster and chisel, without substantial direct contact with the surface. This produced pieces with surface areas of approximately 10–15 mm<sup>2</sup> for use in characterisation before and after fumigation.

A number of methods for characterisation are in progress to fully describe the character of the rock surface and the dust that will be applied in the fumigation experiment with dust.

#### ***Iron ore dust characterisation***

##### ***X-ray diffraction***

XRD provides phase composition information of the crystalline phases of a material. Powder XRD was performed on three replicate samples of iron ore dust from Pilbara Iron.

Analyses of each replicate sample produced almost identical results, and a representative diffraction pattern is shown in Figure 9. The major phase present was hematite, which is to be expected considering the sample was iron ore dust. There was also a moderate amount of goethite and minor indications of quartz and kaolinite.

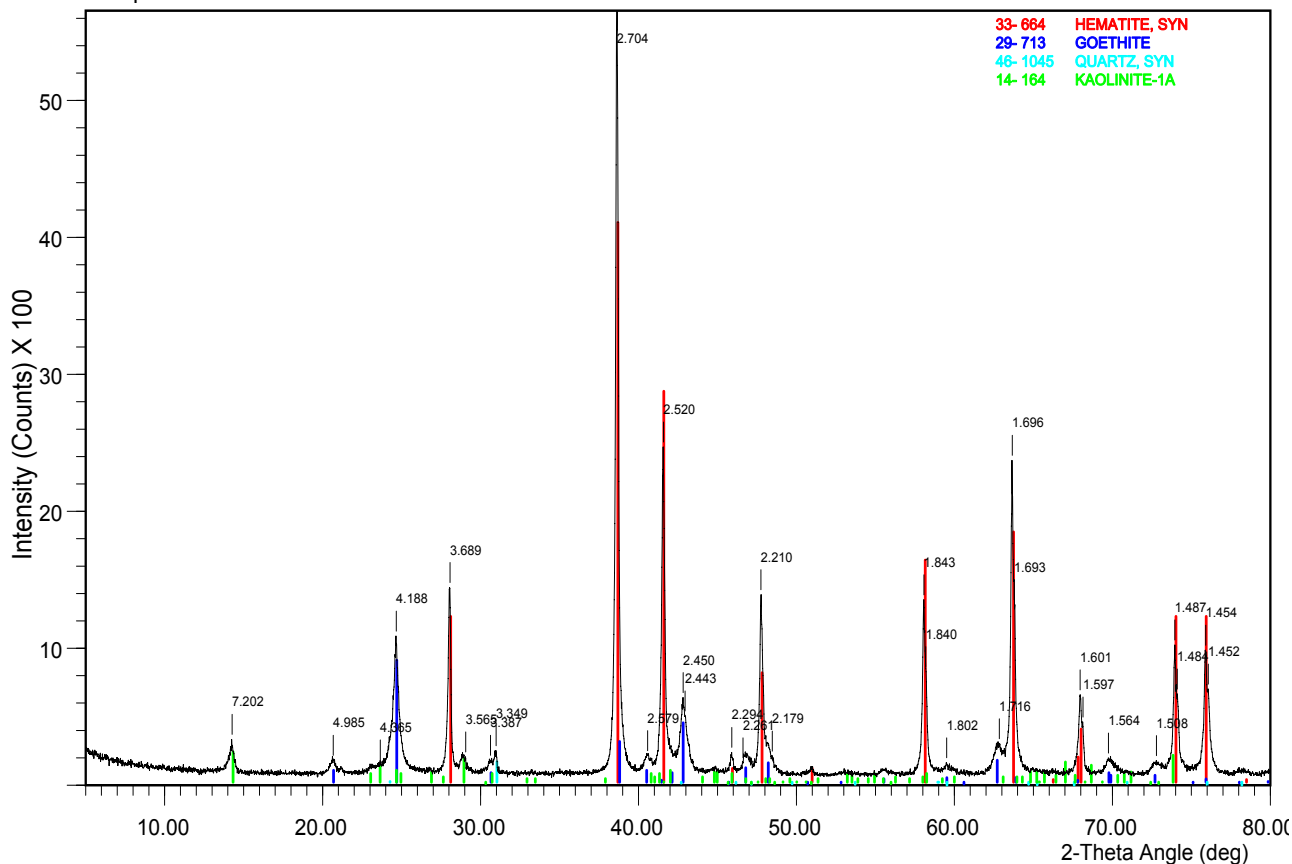


Figure 9: XRD diffraction pattern of iron ore dust.

*Inductively coupled plasma/absorption electron spectroscopy*

ICP/AES provides quantitative information regarding the elemental composition of a dust sample (Table 2). The major components found were consistent with the XRD findings that iron in the form of hematite and goethite is the major constituent of iron ore dust.

Table 4: Elemental composition of iron ore dust (ICP/AES)

Analyte	Ag	Al	As	Ba	Be	Bi	Ca	Cd	Co	Cr	Cu	Fe	K	Mg
Units	ppm	%	ppm	ppm	ppm	ppm	%	ppm	ppm	ppm	ppm	%	%	%
Sample	<0.5	1.34	12	70	1.2	5	0.07	<0.5	<1	22	24	42.2	0.03	0.07
Analyte	Mn	Mo	Na	Ni	P	Pb	S	Sb	Sr	Ti	V	W	Zn	
Units	ppm	ppm	%	ppm	ppm	ppm	%	ppm	ppm	%	ppm	ppm	ppm	
Sample	1445	1	0.05	15	740	6	0.03	<5	18	0.05	25	<10	127	

These findings, together with results from further analyses, provide a comprehensive understanding of the material structure of the dust used in the fumigation study, and allow the

formation of hypotheses regarding any observed changes in rock mineralogy. The concentrations of soluble ions, if in depositing wet aerosols, may influence surface interface mineralogy.

### Interface structure–rock surface characterisation

Mineralogy, chemistry and microtopography of the rock surface are inherently linked to weathering mechanisms. To address the microstructure in these terms, initial studies have concentrated on preparing and examining cross-sections of the rock, revealing the surprisingly thin interface between rock and air.

On the Burrup Peninsula and adjacent islands the predominant rock types are gabbro and granophyre (Figure 9). Without disturbing recognised rock art panels, samples were collected from Site 1 to look at the chemical and physical weathering processes relevant to the key issues.

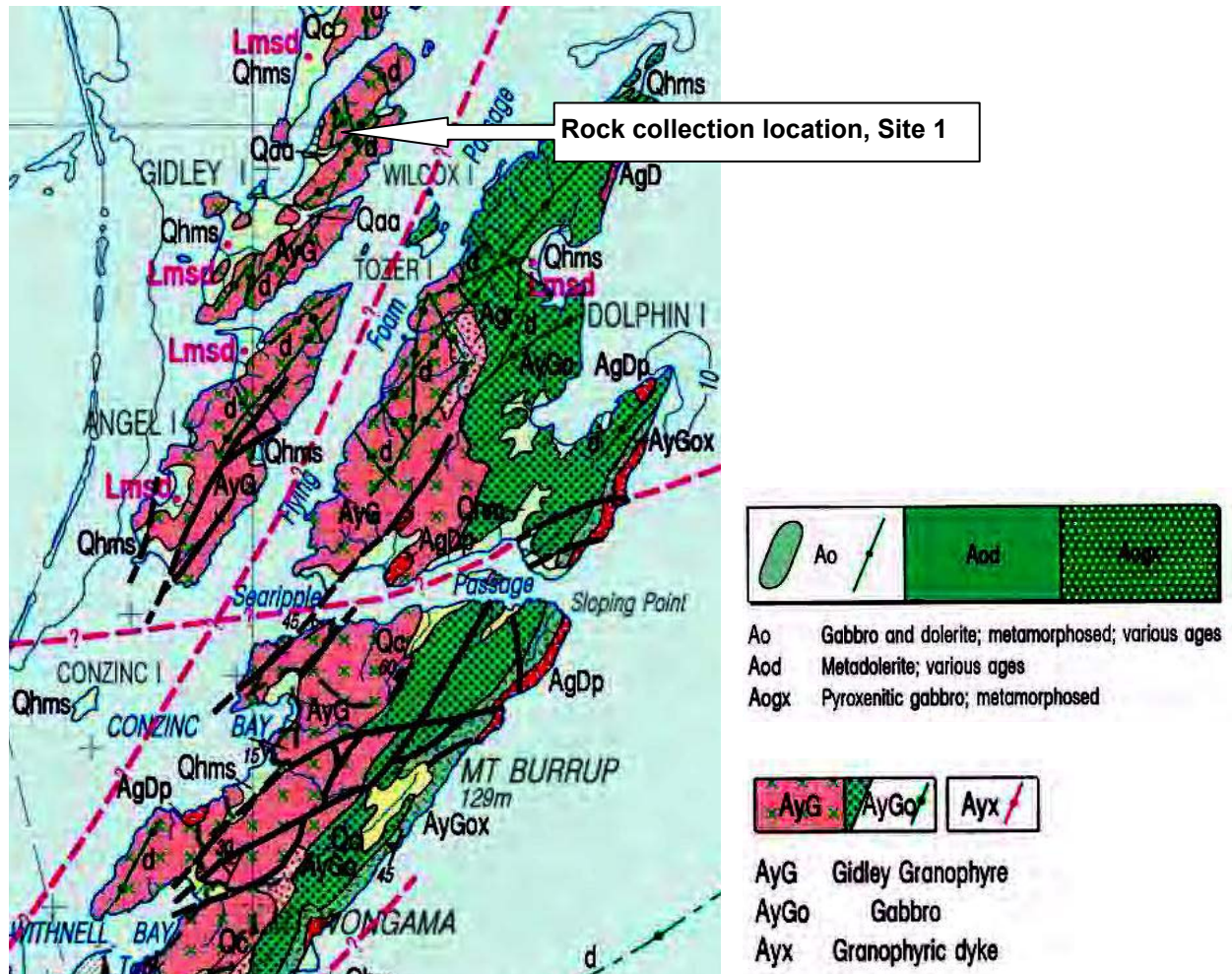


Figure 10: Gabbro and granophyre predominate in the study region (map section reproduced from Geological Survey of WA Sheet SF50-2 [2]).

The underlying mineral assemblages are anticipated to resemble those of other gabbro and determined meta-gabbro terrains, for example meta-gabbro from the Appalachians [3] consisted of (weight per cent):

- 44% andesine,  $\text{Na}_{(70-50\%)} \text{Ca}_{(30-50\%)} (\text{Al}, \text{Si})\text{AlSi}_2 \text{O}_8$ , sodium calcium aluminum silicate.
- 40% hornblende,  $\text{Ca}_2 (\text{Mg}, \text{Fe}, \text{Al})_5 (\text{Al}, \text{Si})_8 \text{O}_{22}(\text{OH})_2$ , calcium magnesium iron aluminum silicate hydroxide.
- 6% quartz,  $\text{SiO}_2$ , silicon dioxide.

- 4% biotite,  $K (Fe, Mg)_3 AlSi_3 O_{10} (F, OH)_2$ , potassium iron magnesium aluminum silicate hydroxide fluoride.
- 3% ilmenite/titanomagnetite/rutile/sphene grains.
- 3% epidote.

Gabbro from the Wellgreen Complex, Yukon Territory, Canada<sup>1</sup>, collected as a certified reference material, consisted of:

- Plagioclase,  $(Ca, Na_2)AlSi_2 O_8$  and other feldspars.
- Pyroxene,  $(Mg, Fe)SiO_3$ .
- Chlorite,  $(Fe, Mg, Al)_6 (Si, Al)_4 O_{10} (OH)_8$ , iron aluminum magnesium silicate hydroxide.
- Prehnite,  $Ca_2 Al_2 Si_3 O_{10} (OH)_2$ , calcium aluminum silicate hydroxide.
- Calcite,  $CaCO_3$ , calcium carbonate.

### *Desert varnish*

Petroglyphs on the Burrup Peninsula have been created through pecking, scraping or icising of the thin red–brown rock patina to reveal contrasting colour from below the surface. The red–brown patina [4] has been referred to with varied descriptive terminology, often as ‘desert varnish’, which makes reference to the shiny appearance the coating can have (see Figure 10). However, although the patina is evident over many rocks in the region, it is variable in the degree of gloss and colouration, from light red to dark brown–red, and most of the rocks in the study region appear matt. The name desert varnish itself is used in a variety of ways and may not always be applicable to all forms of the red patina observed in the Pilbara region. For the purposes of this study, the red colouration on the surface is referred to as background, especially in terms of colour contrast. The cream–white colouration that makes up most of the engraved lines of petroglyphs is referred to as engraved or engraving surface. The blue–green–grey of the gabbro or granophyre when freshly exposed or in the interior of the rock is referred to as the rock interior.



**Figure 11: Glossy desert varnish at Site 5.**

<sup>1</sup> <http://www.nrcan.gc.ca/mms/canmet-mtb/mmsl-lmsm/ccrmp/certificates/wgb-1.htm>.

There has been much speculation as to how a varnish surface coating forms on an exposed rock face, and currently three models are used to describe the process [5] (Figure 11):

- (1) Leaching of the rock substrate followed by precipitation at the rock surface.
- (2) Post-depositional diagenesis, wherein immobile element concentrations are enriched due to net mass loss of Al and Si during conversion of primary silicate minerals to clay minerals.
- (3) Direct aqueous atmospheric deposition, wherein Fe, Mn and trace metals are leached from dust grains into rain/fog droplets, and residual dust/clay grains are physically separated from the aqueous component by water run-off or by wind.

Models (2) and (3) also allow for microbial facilitation.

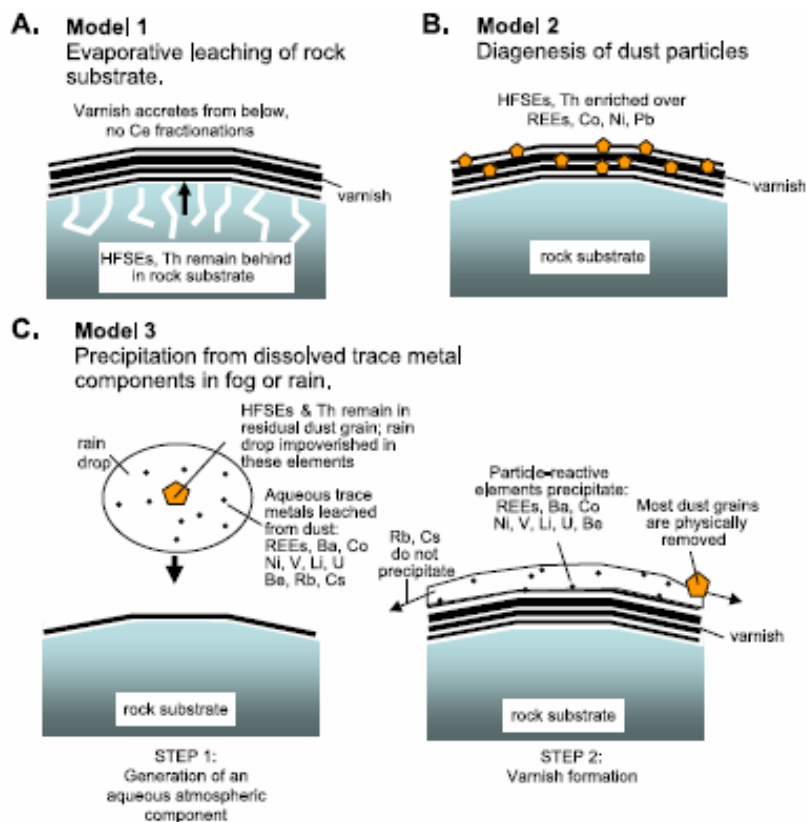


Figure 12: Schematic diagrams of the three models for varnish formation (from Thiagarajan *et al.* [5]).

A recent study has provided evidence for the third situation, discounting the first because it accounts for only a small increase in Mn-Fe and other trace elements, below the observed enrichment observed in the varnish. Leaching is discounted on the basis that varnishes would grow from the inside to the outside and the observed abrupt distinctions in elemental fractionations preclude this. Our cross-sectional examination supports this observation, with clear distinctions between the Fe-oxyhydroxide layers and the substrate.

Given this is a valid scenario for varnish formation, the composition of wet and dry aerosols has critical implications for rock surfaces in the study region. Predicted scenarios for increased industrial activity on the Burrup Peninsula indicate increases in aerosol soluble gases and dust levels, which will affect the solution chemistry of wet aerosols. The formation and aggregation of aerosols is highly dependent of the levels of airborne particulates, with particles acting as nucleation points for the accumulation of water vapour. Together with the evidence that soluble ions leached from dust particles may be the foundation of desert varnish, the combinations of

various solution chemistries provided by elevated levels of airborne pollution will play a vital role in predicting outcomes for the rock art on the Burrup Peninsula.

## ***1.2 Experimental***

### **1.2.2 SEM and Microprobe Cross-Sections**

Cross-sections of Burrup rock surfaces were prepared in epoxy resin and ground to reveal a cross-sectional area through the surface face. They were examined in an ESEM (Quanta FEI 200) at 20 kV and 0.5 torr. Figure 13 and Figure 14 show images obtained from a single example of a rock surface considered representative of the background rock surface.

Cross-sections and a surface view of an engraved surface are shown in Figure 15.

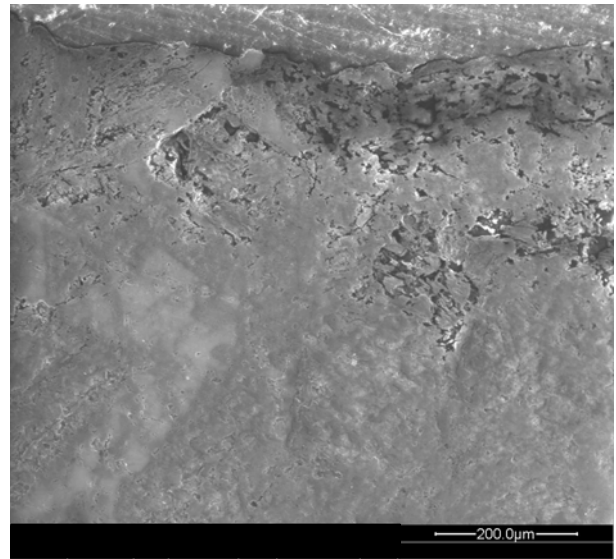
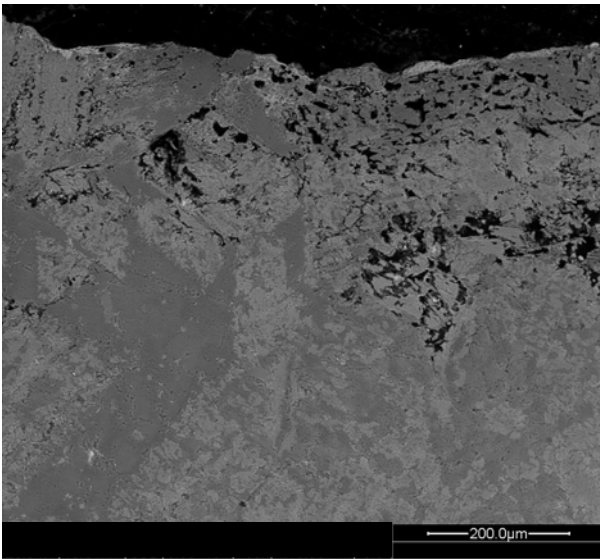
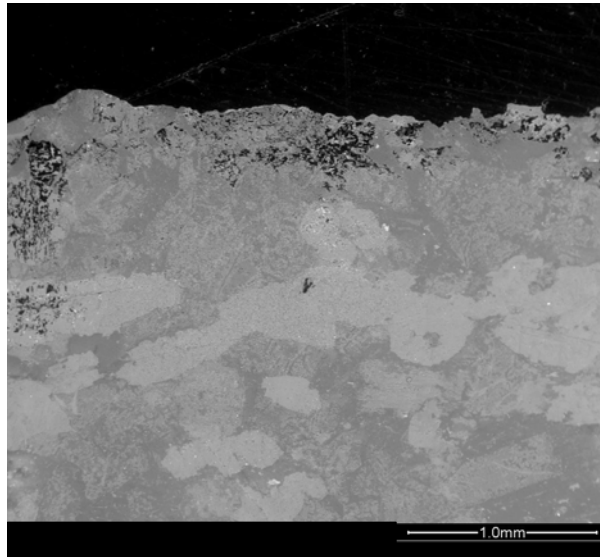
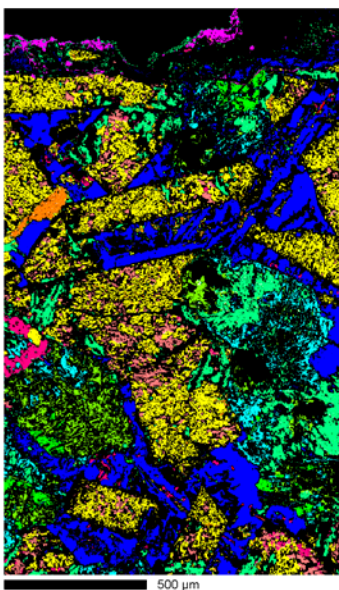
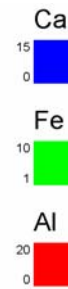
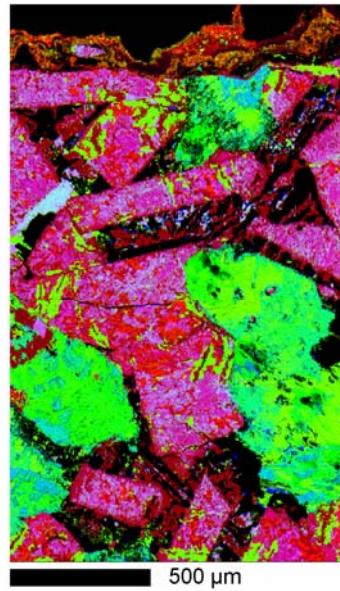
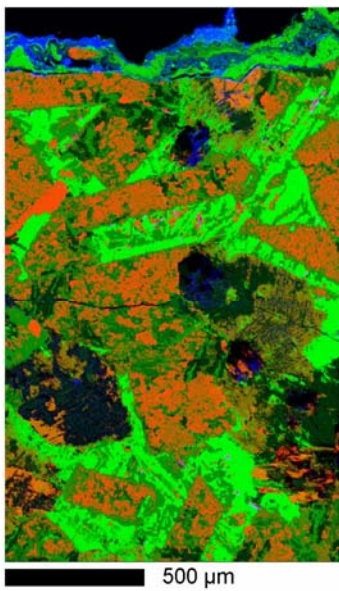


**Figure 13: ESEM images of cross-sections through surface of background rock (BSE top and left, and SE right).**



- Ca(AlFe) oxide
- Ca<sub>2</sub>Al<sub>2</sub>Si<sub>3</sub>O<sub>12</sub>(Fe)
- Ca<sub>2</sub>Al<sub>2</sub>Si<sub>3</sub>O<sub>12</sub>(Fex)
- CaAl<sub>2</sub>Si<sub>2</sub>O<sub>8</sub> Anorthite
- Fe Si (X) oxide
- Fe<sub>16</sub>Al<sub>18</sub>Mg<sub>6</sub>Si<sub>9</sub>
- Feldspar
- KAlSi<sub>3</sub>O<sub>8</sub>
- KMg<sub>3</sub>Fe<sub>3</sub>Si<sub>4</sub>Al<sub>4</sub>O<sub>6</sub> Hydro i
- PAI hydroxide
- SiO<sub>2</sub>

Figure 14: Elemental maps of cross-sections through surface of background rock.

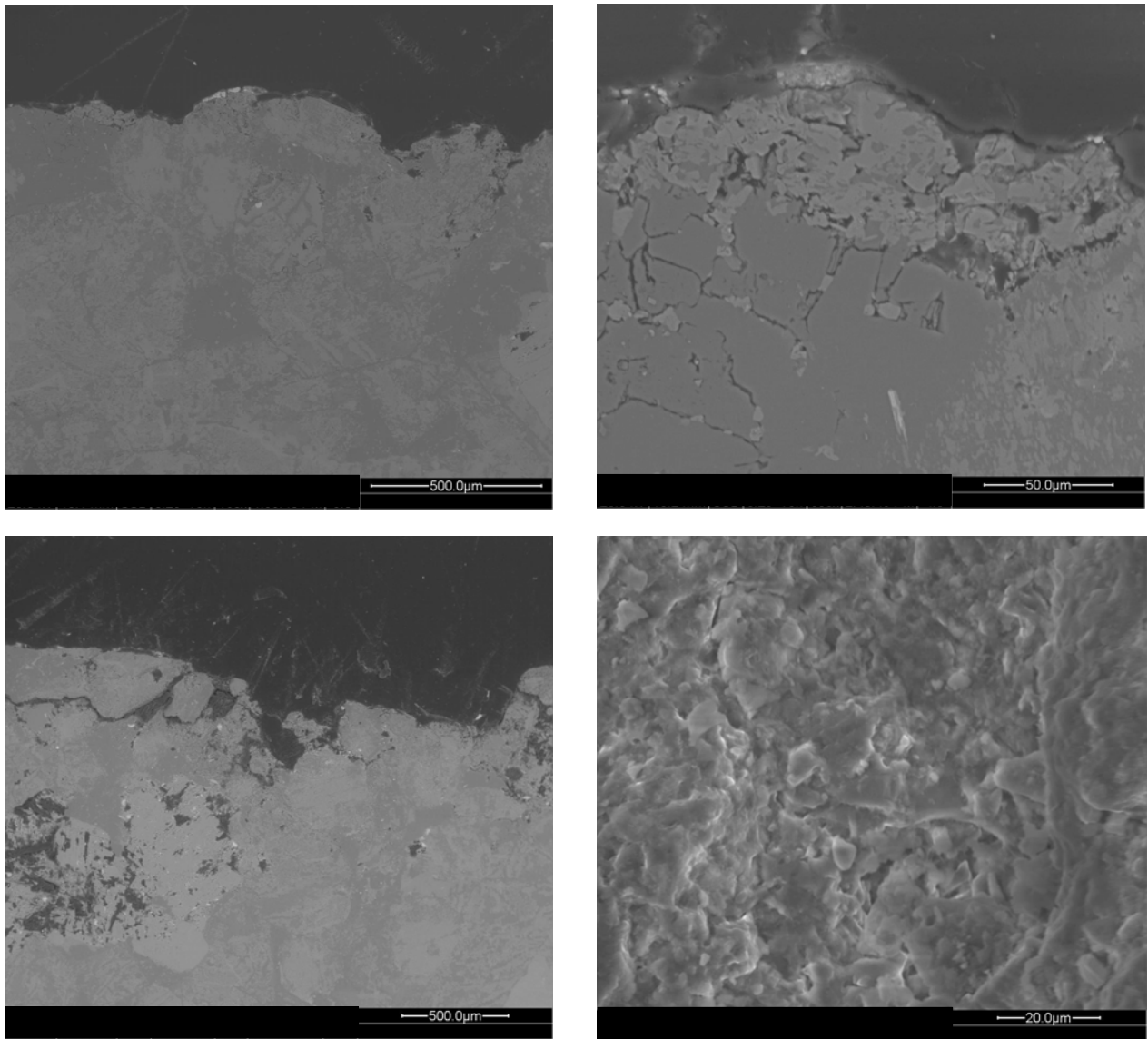


**Figure 15: ESEMs (BSE) of cross-sections through engraved rock surface (top and bottom left) and surface view (bottom right).**

These preliminary studies of the rock interface surface structure most importantly reveal structural differences in near-surface micro-porosity. The engraved surface has very few regions of porous structure, and where they exist they are of the order of up to 50 µm. The background surface has much more extensive regions of porosity that extend to depths of up to 1200 µm.

If desert varnish growth and re-patination of the surface rely on the direct aqueous deposition model, then wettability and the absorption of surface moisture that are defined by porosity and absorptivity of the surface will strongly influence re-patination.

The maps of elemental distribution in cross-sections through the engraved and background surfaces show no enrichment of Fe at the surface interface, as may be expected with the occurrence of hematite as a surface coating. Iron exists predominantly in the iron-containing silicates and aluminosilicates of the bulk rock material.

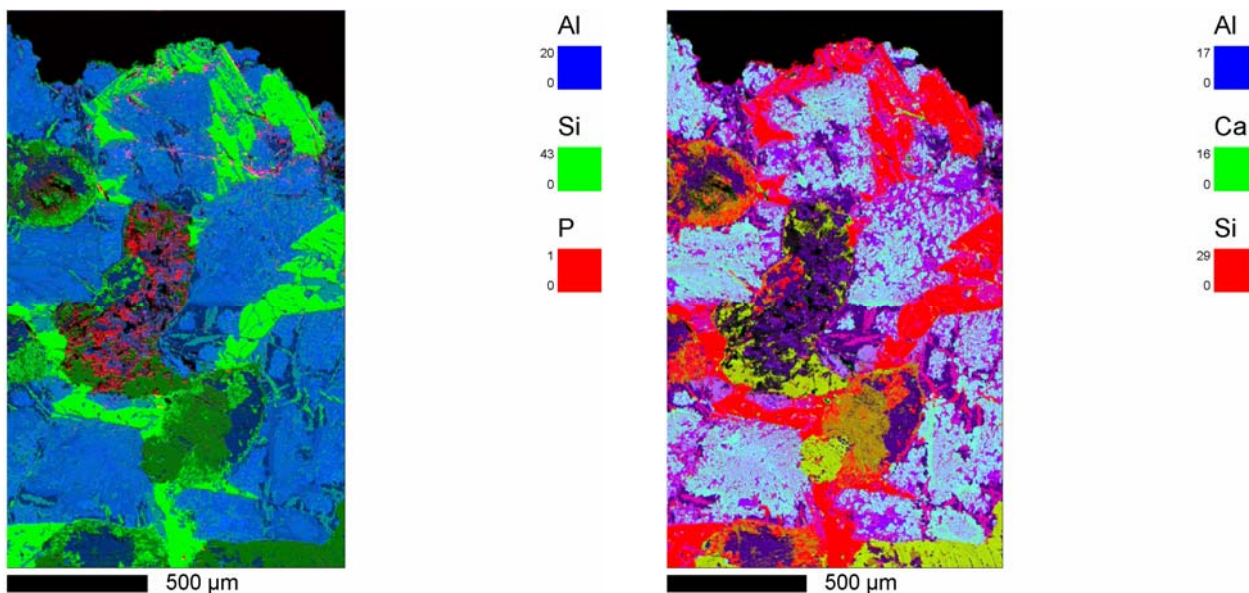


**Figure 16: Elemental maps of cross-sections through surface of engraved rock.**

The microstructure of the surface coating evident on background-type rock surfaces is clearly different in morphology and composition from the bulk rock structure. The patina layer is variable in thickness over the surface, from approximately 20 to 200  $\mu\text{m}$ .

### 1.2.3 Fourier Transform Infrared Spectroscopy

The rock surfaces in this study are being characterised in a number of ways, and an emphasis is being placed on non-destructive methods. A non-destructive technique will allow the analysis of one particular point or sample before and after exposure to chemical modification as part of the fumigation study, thereby reducing the potential for variability in response between different samples, introduced through natural sample variation.

Fourier Transform Infrared Spectroscopy (FTIR) spectroscopy provides information about the chemical make-up of materials, through interrogation the vibrational bonds of molecules by measuring the amount of light absorbed on irradiation with light in the mid-IR region. XRD is widely used to study mineralogy, but it only provides information about crystalline materials. Many iron oxides and hydroxides are poorly crystalline, diminishing the effectiveness of XRD as a tool in this context and, considering the prevalence of these materials on the surfaces, supplementary techniques have been employed.

In order to achieve a fuller understanding of the mineralogical make-up of Burrup rock surfaces, we are using a range of techniques concentrating on the air/rock interface where physiochemical changes can affect the petroglyph image. FTIR provides analysis at a point on a surface with spatial resolution down to 1 micron. The instrumentation used was a Bruker Equinox 55 with a mid-IR prying mantis accessory for collecting reflectance spectra from a surface area of approximately 2 mm in diameter. Conditions for acquisition were 64 scans at 4  $\text{cm}^{-1}$  resolution in the range 400 – 4000  $\text{cm}^{-1}$ . Collected spectra were treated with a Kubelka Munk Transformation. For each sample 3 points were measured then averaged.

**Table 5: Summary of Fumigated samples.**

<i>Exposure x 1</i>	<i>Exposure x 10</i>	<i>Control (unexposed)</i>	<i>Exposure x 1</i>	<i>Exposure x 10</i>	<i>Control (unexposed)</i>	
E1S4	E2S4	E3S4	B1S4	B2S4	B3S4	
E1S5	E2S5	E3S5	B1S5	B2S5	B3S5	With dust
E1S6	E2S6	E3S6	B1S6	B2S6	B3S6	

Results

**Table 6: Before and after exposure: FTIR summary of background type rock surfaces.**

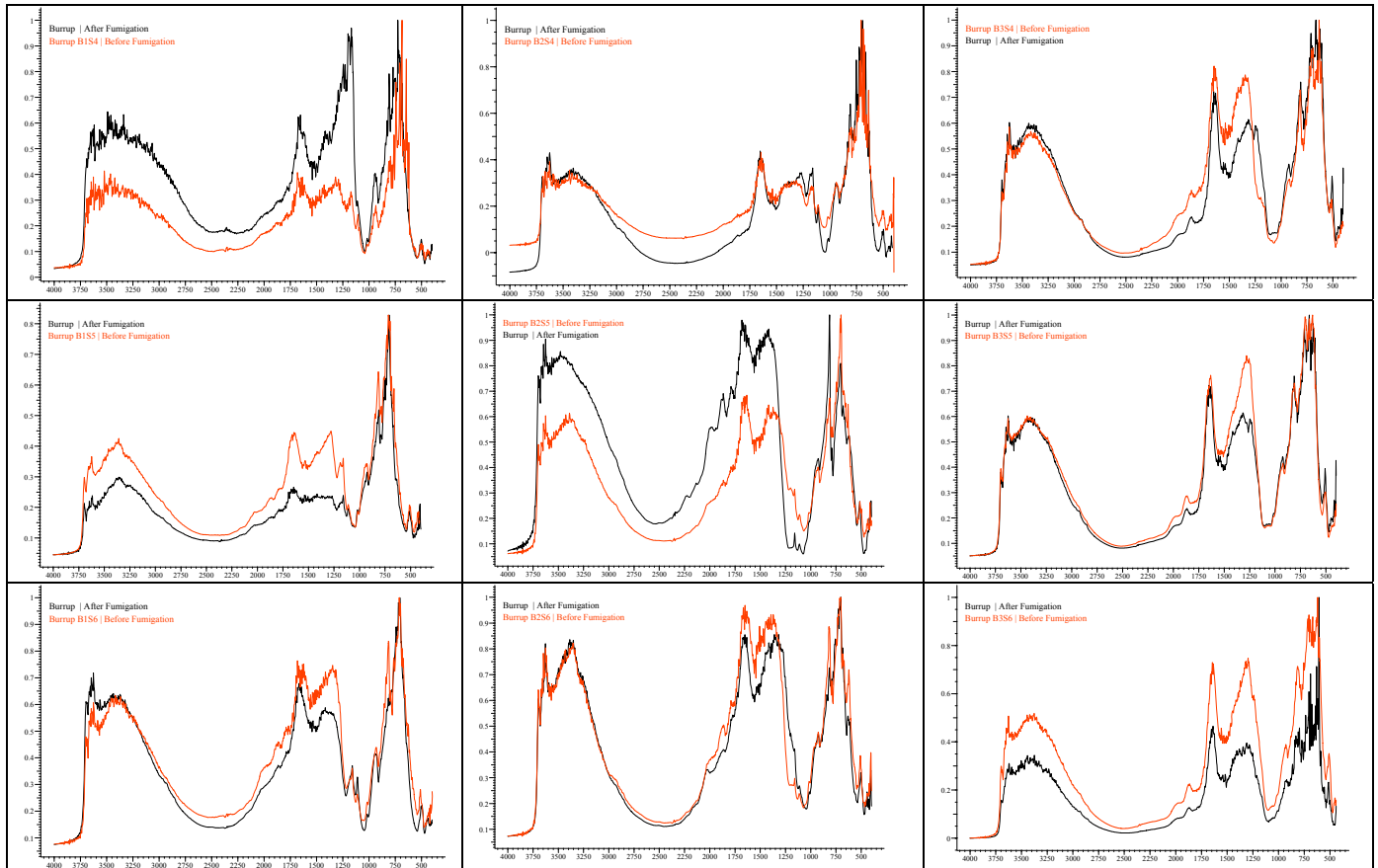
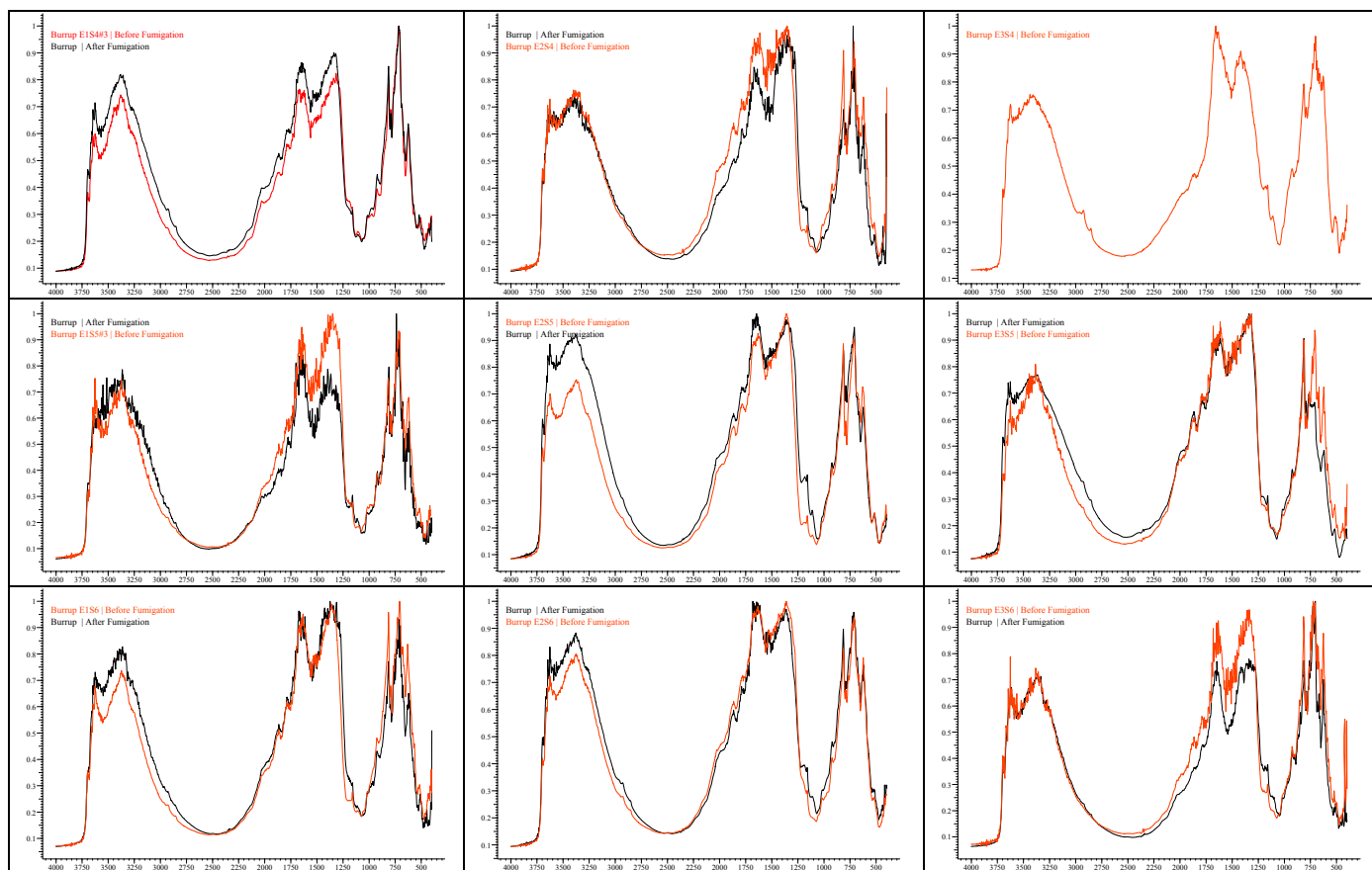


**Table 7: Before and after exposure: FTIR summary of engraved type rock surfaces.**



- Sample E3S4 (engraved control) does not have an average spectrum after fumigation due to excessively noisy spectra, considered unsuitable for comparison with the “before” spectra. However, the sample conditions are duplicated in sample E3S4, also an engraved control.

**Table 8: Normalised intensities of peaks at 1648 and 1369 cm<sup>-1</sup>.**

<b>Normalised Intensity after fumigation</b>						
<b>1648 cm<sup>-1</sup></b>						
<b>Exposure x 1</b>	<b>Exposure x 10</b>	<b>Control (unexposed)</b>	<b>Exposure x 1</b>	<b>Exposure x 10</b>	<b>Control (unexposed)</b>	
E1S4	E2S4	E3S4	B1S4	B2S4	B3S4	
0.9	0.8		0.6	0.4	0.75	
E1S5	E2S5	E3S5	B1S5	B2S5	B3S5	With dust
0.8	1	0.95	0.25	1	0.75	
E1S6	E2S6	E3S6	B1S6	B2S6	B3S6	
0.95	1	0.75	0.7	0.85	0.4	

<b>1369 cm-1</b>						
<i>Exposure x 1</i>	<i>Exposure x 10</i>	<i>Control (unexposed)</i>	<i>Exposure x 1</i>	<i>Exposure x 10</i>	<i>Control (unexposed)</i>	
E1S4	E2S4	E3S4	B1S4	B2S4	B3S4	
0.9	0.95		0.6	0.35	0.6	
E1S5	E2S5	E3S5	B1S5	B2S5	B3S5	With dust
0.75	1	1	0.2	0.95	0.6	
E1S6	E2S6	E3S6	B1S6	B2S6	B3S6	
1	0.95	0.8	0.6	0.85	0.4	
<b>Normalised Intensity before fumigation</b>						
<b>1648 cm-1</b>						
<i>Exposure x 1</i>	<i>Exposure x 10</i>	<i>Control (unexposed)</i>	<i>Exposure x 1</i>	<i>Exposure x 10</i>	<i>Control (unexposed)</i>	
E1S4	E2S4	E3S4	B1S4	B2S4	B3S4	
0.75	0.95		0.35	0.4	0.85	
E1S5	E2S5	E3S5	B1S5	B2S5	B3S5	With dust
0.9	0.95	0.95	0.45	0.7	0.8	
E1S6	E2S6	E3S6	B1S6	B2S6	B3S6	
0.95	1	0.9	0.75	0.95	0.7	
<b>1369 cm-1</b>						
<i>Exposure x 1</i>	<i>Exposure x 10</i>	<i>Control (unexposed)</i>	<i>Exposure x 1</i>	<i>Exposure x 10</i>	<i>Control (unexposed)</i>	
E1S4	E2S4	E3S4	B1S4	B2S4	B3S4	
0.8	1		0.3	0.35	0.8	
E1S5	E2S5	E3S5	B1S5	B2S5	B3S5	With dust
0.95	1	1	0.4	0.6	0.85	
E1S6	E2S6	E3S6	B1S6	B2S6	B3S6	
1	0.95	0.95	0.75	0.9	0.8	

Table 9: Intensity differences before and after fumigation.

### ***Before and after fumigation difference***

<b>1648 cm-1</b>						
<i>Exposure x 1</i>	<i>Exposure x 10</i>	<i>Control (unexposed)</i>	<i>Exposure x 1</i>	<i>Exposure x 10</i>	<i>Control (unexposed)</i>	
E1S4	E2S4	E3S4	B1S4	B2S4	B3S4	

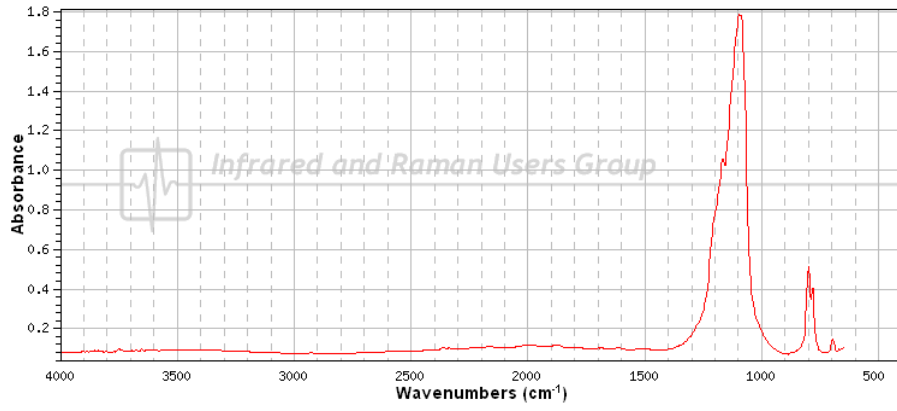
-0.15	0.15	0	-0.25	0	0.1	
E1S5	E2S5	E3S5	B1S5	B2S5	B3S5	With dust
0.1	-0.05	0	0.2	-0.3	0.05	
E1S6	E2S6	E3S6	B1S6	B2S6	B3S6	
0	0	0.15	0.05	0.1	0.3	
<b>1369 cm<sup>-1</sup></b>						
<i>Exposure x 1</i>	<i>Exposure x 10</i>	<i>Control (unexposed)</i>	<i>Exposure x 1</i>	<i>Exposure x 10</i>	<i>Control (unexposed)</i>	
E1S4	E2S4	E3S4	B1S4	B2S4	B3S4	
-0.1	0.05	0	-0.3	0	0.2	
E1S5	E2S5	E3S5	B1S5	B2S5	B3S5	With dust
0.2	0	0	0.2	-0.35	0.25	
E1S6	E2S6	E3S6	B1S6	B2S6	B3S6	
0	0	0.15	0.15	0.05	0.4	

## Discussion

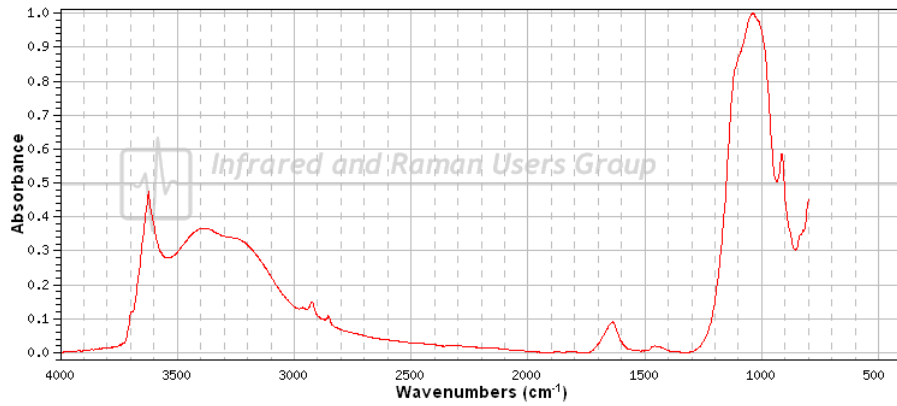
FTIR was used as a surface characterisation technique to examine the rock surface before and after fumigation. Specific absorption bands relate to chemical speciation on the surface and this was used to indicate whether specific mineralogical changes in the rock surfaces could be detected. In a study of ochres using FTIR, Bikiaris et al (2) observed ferric oxide to have two broad peaks at 470 cm<sup>-1</sup> and another at 536 cm<sup>-1</sup> with a shoulder at around 610 cm<sup>-1</sup>. The mineral hematite was similar but with the second peak being shifted towards a higher wavenumber value of 555 cm<sup>-1</sup>.

Red ochre's infrared spectrum is different to that of ferric oxide as ochres generally contain clay and silica. This is more consistent with the mineralogical composition of the surface of the Burrup rocks, and therefore considered a suitable reference spectrum for comparison.

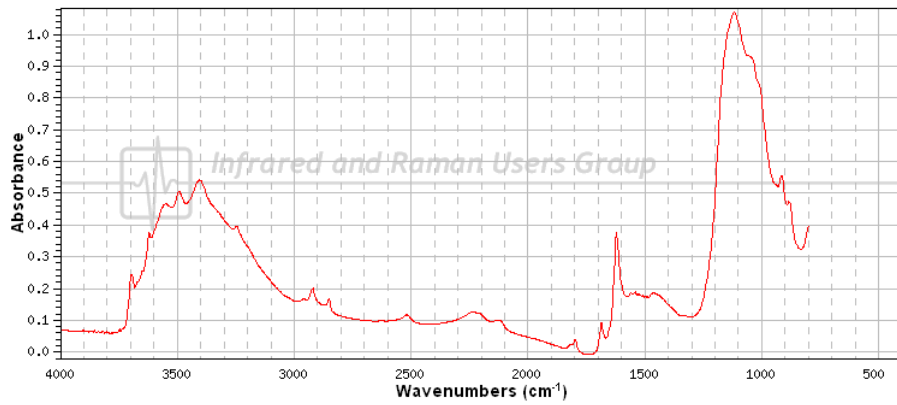
Most clays have strong bands in the region 3670 – 3600 cm<sup>-1</sup>, 3450 – 3400 cm<sup>-1</sup> and 500 – 450 cm<sup>-1</sup> and a very strong band at 1075 – 1050 cm<sup>-1</sup> and a medium/weak band at 1640 cm<sup>-1</sup>, a band at 945 – 905 cm<sup>-1</sup> and a weak band at 885 – 800 cm<sup>-1</sup>. Kaolinite peaks at 1032 (Si-O-Si), 1009 (Si-O-Al), 938 and 914 (Al-O-H), 536 (Si-O-Al) and 479 (Si-O) cm<sup>-1</sup> are common in in kaolinite and red ochre spectra (Figure 17). Clays containing water of crystallization exhibit a distinctive absorption pattern near 3600 cm<sup>-1</sup> with outer hydroxyl ions at 3694, 3669, 3620 and 3652 cm<sup>-1</sup>. In accordance with other layered aluminosilicates, the Si-O peak of chlorite is also at approximately 1000 cm<sup>-1</sup>.



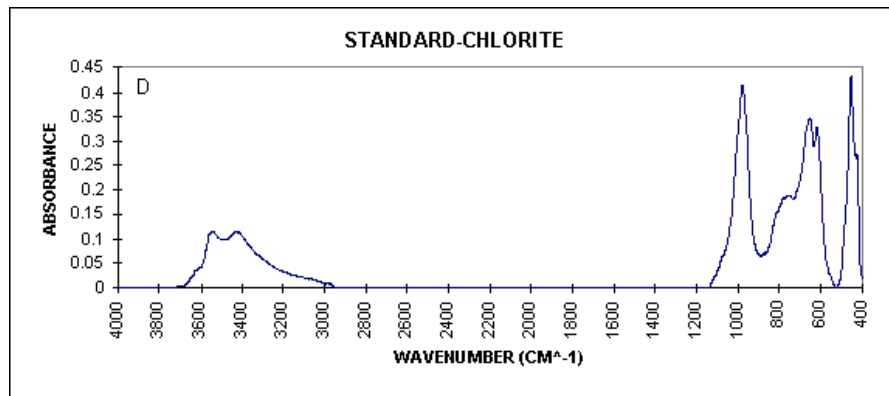
(a) IMP00322 Quartz, silica



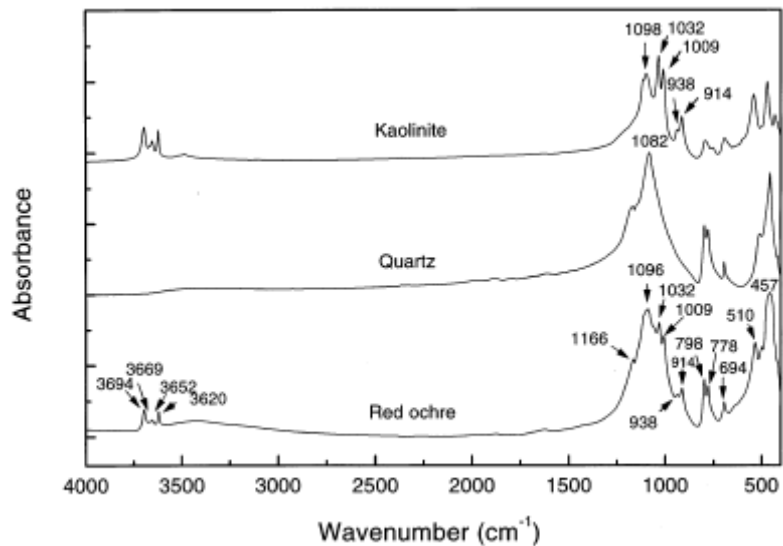
(b) IMP00032 Ochre, dark, German (hematite)



(c) IMP00035 Ochre, yellow, German,



(d) Standard chlorite (from (1))



(e) FTIR spectra of red ochre (hematite), quartz and kaolinite (from (2)).

**Figure 17: Reference mineral FTIR spectra.**

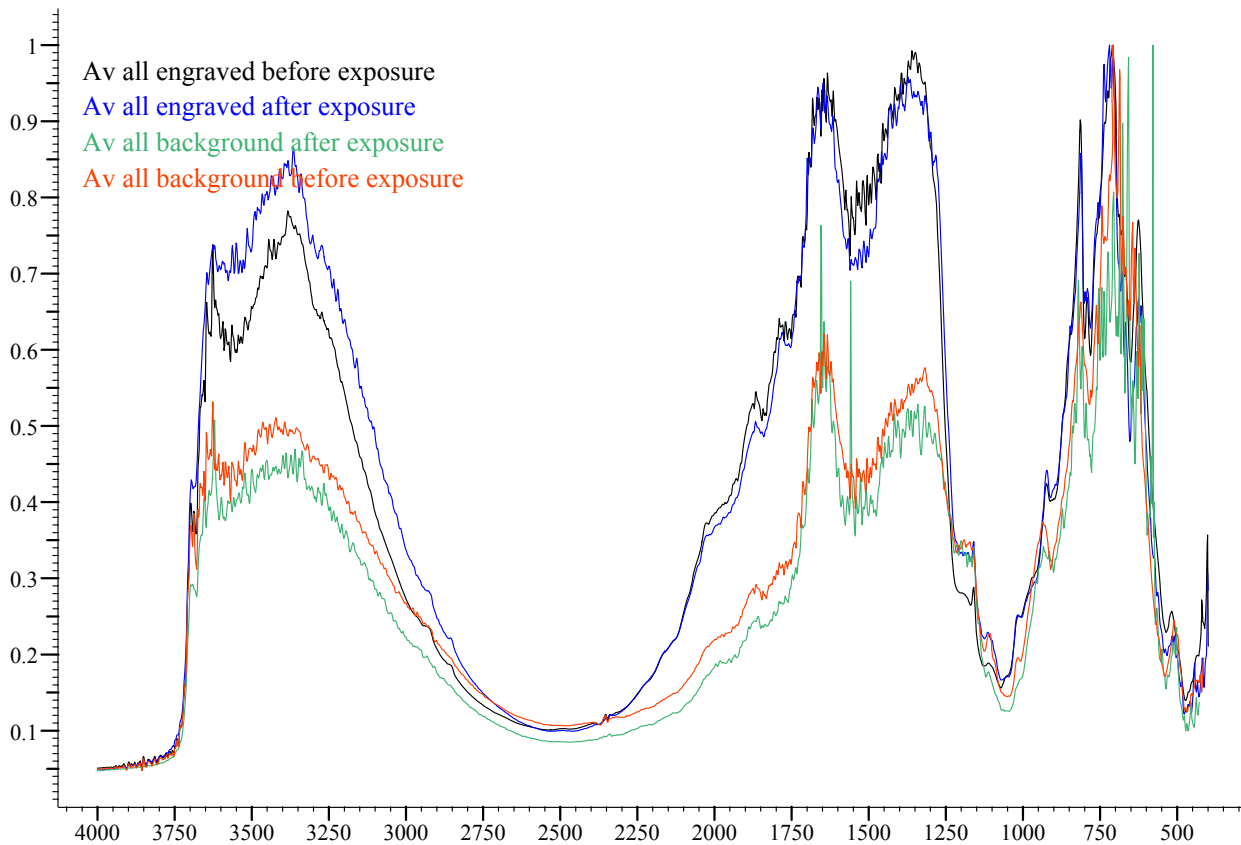


**Figure 18: Average of all spectra including control samples.**

In general, the main peaks in the spectra collected for the pre and post-fumigation samples are 3627, 3367, 1867, 1648 (s), 1369 (s), 1160, 1112, 1014, 921, 816 (s), 719 (s), 620 (s) and 510  $\text{cm}^{-1}$ . There is some difference observed between individual (unaveraged) spectra taken from different points on the same sample which was managed by taking an average of 3 spectra per sample. Figure 18 illustrates the differences observed overall in the before and after spectra. The absorption due to water is slightly decreased for both engraved and background samples. The peak intensity at 1648  $\text{cm}^{-1}$  is unchanged, while the peak intensity at 1369  $\text{cm}^{-1}$  is slightly decreased. This was observed in both the fumigated and control samples, but a single combined plot is presented here for brevity.

The control samples both with and without dust exhibit most difference in the bands at 3627 and 3367  $\text{cm}^{-1}$  (water of crystallization in the layered aluminosilicates) and the band pair at 1648 and 1369  $\text{cm}^{-1}$ . This is also observed in the samples exposed at x1 and x10 dose levels, both with and without dust. The bands at 1648 and 1369  $\text{cm}^{-1}$  were used to quantify any modification at the surface due to changes induced by the fumigation process.

Table 8 lists the normalized intensities from the normalized spectra and Table 9 the differences in peak intensities between the before and after fumigation spectra. It can be seen that there is no consistent decrease or increase in band intensity for either the band at 1648 or 1369  $\text{cm}^{-1}$ . Also, the magnitude of difference observed in the control samples is also greater than that observed for the fumigated samples at both the x1 and x10 exposure levels. This indicates the fumigation process did not induce any measurable change in the mineralogy of either the engraved type or background type rock surfaces.

### **1.2.1 Environmental Scanning Electron Microscopy/Energy Dispersive Spectroscopy (ESEM/EDS) of Rock Surfaces**

The FEI Quanta 200 Environmental Scanning Electron Microscope (ESEM) is a thermal tungsten gun instrument capable of imaging under three vacuum regimes, High-vacuum ( $< 6 \times 10^{-4}$  Pa), Low-vacuum (10 - 130 Pa) and ESEM-vacuum (10 - 2600 Pa). The microscope is equipped with an Oxford Inca Energy Dispersive X-ray (EDX) system for chemical analysis. In analysing and imaging the rock samples the Low-vacuum secondary electron detector (LFD), and the solid-state back-scatter electron detector (BSE) were employed. ESEM is able to image uncoated and hydrated samples by means of a differential pumping system and the gaseous secondary electron detector.

The elemental composition of the rock samples was determined in Low-vacuum mode using two pressure ranges (40 Pa and 107 Pa) for quantification. The conditions used were an accelerating voltage (HV) of 20kV, spot size 6.0, working distance 10mm, magnification x 40 and counting time of 100 sec

The rock samples were adhered to a large pin-type 25mm diameter SEM mount without any further sample preparation. At least 2 points on each rock were analysed quantitatively and the average result presented. An example ESEM image of a rock surface is shown in Figure 13.



Figure 19: Optical microscopy of rock subsample prepared for fumigation.

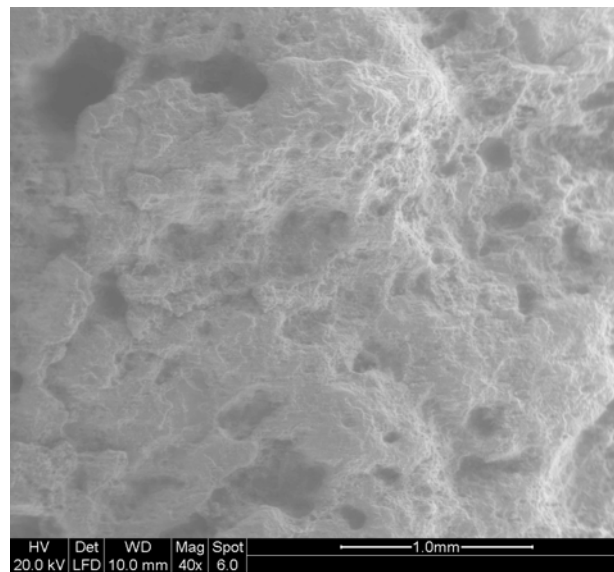


Figure 20: ESEM image of a rock surface.

Table 10: Elemental profile of rock surfaces before and after fumigation (% composition).

<b>Sample</b>	<b>C</b>	<b>O</b>	<b>Na</b>	<b>Mg</b>	<b>Al</b>	<b>Si</b>	<b>K</b>	<b>Ca</b>	<b>Fe</b>
<b>x1</b>									
Bgnd1, s4 - Before	4.76	42.88	0.54	0.98	12.78	16.24	0.76	1.34	15.97
Bgnd1, s5 - Before	12.7	42.46	0.61	1.18	11.77	18.17	1.02	0.6	9.23
Bgnd1, s6 - Before	21.98	40.56	0.68	1.06	9.53	13.49	0.81	0.86	9.03
<b>x10</b>									
Bgnd2, s4 - Before	10.73	42.91	0.62	1.11	10.89	18.32	1.19	1.03	11.64
Bgnd2, s5 - Before	14.91	41.75	1.09	1.12	8.92	18.65	1.18	1.67	9.25
Bgnd2, s6 - Before	13.83	42.29	0.64	1.24	8.72	16.19	0.84	2.14	12.79
<b>control</b>									
Bgnd3, s4 - Before	13.75	42.31	1	1.88	6.25	19.13	1.11	1.79	10.98
Bgnd3, s5 - Before	5.98	47.05	0.42	0.73	4.11	28.67	0.5	0.5	11.39
Bgnd3, s6 - Before	9.78	44.54	0.57	1.24	5.4	29.81	0.73	0.85	6.48
<b>x1</b>									
Bgnd1, s4 - After	4.41	32.07	0.76	1.27	12.04	19.43	1.05	2.64	21.9
Bgnd1, s5 - After	7.54	34.19	0.38	1.05	12.06	18.84	0.98	2.58	20.06
Bgnd1, s6 - After	7.79	34.12	0.47	0.94	13.53	19.64	0.94	1.3	16.62

**x10**

Bgnd2, s4 - After	13.09	34.36	0.5	0.87	9.22	24.66	1.25	1.64	9.94
Bgnd2, s5 - After	9.33	35.11	0.78	1.14	11.08	18.3	1.26	2.08	14.54
Bgnd2, s6 - After	9.55	36.49	1.38	1.52	10.5	23	1.58	3.61	10.24

**control**

Bgnd3, s4 - After	5.11	43.08	0.45	1.31	6.46	36.92	0.49	1.01	3.77
Bgnd3, s5 - After	5.15	40.59	0.4	1.35	5.66	37.76	0.71	0.89	7.28
Bgnd3, s6 - After	5.9	40.45	0.32	1.37	6.77	33	1.16	1.13	9.38

**Sample**

**C O Na Mg Al Si K Ca Fe**

**x1**

Engr1, s4 - Before	10.33	41.14	2.17	3.23	7.06	24.38	0.67	3.6	7.42
Engr1, s5 - Before	13.47	39.82	1.41	1.69	7.3	21.93	1.09	2.35	10.32
Engr1, s6 - Before	12.71	38.81	1.63	2.27	7.55	22.78	1.19	3.43	9.36

**x10**

Engr2, s4 - Before	6.46	41.73	0.83	2.5	9.55	21.23	1.37	4.17	11.7
Engr2, s5 - Before	14	41.82	0.86	1.97	7.92	20.38	1.19	2.62	8.88
Engr2, s6 - Before	15.45	40.96	0.64	2.59	6.72	18.9	0.79	2.84	8.96

**control**

Engr3, s4 - Before	16.35	39.2	0.71	2.08	7.62	20.48	1.14	3.07	9.04
Engr3, s5 - Before	4.05	40.36	2.62	2.71	9.15	25.33	0.86	4.52	9.33
Engr3, s6 - Before	6.26	42.12	1.96	3.58	6.75	22.35	0.56	3.21	12.81

**x1**

Engr1, s4 - After	5.58	33.1	0.88	2.08	8.31	23.74	1.67	5.52	17.43
Engr1, s5 - After	4.94	33.39	1.38	1.97	10.2	24.25	1.58	4.98	15.83
Engr1, s6 - After	9.87	38.55	1.12	1.81	9.19	25.54	1.33	3.37	8.16

**x10**

Engr1, s4 - After	14.04	34.85	0.41	0.89	9.61	22.86	1.13	1.77	9.8
Engr1, s5 - After	14.01	34.78	0.41	0.89	9.61	22.88	1.13	1.78	9.84
Engr1, s6 - After	13.89	36.4	0.41	0.87	9.5	22.72	1.13	1.79	4.93

**control**

Engr3, s4 - After	7.75	33.95	0.61	2.03	8.94	25.86	1.72	4.35	14.15
Engr3, s5 - After	1.77	38.04	0.55	1.34	12.47	26.19	1.39	6.74	10.95
Engr3, s6 - After	4.19	36.48	1.19	2.09	9.28	26.3	1.59	3.83	14.19

**Table 11: Average pre-exposure surface concentration for all samples.**

	<b>C</b>	<b>O</b>	<b>Na</b>	<b>Mg</b>	<b>Al</b>	<b>Si</b>	<b>K</b>	<b>Ca</b>	<b>Fe</b>
background	12.05	42.97	0.69	1.17	8.71	19.85	0.90	1.20	10.75
engraved	11.01	40.66	1.43	2.51	7.74	21.97	0.98	3.31	9.76

**Table 12: Percentage change in elemental composition before and after fumigation.**

<b>% change before-after</b>	<b>C</b>	<b>O</b>	<b>Na</b>	<b>Mg</b>	<b>Al</b>	<b>Si</b>	<b>K</b>	<b>Ca</b>	<b>Fe</b>
<b>x1</b>									
Bgnd1, s4	-7.35	-25.21	40.74	29.59	-5.79	19.64	38.16	97.01	37.13
Bgnd1, s5	-40.63	-19.48	-37.70	-11.02	2.46	3.69	-3.92	330.00	117.33
Bgnd1, s6	-64.56	-15.88	-30.88	-11.32	41.97	45.59	16.05	51.16	84.05
<b>x10</b>									
Bgnd2, s4	21.99	-19.93	-19.35	-21.62	-15.34	34.61	5.04	59.22	-14.60
Bgnd2, s5	-37.42	-15.90	-28.44	1.79	24.22	-1.88	6.78	24.55	57.19
Bgnd2, s6	-30.95	-13.71	115.63	22.58	20.41	42.06	88.10	68.69	-19.94
<b>control</b>									
Bgnd3, s4	-62.84	1.82	-55.00	-30.32	3.36	93.00	-55.86	-43.58	-65.66
Bgnd3, s5	-13.88	-13.73	-4.76	84.93	37.71	31.71	42.00	78.00	-36.08
Bgnd3, s6	-39.67	-9.18	-43.86	10.48	25.37	10.70	58.90	32.94	44.75
<b>% change before-after</b>	<b>C</b>	<b>O</b>	<b>Na</b>	<b>Mg</b>	<b>Al</b>	<b>Si</b>	<b>K</b>	<b>Ca</b>	<b>Fe</b>
<b>x1</b>									
Engr1, s4	-45.98	-19.54	-59.45	-35.60	17.71	-2.63	149.25	53.33	134.91
Engr1, s5	-63.33	-16.15	-2.13	16.57	39.73	10.58	44.95	111.91	53.39
Engr1, s6	-22.34	-0.67	-31.29	-20.26	21.72	12.12	11.76	-1.75	-12.82
<b>x10</b>									
Engr2, s4	117.34	-16.49	-50.60	-64.40	0.63	7.68	-17.52	-57.55	-16.24
Engr2, s5	0.07	-16.83	-52.33	-54.82	21.34	12.27	-5.04	-32.06	10.81
Engr2, s6	-10.10	-11.13	-35.94	-66.41	41.37	20.21	43.04	-36.97	-44.98
<b>control</b>									
Engr3, s4	-52.60	-13.39	-14.08	-2.40	17.32	26.27	50.88	41.69	56.53
Engr3, s5	-56.30	-5.75	-79.01	-50.55	36.28	3.40	61.63	49.12	17.36
Engr3, s6	-33.07	-13.39	-39.29	-41.62	37.48	17.67	183.93	19.31	10.77

The elemental profiles of the rock surfaces are presented in Table 10 and the percentage differences in Table 12. The pre-exposure differences between the engraved and background types are consistent with the mineralogy identified in the cross sections and with XRD. Iron is observed in relatively higher average pre-exposure concentration on the background type rock surface, and lower average pre-exposure concentration on the engraved type. Silicon is in greater average pre-exposure concentration on the engraved rock surface due to the greater surface exposure of silica, along with calcium due do calcium containing sub-surface minerals. Iron, silicon and calcium are the elements used to indicate whether the rock surface has changed from a background to engraved type due to the fumigation procedure.

For the background type rock surfaces, the percentage change in the control samples is not consistently greater than the exposed specimens for iron and calcium. There is a slight increase in the silicon concentration compared with the controls, but given there is not a measurable parallel decrease in iron and calcium, it is not possible to attribute this change in composition to becoming more like the engraved type. The differences in iron and calcium concentration do not increase from the x1 to the x10 exposure so concentration changes are not considered to be related to the increased pollutant exposure.

The engraved type rock surfaces did not demonstrate a consistent increase in silicon concentration or decrease in calcium or iron.

Overall, the elemental concentrations of the background and engraved surface types after the x1 pollutant exposure were not measurably different from the unexposed samples. Also, the x10 exposure did not produce a greater change in the concentrations of elements compared with either the x1 exposure or the control samples.

### 1.2.4 Surface Colour Measurements

In accord with the colour measurements made in situ, the fumigated samples were monitored for colour change before and after exposure.

The difference between two colours measured instrumentally is  $\Delta E$ . It derives from the German word for sensation – *Empfindung* – which means a difference in sensation. A  $\Delta E$  value of zero represents an exact match. It is the standard CIE colour difference method, and measures the distance between the two colours, calculated in 3D L\*a\*b\* colour space. In this way, colour difference can be evaluated through measuring the tristimulus values of points over time, and calculating to evaluate the colour difference with time.

The difference between two colours,  $\Delta E$ , can be evaluated using the 1976 CIE colour difference formula [11]. In CIE L\*a\*b\* space, the difference is:

$$\Delta E^*_{ab} = [(\Delta L^*)^2 + (\Delta a^*)^2 + (\Delta b^*)^2]^{0.5}$$

This principle was used to measure the fumigated samples before and after exposure.

Table 13: Colour measurements before and after fumigation.

Sample	Comment:	Color scale						$\Delta$ CMC
		L*	a*	b*	L*	a*	b*	
		<b>Pre-exposure</b>			<b>Post exposure</b>			
engraved#1,s4	<b>AVERAGE</b>	<b>28.71</b>	<b>5.80</b>	<b>11.42</b>	<b>42.82</b>	<b>12.80</b>	<b>19.96</b>	17.91
engraved#1,s5	<b>AVERAGE</b>	<b>26.48</b>	<b>11.14</b>	<b>18.79</b>	<b>33.74</b>	<b>11.83</b>	<b>16.62</b>	7.61
engraved#1,s6	<b>AVERAGE</b>	<b>33.38</b>	<b>8.91</b>	<b>18.65</b>	<b>38.47</b>	<b>12.00</b>	<b>20.10</b>	6.13
engraved#2,s4	<b>AVERAGE</b>	<b>29.90</b>	<b>9.74</b>	<b>15.66</b>	<b>35.09</b>	<b>9.162</b>	<b>15.352</b>	5.23
engraved#2,s5	<b>AVERAGE</b>	<b>33.72</b>	<b>12.92</b>	<b>18.29</b>	<b>36.64</b>	<b>12.27</b>	<b>16.97</b>	3.27
engraved#2,s6	<b>AVERAGE</b>	<b>16.46</b>	<b>7.45</b>	<b>12.22</b>	<b>35.945</b>	<b>10.115</b>	<b>16.5625</b>	20.14
engraved#3,s4	<b>AVERAGE</b>	<b>28.32</b>	<b>7.27</b>	<b>14.88</b>	<b>35.71</b>	<b>5.14</b>	<b>14.17</b>	7.72
engraved#3,s5	<b>AVERAGE</b>	<b>31.57</b>	<b>4.20</b>	<b>8.28</b>	<b>37.18</b>	<b>5.71</b>	<b>13.23</b>	7.62
engraved#3,s6	<b>AVERAGE</b>	<b>47.05</b>	<b>11.11</b>	<b>20.26</b>	<b>43.07</b>	<b>8.966</b>	<b>16.72</b>	5.75
background#1, s4	<b>AVERAGE</b>	<b>23.04</b>	<b>9.85</b>	<b>10.48</b>	<b>35.74</b>	<b>10.93</b>	<b>14.93</b>	13.50

background#1, s5	<b>AVERAGE</b>	<b>24.70</b>	<b>10.96</b>	<b>10.10</b>	<b>26.84</b>	<b>9.72</b>	<b>11.43</b>	2.81
background#1, s6	<b>AVERAGE</b>	<b>29.40</b>	<b>14.12</b>	<b>16.66</b>	<b>35.12</b>	<b>15.55</b>	<b>19.21</b>	6.43
background#2, s4	<b>AVERAGE</b>	<b>21.27</b>	<b>13.27</b>	<b>15.48</b>	<b>31.68</b>	<b>14.60</b>	<b>19.61</b>	11.27
background#2, s5	<b>AVERAGE</b>	<b>19.01</b>	<b>12.78</b>	<b>14.69</b>	<b>30.64</b>	<b>14.53</b>	<b>18.59</b>	12.39
background#2, s6	<b>AVERAGE</b>	<b>30.37</b>	<b>13.07</b>	<b>19.76</b>	<b>34.56</b>	<b>12.18</b>	<b>18.95</b>	4.36
background#3, s4	<b>AVERAGE</b>	<b>40.68</b>	<b>12.80</b>	<b>22.60</b>	<b>36.28</b>	<b>13.18</b>	<b>20.78</b>	4.78
background#3, s5	<b>AVERAGE</b>	<b>20.36</b>	<b>9.72</b>	<b>18.88</b>	<b>33.16</b>	<b>13.57</b>	<b>19.57</b>	13.39
background#3, s6	<b>AVERAGE</b>	<b>45.34</b>	<b>17.46</b>	<b>27.17</b>	<b>39.69</b>	<b>16.32</b>	<b>23.40</b>	6.89

Table 14: Colour change ( $\Delta$  CMC) measurements of fumigated samples

<i>Exposure x 1</i>	<i>Exposure</i>	<i>Control</i>	<i>Exposure</i>	<i>Exposure</i>	<i>Control</i>	
	<i>x 10</i>	<i>(unexposed)</i>	<i>x 1</i>	<i>x 10</i>	<i>(unexposed)</i>	
E1S4	E2S4	E3S4	B1S4	B2S4	B3S4	
17.9	5.23	7.72	13.5	11.27	4.78	
E1S5	E2S5	E3S5	B1S5	B2S5	B3S5	With dust
7.6	3.27	7.62	2.85	12.39	13.39	
E1S6	E2S6	E3S6	B1S6	B2S6	B3S6	
6.13	20.14	5.75	6.43	4.35	6.89	

The averaged colour measurements are shown in Table 13 and the colour changes in Table 14. The overall values for colour change are higher than the field measurements for both the control and exposed samples, possibly indicating differences in the manner that the measurements were taken.

However, the comparison between the control samples and the exposed samples measured in the laboratory shows that the colour change values are within the same range for both groups. The samples that were exposed with dust did not show a significantly different colour change either. There was not a consistent increase in the colour change value with the exposure concentration increase from x1 to x10.

### 1.3 Results and Discussion

#### 1.3.1 Extreme pollutant exposure response colour measurements

The response of iron ore dust to extreme pollutant exposure was used to represent endpoints in any degradation process due to individual pollutants. It is important to understand this process for two main reasons: firstly to indicate the interaction between industrially generated dust and individual pollutants, and secondly as a predictor of how hematite on rock surfaces may eventually respond to highly concentrated individual pollutants.

#### *Experimental*

Samples of iron ore (which have been previously shown to be mineralogically similar to that of iron ore dust) were treated with pollutants and the effect on colour change was evaluated. Samples were exposed to water, concentrated solvent (benzene, toluene, xylene) or acid/base (1M nitric acid, concentrated nitric acid, 1M sulfuric acid, concentrated sulfuric acid, 1M ammonia and concentrated ammonia) individually in vials for 22 days, and then rinsed with water and

dried in ambient conditions. Mineralogy was characterised with powder XRD and colour change was measured. The same experiments were repeated with temperatures elevated to 50°C.

## Results/discussion

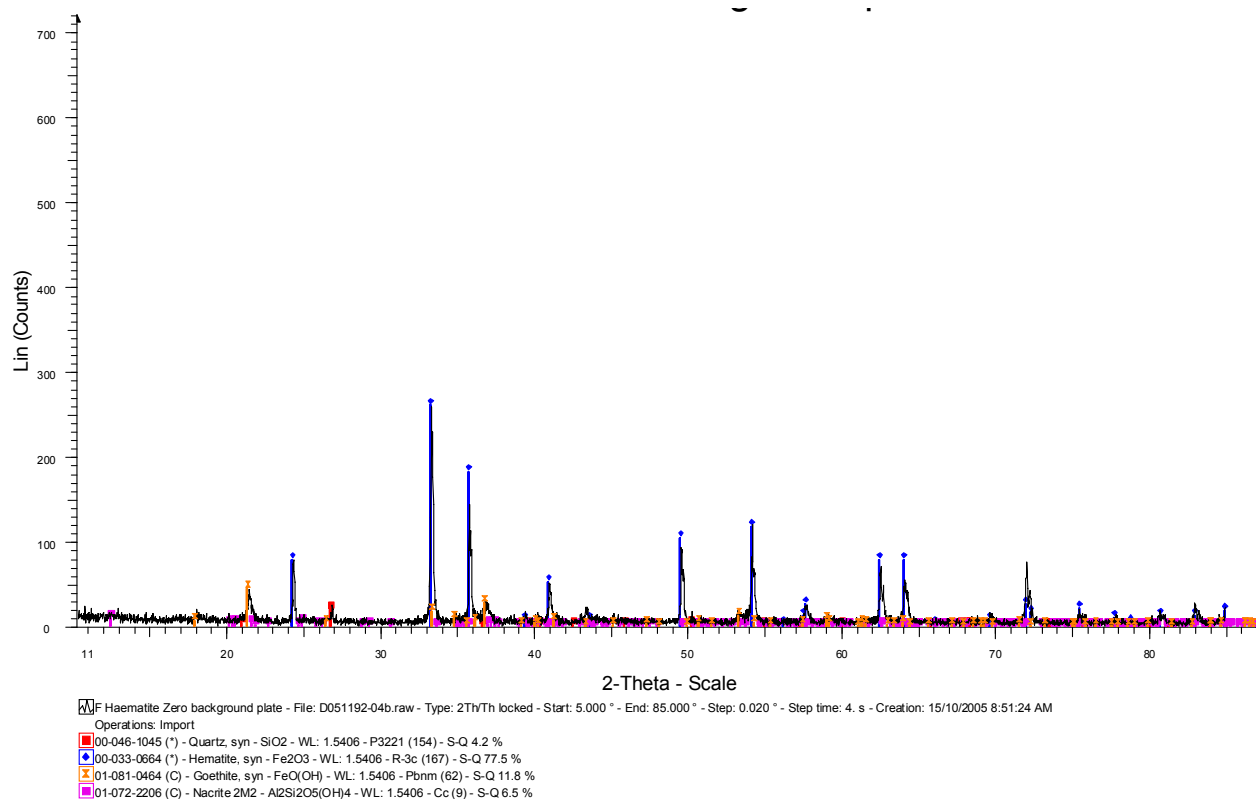


Figure 21: Iron ore XRD analysis.

Rietveld quantitative analysis of the XRD results gave

- 73% Hematite
- 20% Goethite
- 2% Quartz
- 5% Nacrite

Table 15: Colour measurements of pollutant-treated hematite (ambient conditions, 22 days)

Sample	Colour scale			Sample	Colour scale		
	L*	a*	b*		L*	a*	b*
Iron ore untreated	38.51	14.43	21.72	Benzene	40.48	13.96	21.19
Iron ore untreated	38.60	14.68	21.75	Benzene	40.46	13.65	21.50
Iron ore untreated	38.98	14.58	21.99	Benzene	40.93	13.91	21.35
Water	41.21	14.25	20.98	Benzene	41.07	13.75	21.68
Water	41.60	14.45	21.60	Toluene	41.24	13.70	21.34

Water	40.77	14.04	20.34	Toluene	41.16	13.71	21.42
Water	40.75	13.82	20.22	Toluene	41.29	13.78	21.51
1M HNO <sub>3</sub>	42.69	13.53	19.74	Toluene	41.48	13.77	21.68
1M HNO <sub>3</sub>	42.58	13.59	20.28	Xylene	42.58	14.44	22.49
1M HNO <sub>3</sub>	42.43	13.47	20.45	Xylene	42.58	14.44	22.49
Conc. HNO <sub>3</sub>	42.69	13.47	20.14	Xylene	42.19	14.60	22.23
Conc. HNO <sub>3</sub>	39.13	13.38	20.13	Xylene	42.26	14.57	22.40
Conc. HNO <sub>3</sub>	39.29	13.40	20.26	1M NH <sub>3</sub>	42.00	14.23	21.24
Conc. HNO <sub>3</sub>	39.29	13.50	20.15	1M NH <sub>3</sub>	42.36	14.20	21.24
Conc. HNO <sub>3</sub>	39.30	13.45	20.17	1M NH <sub>3</sub>	42.49	14.06	21.57
1M H <sub>2</sub> SO <sub>4</sub>	40.10	13.38	19.55	1M NH <sub>3</sub>	42.30	14.05	21.68
1M H <sub>2</sub> SO <sub>4</sub>	40.09	13.30	19.79	Conc. NH <sub>3</sub>	40.11	14.16	21.72
1M H <sub>2</sub> SO <sub>4</sub>	39.35	13.49	19.90	Conc. NH <sub>3</sub>	40.07	14.09	21.68
Conc. H <sub>2</sub> SO <sub>4</sub>	43.14	8.97	11.19	Conc. NH <sub>3</sub>	39.90	14.09	21.46
Conc. H <sub>2</sub> SO <sub>4</sub>	42.03	8.92	11.30	Conc. NH <sub>3</sub>	39.90	14.09	21.46
Conc. H <sub>2</sub> SO <sub>4</sub>	41.91	8.91	11.00				
Conc. H <sub>2</sub> SO <sub>4</sub>	41.37	8.89	11.53				

**Table 16: Pollutant treatment of iron ore**

Treatment	Mineralogical products
Iron ore untreated	Quartz, goethite, hematite, nacrite
Water	Unchanged
1M HNO <sub>3</sub>	Unchanged
Conc. HNO <sub>3</sub>	Unchanged
1M H <sub>2</sub> SO <sub>4</sub>	Quartz, goethite, hematite, nacrite, cordierite, rhomboclase
Conc. H <sub>2</sub> SO <sub>4</sub>	Rhomboclase
Benzene	Unchanged
Toluene	Unchanged
Xylene	Unchanged
1M NH <sub>3</sub>	Unchanged
Conc. NH <sub>3</sub>	Unchanged

Treatment with water did not produce a significant change in colour, nor did exposure to concentrated solvent (benzene, toluene, xylene) or acid/base (1M nitric acid, concentrated nitric acid, 1M sulfuric acid, 1M ammonia and concentrated ammonia at ambient conditions or at 50°C. However, treatment with concentrated sulfuric acid produced colour change after 22 days in ambient conditions (as shown in Table 5). Concentrated sulfuric acid at 50°C caused the material to harden and become white. It is interesting to note that concentrated nitric acid did not produce any observable colour change.

The set of samples elevated to 50°C were characterised using powder XRD. The samples exposed to water, ammonia or concentrated solvent (benzene, toluene, xylene) did not produce any mineralogical changes compared to the original ore. Most significantly, the sample exposed to concentrated sulfuric acid was digested almost completely to rhomboclase, a hydrated iron sulfate, with less change observed when exposed to 1M sulfuric acid.

## Part 2: Dust Deposition

---

### 2.1 Introduction

Petroglyphs on the Burrup Peninsula have been created through pecking, scraping or incising through the thin red–brown rock patina (<200 µm) to reveal contrasting colour from below the surface. The colour of rock patina is similar to and has been shown to contain hematite. Hematite exists in the local soil and in the iron ore being transported in the region, thereby representing an opportunity for airborne dust to be deposited on rock surfaces, potentially altering petroglyph images that are defined by the contrast between the rock engraving and background. This study is designed to monitor dust deposition on rock surfaces and investigate the chemistry and mineralogy of that deposition, in order to establish whether the source of depositing dust is from naturally occurring local dust or iron ore transportation.

In designing a way to measure deposited dust, methods that involved brushing or vacuuming rock surfaces *in situ* were discounted because the rock surface contains hematite, and the mineralogical composition resembles both iron ore dust and local soil. This dictated a method that would collect dust through direct deposition without contamination of the deposited material.

A number of standard techniques for dust collection exist, and these are classified as either *active* or *passive*. With active sampling, a known volume of air is pumped through a filter for a defined period of time. Passive sampling collects only the particulates that have fallen and settled on a known surface area over a defined period of time. The design for passive samplers is often based on a funnel-type collector that is washed into a bottle beneath for storage until collection at regular intervals. A modification of this is the ‘Frisbee’ collector, which collects deposited dust on a supported foam disc, designed to reduce loss which may occur when rain splashes dust in the collector. For both techniques, deposition rates are generally expressed as mg/m<sup>2</sup>/day.

Many international and Australian standard techniques employ these principles, and CMAR is using both active and passive techniques to measure dust deposition as part of the Burrup rock art monitoring project.

#### 2.1.1 Considerations for Particulate Deposition

There are many factors that affect the settling of airborne particulates on a surface – global weather patterns, local weather patterns, meso-scale structures of the scale of hills and rock piles on the Dampier Archipelago, in addition to microstructures such as surface topography and roughness. All these factors influence eddies and turbulence around a rock face and the substantially control the deposition process.

The interaction of a surface with its environment will define deposition and retention processes. Previous work has shown that particle size distribution of deposited particulates is influenced by surface roughness, and rougher surfaces inhibit the deposition of smaller particle fractions. Washing by rain and dew run-off can be expected to be dictated by microchannelling and micropooling on the surface. The composition of ongoing collective particulate deposit on rock surfaces in the region will therefore depend on the microtopography of Burrup rock surfaces.

Because the character of deposited particulates relies on the rock surface microtopography, the collector design used in this study emulates the rock surface structure. The simulated rock surfaces are then exposed in order to collect dust representative of that depositing on rock surfaces and petroglyphs on the Burrup Peninsula.

### 2.1.2 Rock Washing in the Field

During the August 2006 site visits, field measurements of rock washings were undertaken to investigate the current deposition of acidic gaseous species directly on the surface of rocks. The two Northern Sites (1 & 2) and a Southern Site (6) close to industry were measured.

The sampler was constructed by Atmospheric Research and comprised a silicone rubber washer at the base of an open base plastic container with internal diameter 50 mm. The open base was pressed up against suitable rock surfaces. 14 mL of deionised water was placed in the sampler and allowed to remain on the rock surface for 20 s. The water was withdrawn from the sampler and collected. A blank for each site was performed on a clean ceramic tile.

Nitrate and sulfate in the 12 solution samples were analysed as original by direct injection into an ion-chromatography system. There was not any pre-treatment such as neutralisation or dilution involved. There was neither nitrate nor sulfate found in any of the solutions (Table 17).

**Table 17: IC results of rock washings.**

	<b>NO<sub>3</sub><sup>-</sup></b>	<b>SO<sub>4</sub><sup>2-</sup></b>
	<b>(mg/L)</b>	<b>(mg/L)</b>
Site 1 Blank	<DL	<DL
Site 1 Rock Wash 1	<DL	<DL
Site 1 Rock Wash 2	<DL	<DL
Site 2 Blank	<DL	<DL
Site 2 Rock Wash 1	<DL	<DL
Site 2 Rock Wash 2,	<DL	<DL
Blank from tile site 6	<DL	<DL
Site 6 Rock Wash 1	<DL	<DL
Site 6 Rock Wash 2	<DL	<DL
Site 8 Blank	<DL	<DL
Site 8 Sample 1	<DL	<DL
Site 8 Sample 2	<DL	<DL
Detection Limit (DL)	0.3	0.5

## 2.2 Experimental Methodology

### 2.2.1 Tile Construction and Installation

Exposure conditions in the region are considered extreme, with cyclones and extended periods of heat above 40°C. The material that was to be used for synthetic rock surfaces must withstand these rigorous conditions, and also behave in some way like natural rock. Metallic surfaces were considered unsuitable as the thermal response at the interface was too dissimilar. Given the requirement for weatherability, the final decision was a polyurethane polymer with silica filler cast to a depth of 5–8 mm, mounted on an aluminium backing for strength. Prototypes were prepared and artificially aged in a weatherometer for two weeks to evaluate structural stability. This allowed for design modifications so that the resin did not delaminate from the aluminium base.

Representative rock surfaces were selected by Bill Carr, Technical Advisor to the Burrup Rock Art Monitoring Management Committee. A silicon moulding resin that can reproduce detail to 1 µm was applied to the rock surfaces over an area slightly larger than 100 × 150 mm. Polyurethane resin was cast into the moulds and a 100 × 150 × 3 mm aluminium support backing was applied. Cured tiles were removed from the moulds, trimmed and washed with soapy water, then rinsed with deionised water and stored with the surface protected until exposure at monitoring sites 1, 5 and 8 (listed in Table 18).

Table 18: Dust Collection Sites

Site	Site name	Coordinates (GDA 94, Zone 50)	
1	Dolphin Island	484,975	7,738,503
5	Burrup Rd	475,959	7,719,771
8	King Bay South	474,082	7,717,229



Figure 22: Exposure rack at Site 1.

## 2.3 Results and Discussion

### 2.3.1 Comparative Dust Analysis

Iron ore dust and local soil are identifiable through their XRD spectra. Iron ore and iron ore dust are predominantly hematite, with some goethite and traces of quartz and kaolinite. The major component of local soil is quartz, with a small amount of hematite and traces of albite, microcline, muscovite and kaolinite.

XRD is a technique of analysis that only identifies crystalline components in a sample, and amorphous or disordered compounds such as amorphous iron oxides or disordered clays may not be accounted for. However, in a diffraction pattern, the amount of amorphous or disordered material in a sample is indicated by an elevated baseline and peak broadening. These samples show no elevation of the baseline and peak shapes indicate there is little non-crystalline component. From this evidence, it appears this technique provides a good representation of the material component in the samples examined here.

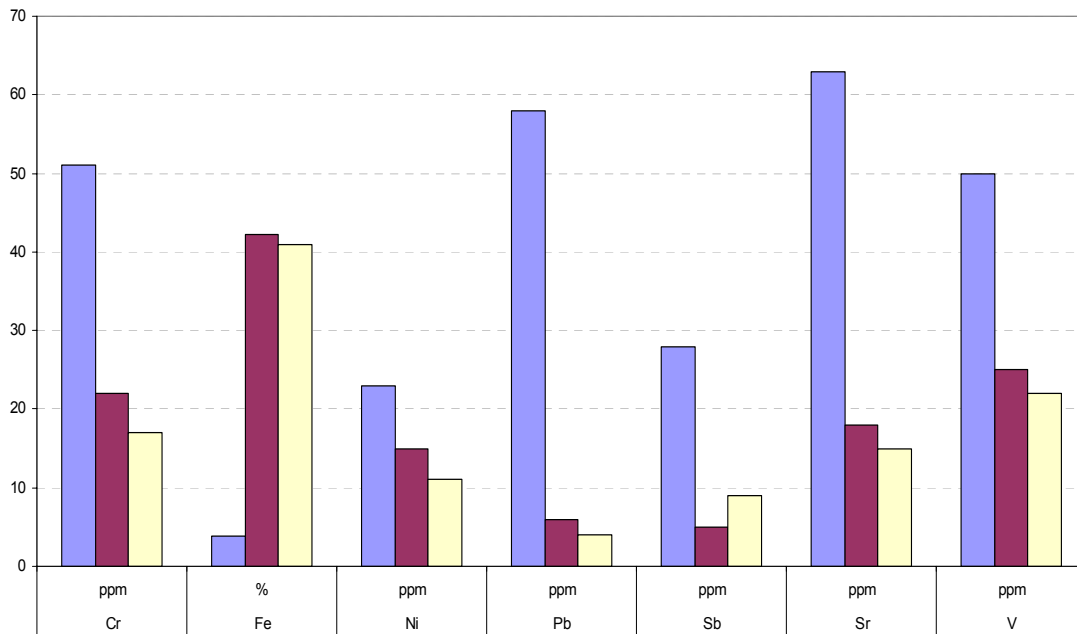
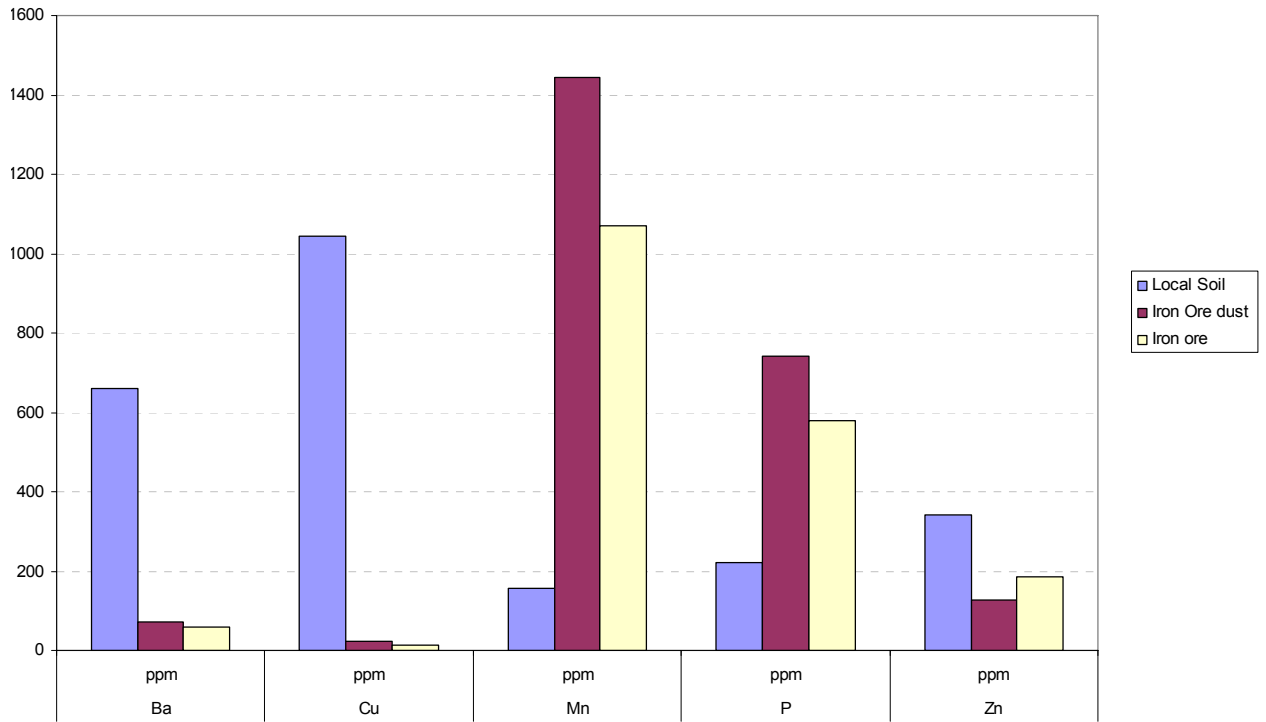
Both iron ore and local soil are dark red–brown in appearance, but are mineralogically dissimilar. This analysis shows a distinct difference in the mineral composition of the two alternative sources – iron ore and local soil. The iron ore is largely hematite with smaller quantities of other minerals. Local soil is largely quartz with much less hematite than iron ore.

### 2.3.2 Iron Ore Dust Elemental Composition

The elemental composition of dust is provided by ICP/AES. Consistent with the XRD analysis, iron is a major component of iron ore dust, accounting for 42.2% by weight of the sample (see below).

The elemental profiles of iron ore dust and iron ore are quite similar, and both are distinguishable from that of local soil. Most notable differences occur in the concentrations of Ba, Cu, Mn, P, Cr, Fe, Pb, Sb, Sr, V, K, Na and Ti.

<b>Analyte</b>	<b>Ag</b>	<b>Al</b>	<b>As</b>	<b>Ba</b>	<b>Be</b>	<b>Bi</b>	<b>Ca</b>	<b>Cd</b>	<b>Co</b>	<b>Cr</b>	<b>Cu</b>	<b>Fe</b>	<b>K</b>	<b>Mg</b>
Units	ppm	%	ppm	ppm	ppm	ppm	%	ppm	ppm	ppm	ppm	%	%	%
Local soil	<0.5	4.46	7	660	0.7	<2	0.51	<0.5	8	51	1045	3.80	2.74	0.30
Iron ore dust	<0.5	1.34	12	70	1.2	5	0.07	<0.5	<1	22	24	42.2	0.03	0.07
Iron ore	<0.5	0.92	7	60	0.9	4	0.11	<0.5	<1	17	13	40.9	0.03	0.06
<b>Analyte</b>	<b>Mn</b>	<b>Mo</b>	<b>Na</b>	<b>Ni</b>	<b>P</b>	<b>Pb</b>	<b>S</b>	<b>Sb</b>	<b>Sr</b>	<b>Ti</b>	<b>V</b>	<b>W</b>	<b>Zn</b>	
Units	ppm	ppm	%	ppm	ppm	ppm	%	ppm	ppm	%	ppm	ppm	ppm	
Local soil	156	<1	0.81	23	220	58	0.02	28	63	0.36	50	<10	340	
Iron ore dust	1445	1	0.05	15	740	6	0.03	<5	18	0.05	25	<10	127	
Iron ore	1070	1	0.09	11	580	4	0.04	9	15	0.04	22	10	186	



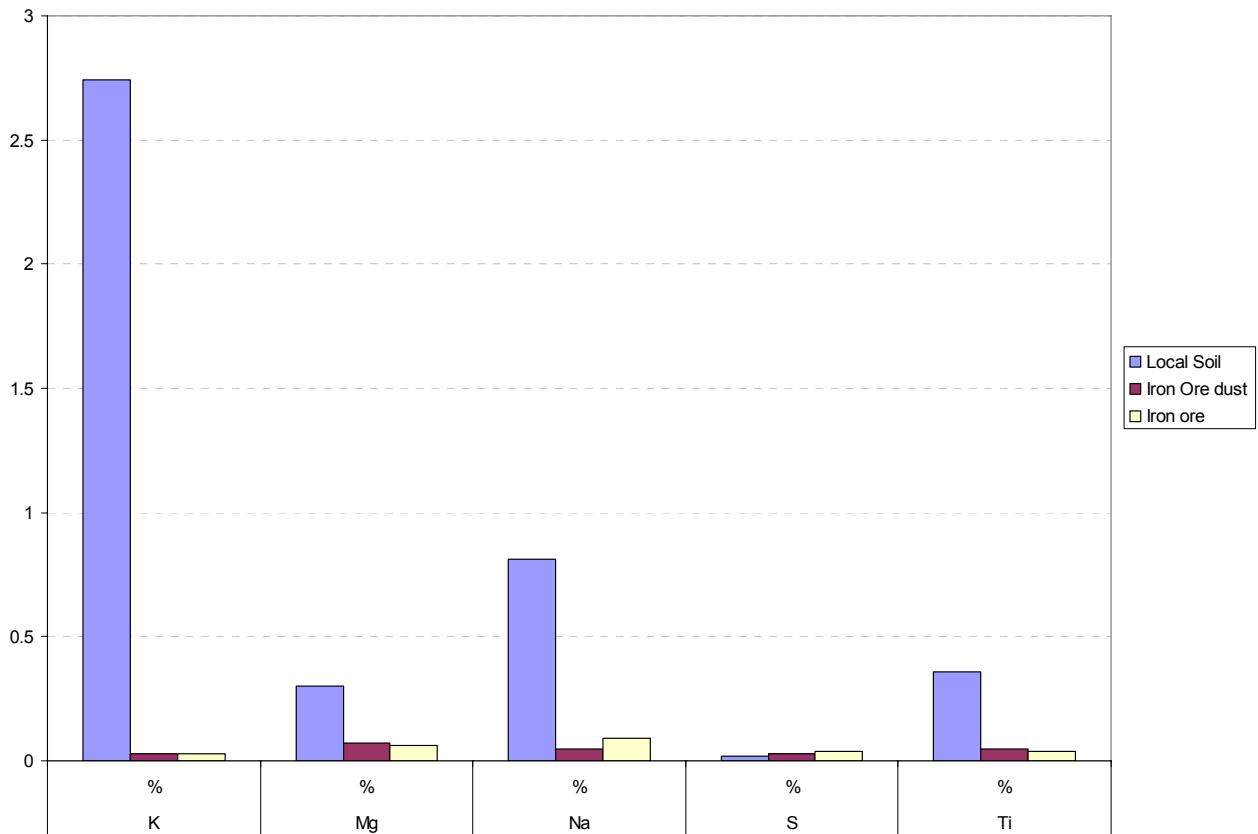


**Figure 23: Compositional differences in local soil, iron ore dust and iron ore.**

### 2.3.3 Dust Collection

The first tile exposure period was for three months from August 2004. Unfortunately, an insufficient quantity of dust was collected to allow a comparative diagnosis of the particulate deposit. A small amount of dust was visually discernible in the deepest depressions of tiles from Site 5. Less was evident in tiles from Site 8. Virtually no dust was evident on tiles from Site 1. These results are consistent with dust deposition rate measurements being performed by CMAR.

Results from micro-XRD performed on the small grains evident on the tiles indicate hematite. Quartz in the diffraction patterns, as shown in Figure 24, are from the silica filler used in the polyurethane.

**Figure 24: Image of dust on synthetic rock tile.**

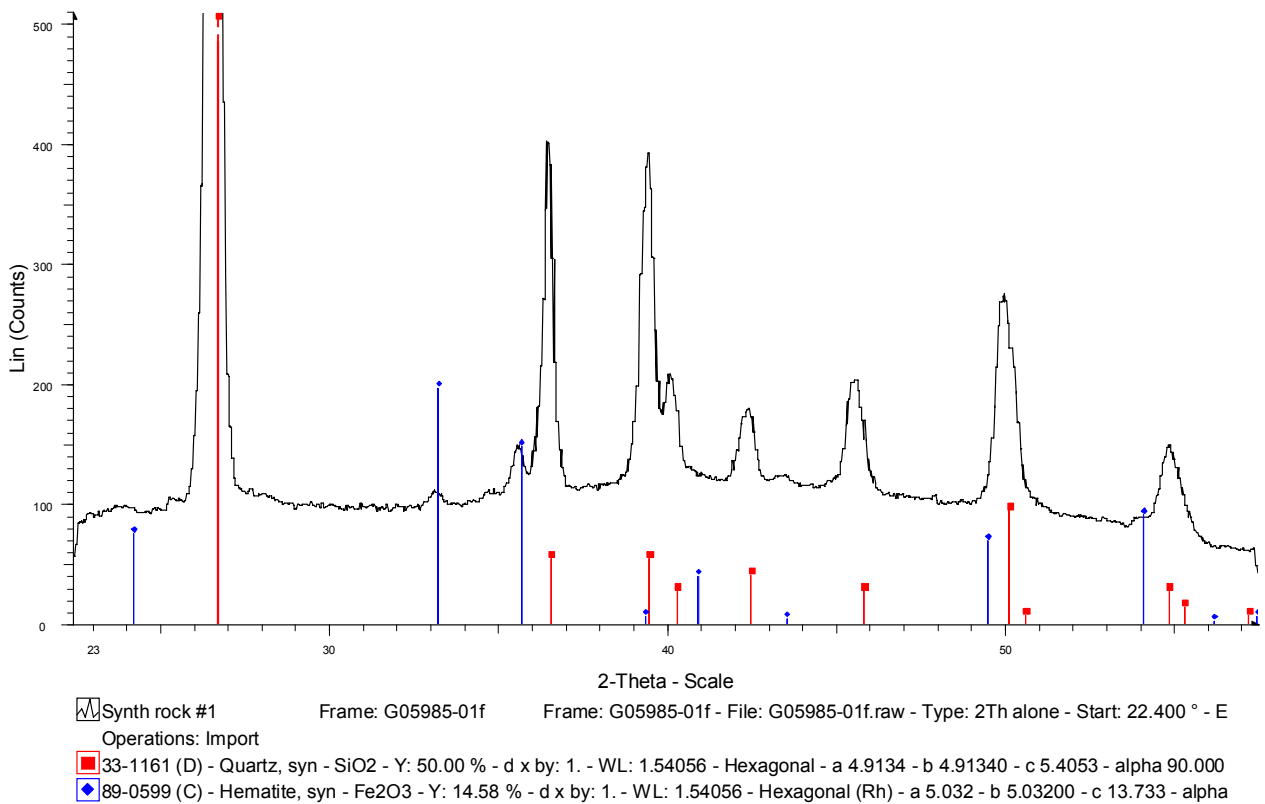
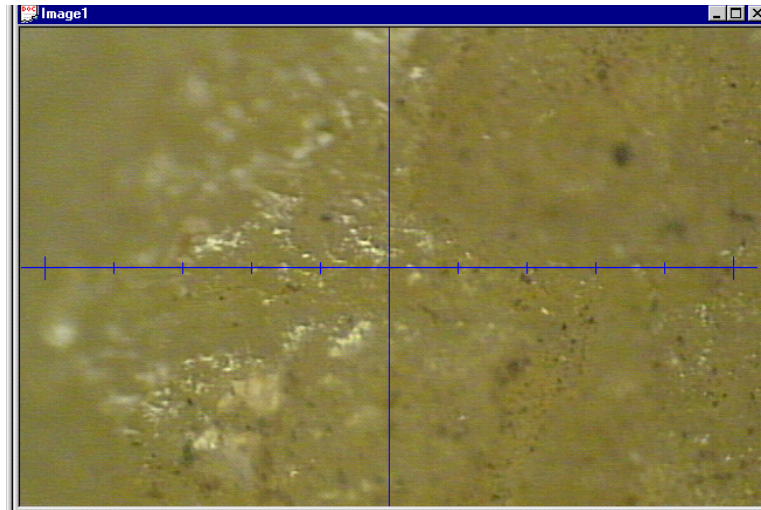


**Figure 25: Micro-XRD trace of dust in situ on synthetic rock tile. The quartz detected is from the tile filler.**

Considering the negligible amounts of dust collected on the tiles, a decision was made to expose tiles for periods of six months in an attempt to improve the amount collected. This did not produce any observable effect. A combination of wind and/or washing from rain on the exposed tile surfaces removes any substantial build-up of deposited material.

In order to collect sufficient material to characterise, a modified approach was employed. Dust was collected from the protected interleaved horizontal surfaces of the RH and temperature logger housing (Figure 26) at the nominated sites. Dust was collected in this manner from the three sites (two southern and one northern) and characterised with powder XRD (Figure 27, Figure 28 and Figure 29).

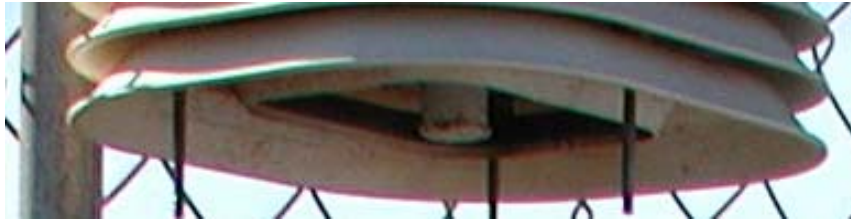


Figure 26: Dust deposited on datalogger housing.

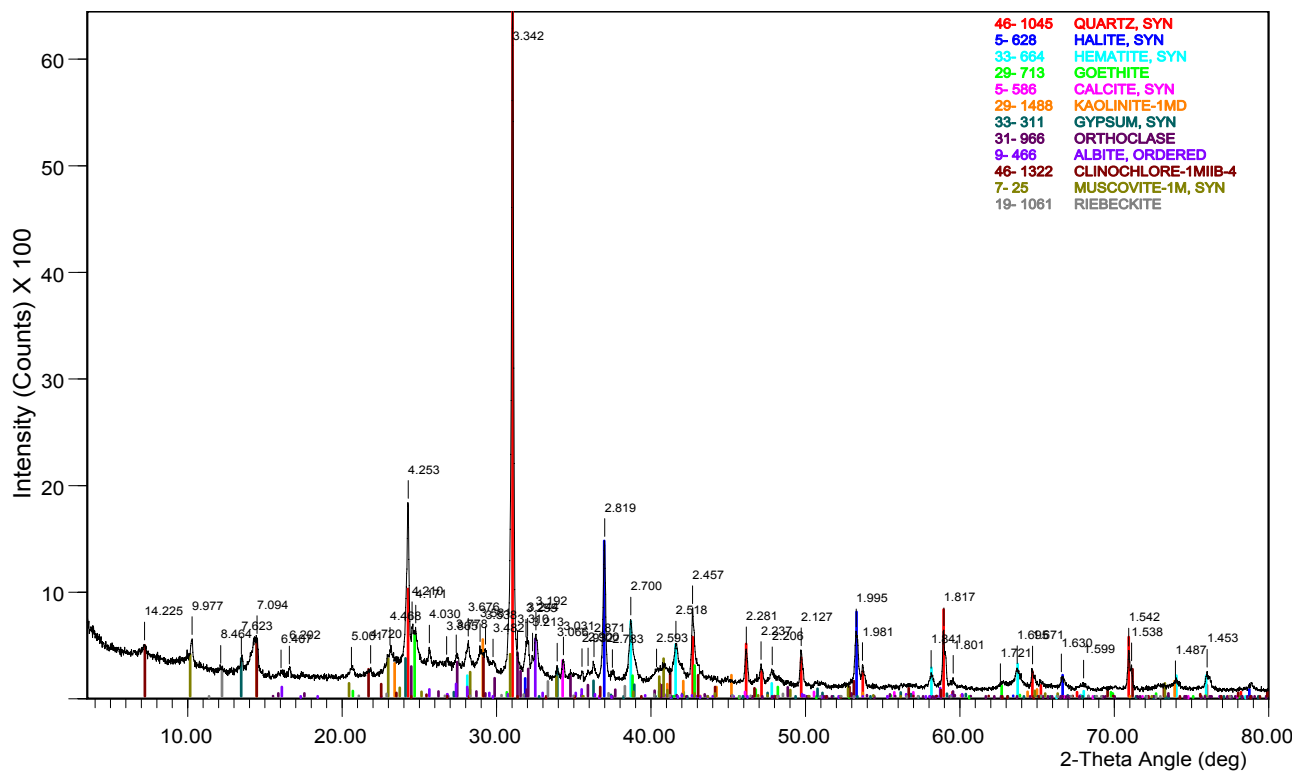


Figure 27: XRD trace of surface dust from Site 1.

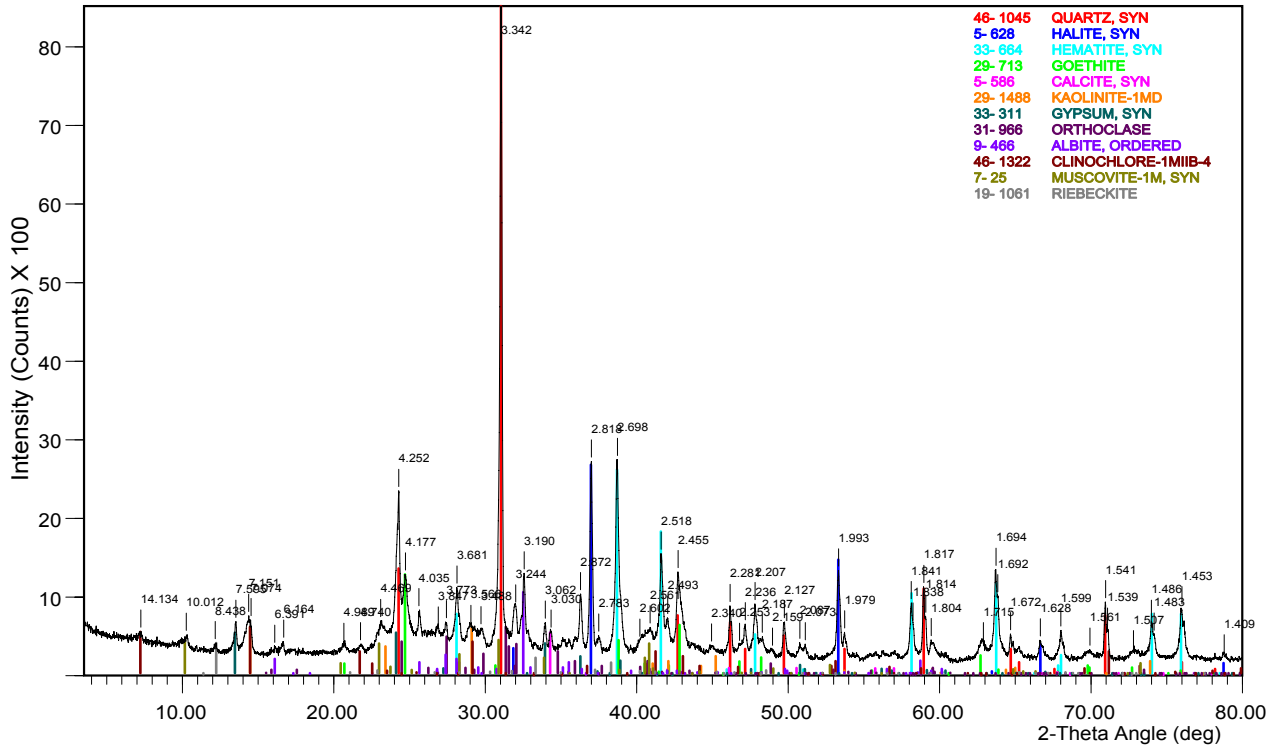


Figure 28: XRD trace of surface dust from Site 5.

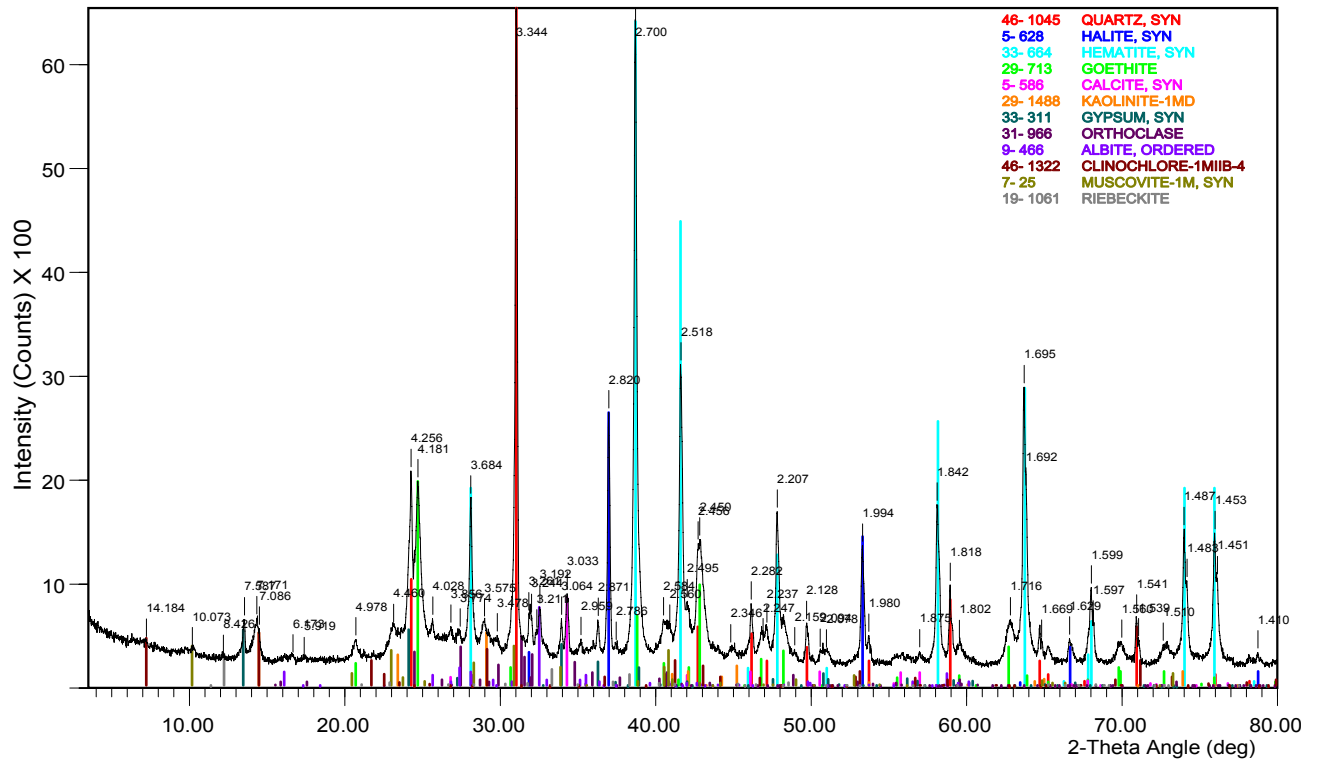


Figure 29: XRD trace of surface dust from Site 8.

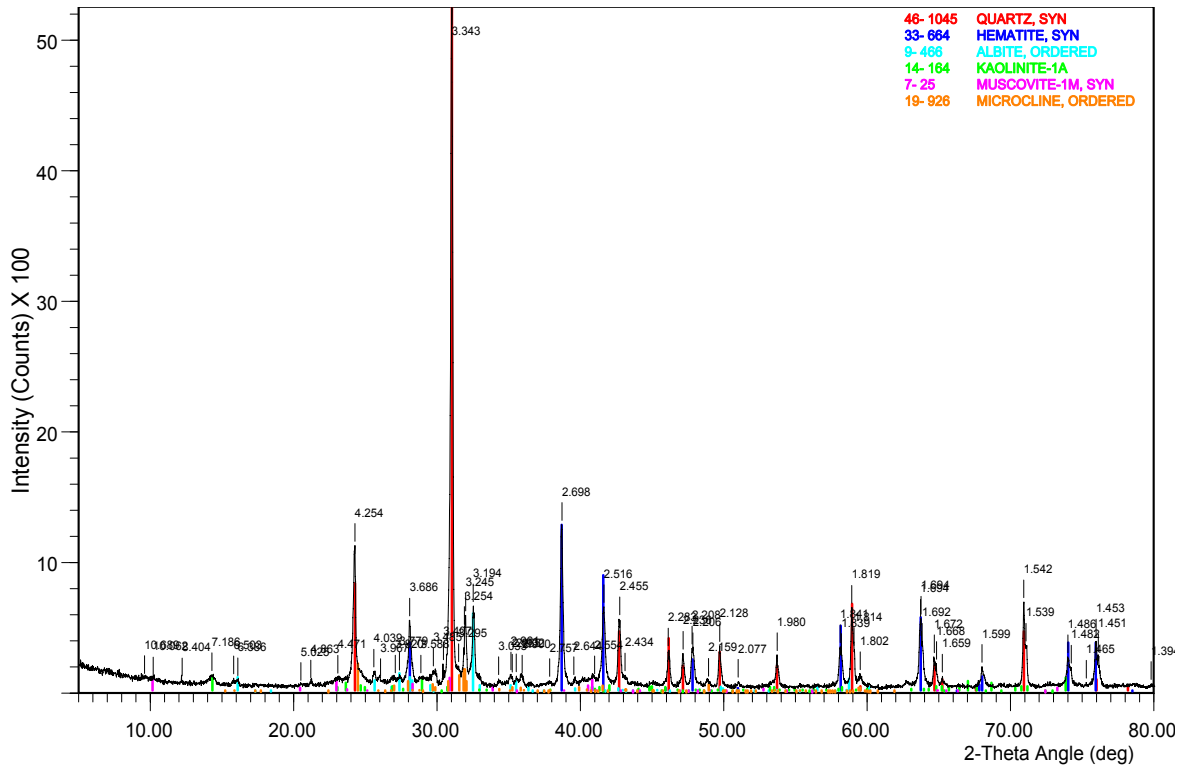


Figure 30: XRD trace of local soil sample.

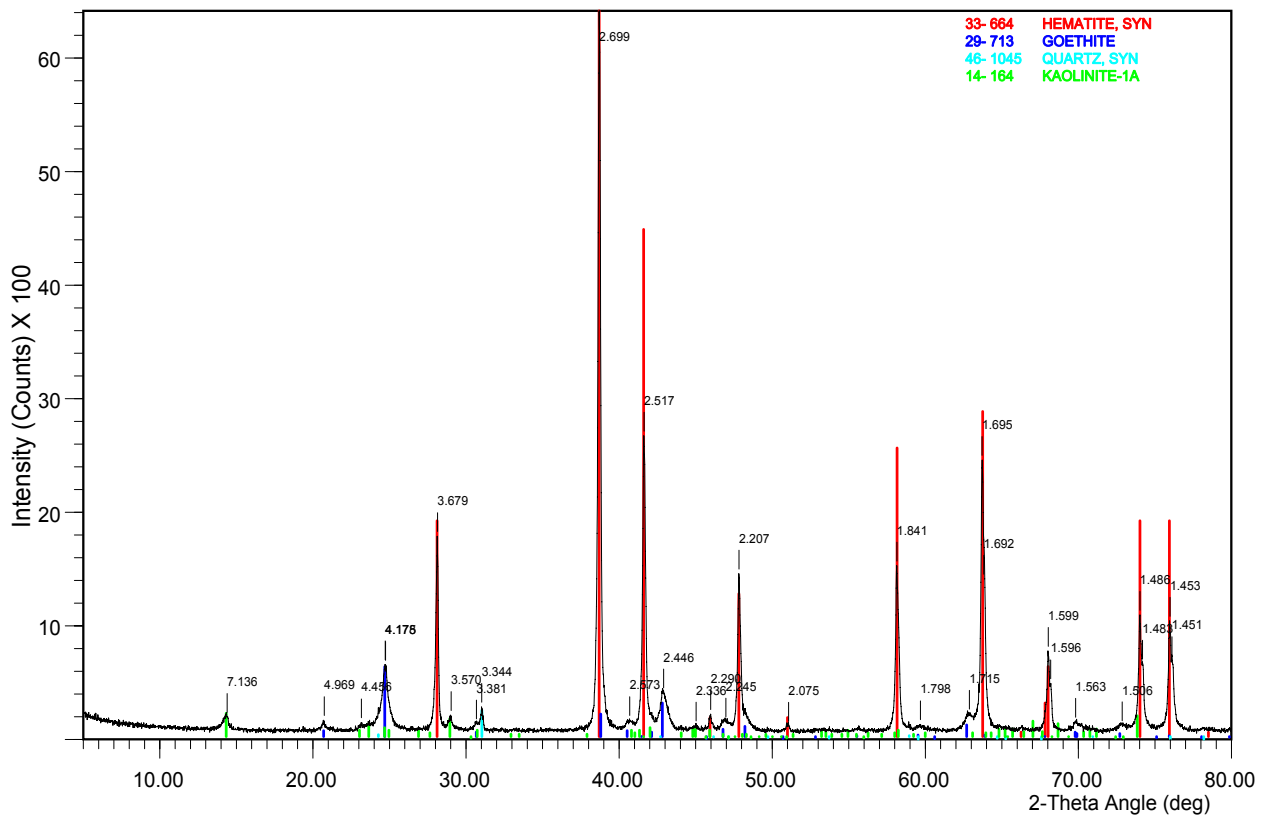


Figure 31: XRD trace of iron ore sample.

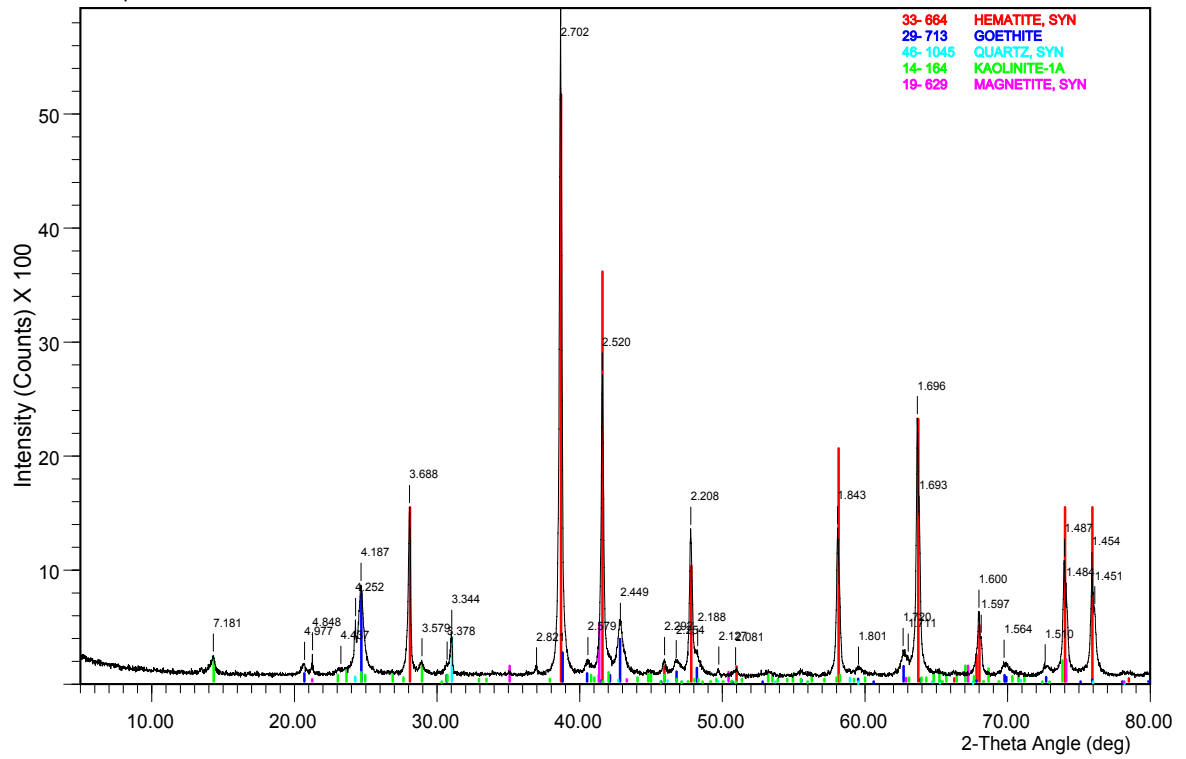


Figure 32: XRD trace of iron ore dust sample.



Table 19: Tiles after exposure (12 months) Site 1; Dolphin Island.



**Figure 33: Tiles after exposure (12 months) Site 5; Burrup Rd.**



**Figure 34: Tiles after exposure (12 months) Site 8; King Bay South.**

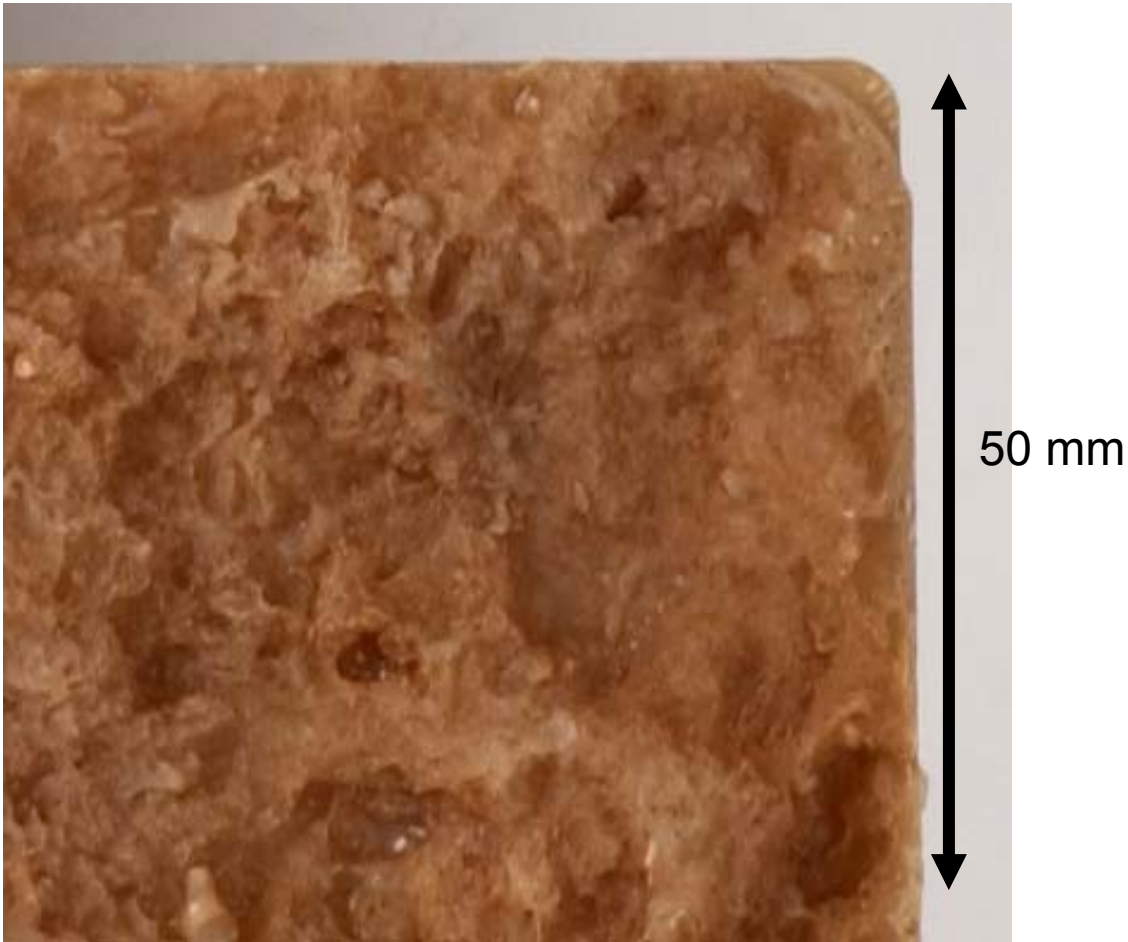


Figure 35: Magnified area of extremely rough tile surface showing deposition only in the deepest crevices.

## ***2.4 Results and Discussion***

Tiles for the second collection period were exposed for 12 months and did not accumulate any more dust than for the 3 month exposure period. From this it can be assumed that a steady state of accumulation and removal is achieved.

Dust accumulates differentially, dependent on the surface roughness. It was observed that in areas of surface roughness average 2 mm and below, no dust accumulated. Dust only lodged in the deepest crevices of the roughest tile, and not more than a few micrograms were detected.

A clear correlation exists between the location of the site and the composition of deposited dust. From characterisation of the iron ore dust, we know it is primarily comprised of hematite and lesser amounts of goethite. Local soil is primarily quartz with a lesser quantity of hematite.

Deposited dust at Sites 5 and 8 (southern sites) has quartz, NaCl (sea salt), hematite and goethite predominating. For Site 1 (northern site), there is much less hematite evident and the predominant depositing species are quartz and sea salt.

From the knowledge that iron ore dust is produced as particulate aerosols in the region and is predominantly hematite, the findings suggest the dust deposited at Sites 5 and 8 is principally from iron ore. We were unable to characterise the composition of the hematite in order to ascribe

a source of its origin on the basis of the hematite chemistry due to the limited amount of sample material collected.

Because of its remote location and choice as a control site, the dust collected on surfaces at Site 1 is believed to originate from natural sources. Quartz is the major component of the local soil and is found in the greatest quantity on the surfaces, and aerosol sea salt is the source of halite.

From these observations, it is shown that the character of the dust depositing at the southern sites close to industrial activity is different from the dust naturally deposited on northern control sites.

## Part 3: Colour Measurement

---

### 3.1 Introduction

In response to tender number 34DIR0603 issued by WA DoIR, CMMT have been engaged in measuring the colour of selected petroglyphs on the Burrup Peninsula over a period of four years. The requirements stipulated by the project are the measurement of relocatable sample points on petroglyphs annually for the measurement period.

An alternative technique for in situ monitoring of degradative change through colour measurement has been reported by Mirmehdi *et al.* [9], who undertook a pilot study designed for monitoring and modelling the deterioration of paint residues in a cave environment through digital image comparisons with a reference image. The template-matching technique was considered unsuitable and impractical for the Burrup study because:

- (a) Template matching, as described by Mirmehdi *et al.*, would require the collection of digital images with repeatable and controlled spectral illumination, angle of incidence and collection. Burrup petroglyphs are located in remote, exposed locations, and it would not be possible to control the colour temperature and angle of the ambient lighting easily without blocking all the ambient daylight, or collecting images in the night with the ambient moon and starlight removed.
- (b) The effect of metamerism in relation to the reference template and rock surface has not been accounted for. It is well known that surfaces appearing similar in colour under one set of illumination conditions can appear dramatically different with another spectral illuminant or angle of incidence. The reference template is a glossy (laminated) smooth surface, while the rocks in this study are significantly rougher.

Portable, hand-held spectrophotometry was identified as a suitable technique. It has been recognised as a repeatable way of recording colour in units of standard CIE chromaticity coordinates, in many contexts including archaeological situations [10]. CIE chromaticity coordinates are an internationally recognised numerical system of permanently and objectively describing the colour of a surface or material as a point in three-dimensional L\*a\*b\* colour space, identifying a tristimulus value (L\*a\*b\*) for each sample point.

### 3.2 Experimental Methodology

#### 3.2.1 Measurement Principles

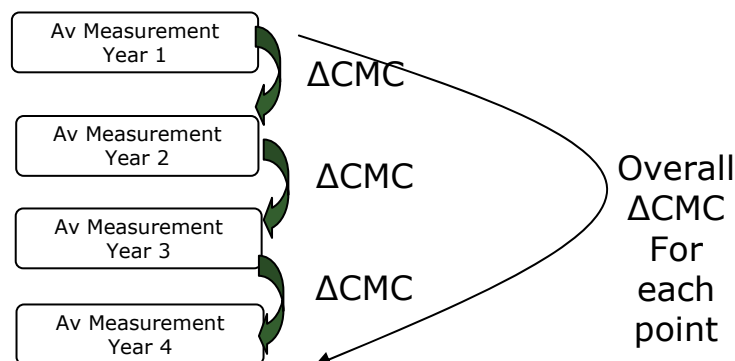
The difference between two colours measured instrumentally is  $\Delta E$ . It derives from the German word for sensation – *Empfindung* – which means a difference in sensation. A  $\Delta E$  value of zero represents an exact match. It is the standard CIE colour difference method, and measures the distance between the two colours, calculated in 3D L\*a\*b\* colour space. In this way, colour difference can be evaluated through measuring the tristimulus values of points over time, and calculating to evaluate the colour difference with time.

This means the colour contrast between the engraving and rock surface can be monitored to evaluate whether it is decreasing.

The difference between two colours,  $\Delta E$ , can be evaluated using the 1976 CIE colour difference formula [11]. In CIE  $L^*a^*b^*$  space, the difference is:

$$\Delta E^*_{ab} = [(\Delta L^*)^2 + (\Delta a^*)^2 + (\Delta b^*)^2]^{0.5}$$

This will be used to evaluate colour change of single points between the four consecutive years over which the monitoring will occur.



The instrument used for colour measurement is a portable spectrophotometer (BYK Gardner<sup>2</sup>) with inbuilt spectral illuminants: CIE illuminant A, D65 and F2 (see Figure 32 and Table 8). A CIE standard illuminant represents an aimed spectral power distribution of a theoretical real light source. For example, CIE illuminant A is a mathematical representation of tungsten halogen (incandescent), and CIE illuminant D65 is a mathematical representation of a phase of daylight, recommended by the CIE if daylight is of interest. F illuminants are similar to fluorescent light sources.



**Figure 36: Portable spectrophotometer used for colour measurements.**

It is essential to use an artificial light source for reproducibility and determination of colour change, as the fluctuations in the natural daylight spectrum due to time of day, season and weather, means naturally illuminated measurements would be inconsistent and unreliable.

The geometry of the measuring head on the measuring device is designed to exclude light on flat surfaces. As rock surfaces are not always flat, a collar of black fabric was used when necessary for the complete exclusion of natural light.

<sup>2</sup> Spectrophotometer website: <http://www.bykgardner.com/englisch/products.php?lv3=2>.

**Table 20: Portable spectrophotometer specifications**

<u>Repeatability</u>	<u>Inter-Instrument Agreement</u>	<u>Color System</u>	<u>Color Differences</u>	<u>Indices</u>	<u>Spectral Interval</u>
0.01 $\Delta E$ , $1\sigma$	0.02 $\Delta E$ , $1\sigma$	CIE Lab/Ch; Lab(h); XYZ; Yxy; RxRyRz	$\Delta E$ ; $\Delta E(h)$ ; $\Delta$ E <sub>FMC2</sub> ; $\Delta E_{94}$ ; $\Delta$ E <sub>CMC</sub> ; Component differences	YIE313; YID1925; WIE313; CIE; Berger; Color strength; Opacity; Metamerism	20 nm
<u>Observer</u>	<u>Language</u>	<u>Power Supply</u>	<u>Operating Temperature</u>	<u>Illuminants</u>	<u>Spectral Range</u>
2°; 10°	English; German; French; Italian; Spanish; Japanese	4 AA alkaline; NiCd or MH	50 to -110 °F (10 to -42 °C)	A; C; D50; D55; D65; F2; F6; F7; F8; F10; F11	400 - 700 nm
<u>Geometry</u>	<u>Aperture</u>	<u>Humidity</u>			
45/0	4 mm	< 85% relative humidity, non- condensing / 35 °C (95 °F)			

### 3.2.2 Sampling Protocol

Monitoring site locations were determined by the Rock Art Monitoring Management Committee, and the final decision for a representative petroglyph at each site was determined in consultation with the Committee’s Technical Advisor and nominated representatives from the local indigenous communities. Petroglyphs at each site were firstly evaluated for their suitability for scientific study, in order to respect the cultural laws of the traditional owners for the entitlement of access. The second consideration from a scientific perspective was aspect, including elevation and direction of exposure.

**Table 21. Details of the sites for colour and spectral mineralogy measurements (Site 3 is not included in this study)**

<u>Site</u>	<u>Site name</u>	<u>Coordinates (GDA 94, Zone 50)</u>	
1	Dolphin Island	484,975	7,738,503
2	Gidley Island	482,166	7,740,857
4	Woodside	477,398	7,721,980
5	Burrup Rd	475,959	7,719,771
6	Water Tanks	477,698	7,720,137
7	Deep Gorge	477,956	7,717,987
8	King Bay South	474,082	7,717,229

Each site contains one or more petroglyphs. Petroglyphs were measured at six sampling points. Each sampling point gave a measurement based on an average of a minimum of seven readings. For each sampling point in a petroglyph, the adjacent rock surface (which provides the visual contrast of the petroglyph image) was measured in the same way.

Measurements were taken from areas defined as ‘background’ or ‘engraving’. Background refers to the rock surface area unmarked by the petroglyph. Engraving refers to the area defined by sgraffito lines or pecking marks, constituting the image. The sampling area was defined as having

relatively uniform colour at that point over an area of a minimum of 20 mm, so that comparative measurements could be made with fibre optic reflectance spectroscopy, performed concurrently by CEM.

### ***3.3 Results and Discussion***

The following pages illustrate the sampling points for the engraved and background spots on each petroglyph for each site, and the measurements collected from that point in the first year.

The original intention was to take an average of seven colour measurements ( $L^*a^*b^*$ ) from each sample point. When in the field, it became apparent that additional measurements would be useful to statistically evaluate the variability of measurements, so for many sample points there are more than one set of average measurements.

In the second year of colour measurements, 21 independent measurements were taken from each sample point (3 times the originally intended 7 measurements), to reduce sample variance introduced by surface inhomogeneity or roughness, and systematic error. For clarity, the raw data has not been included here, but averages of the data are presented with the colour difference measurements calculated with 2 accepted CIE standard methods –  $\Delta E$  and  $\Delta CMC$ .

## Site 1: Dolphin Island



Sample	Colour scale			Colour difference* ΔE
	L*	a*	b*	
Site 1 Spot 1 Engraved				
AVERAGE 2006	16.791	3.833	11.593	3.040
AVERAGE 2005	14.970	6.081	12.525	2.155
AVERAGE 2004	14.315	8.080	12.995	
Site 1 Spot 1 Background				
AVERAGE 2006	28.969	10.287	10.332	1.842
AVERAGE 2005	27.662	11.255	11.196	2.243
AVERAGE 2004	29.867	11.200	10.787	
Site 1 Spot 2 Engraved				
AVERAGE 2006	8.372	8.216	9.257	1.838
AVERAGE 2005	7.911	9.837	9.991	0.690
AVERAGE 2004	8.427	9.620	9.587	
Site 1 Spot 2 Background				
AVERAGE 2006	28.819	10.210	11.064	7.881
AVERAGE 2005	20.984	9.460	11.461	6.744
AVERAGE 2004	27.657	10.350	11.870	
Site 1 Spot 3 Engraved				
AVERAGE 2006	23.218	10.682	16.272	3.159
AVERAGE 2005	25.669	12.246	17.506	3.024
AVERAGE 2004	28.672	12.117	17.175	
Site 1 Spot 3 Background				
AVERAGE 2006	13.069	7.302	9.247	2.429
AVERAGE 2005	11.449	8.754	10.328	2.437
AVERAGE 2004	13.417	7.983	9.113	

## Site 2: Gidley Island



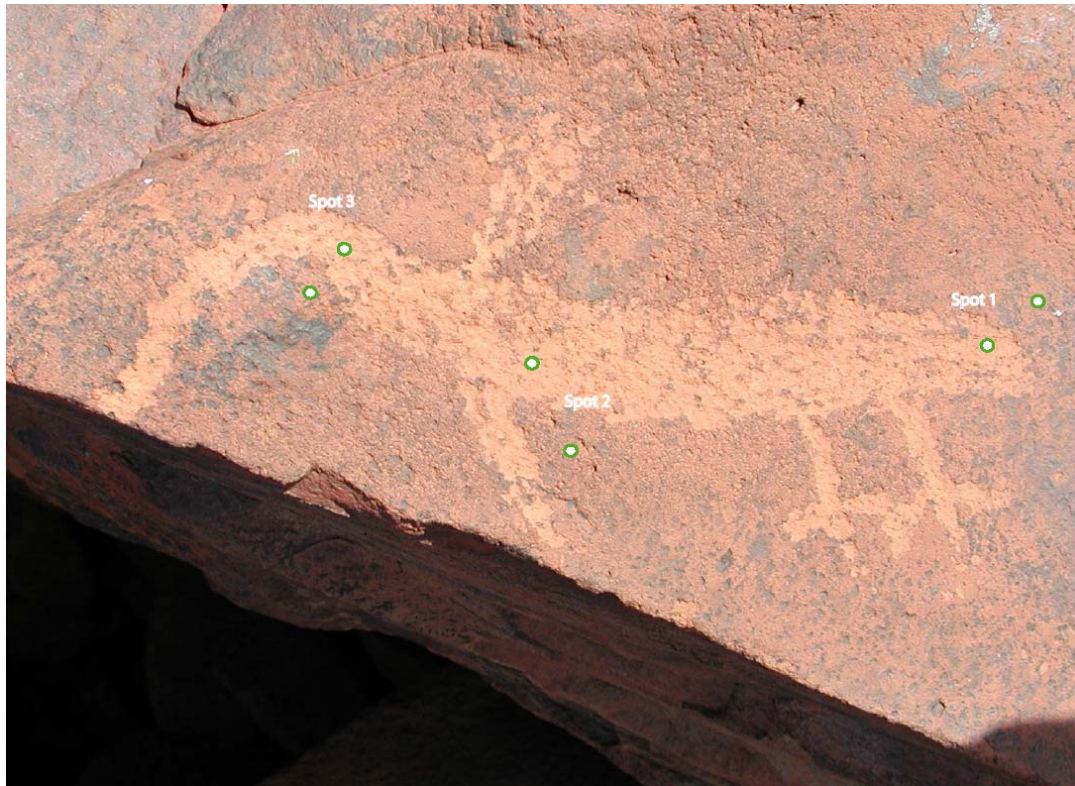
Sample	Colour scale			Colour difference*
	L*	a*	b*	$\Delta E$
Site 2 Spot 1 Engraved				
AVERAGE 2006	34.104	7.790	17.069	1.620
AVERAGE 2005	33.581	9.261	17.502	2.292
AVERAGE 2004	31.900	8.957	15.975	
Site 2 Spot 1 Background				
AVERAGE 2006	26.536	9.159	11.817	2.138
AVERAGE 2005	27.010	9.883	13.772	4.626
AVERAGE 2004	22.505	9.000	13.197	
Site 2 Spot 2 Engraved				
AVERAGE 2006	34.100	9.113	19.374	1.724
AVERAGE 2005	34.018	10.670	20.110	3.302
AVERAGE 2004	31.013	10.153	18.840	
Site 2 Spot 2 Background				
AVERAGE 2006	26.990	11.490	11.491	2.086
AVERAGE 2005	26.424	12.705	13.089	2.889
AVERAGE 2004	25.803	10.770	11.037	
Site 2 Spot 3 Engraved				
AVERAGE 2006	33.042	10.817	20.022	0.824
AVERAGE 2005	33.224	10.556	19.262	5.569
AVERAGE 2004	27.683	10.563	18.697	
Site 2 Spot 3 Background				
AVERAGE 2006	15.815	10.243	14.722	6.402
AVERAGE 2005	21.395	12.573	16.824	2.678
AVERAGE 2004	18.823	12.247	16.153	

## Site 4: Woodside



Sample	Colour scale			Colour difference*
	L*	a*	b*	$\Delta E$
Site 4 Spot 1 Engraving				
AVERAGE 2006	25.363	13.070	17.961	2.44
AVERAGE 2005	23.266	14.259	18.341	1.17
AVERAGE 2004	22.717	13.835	17.400	
Site 4 Spot 1 Background				
AVERAGE 2006	20.706	11.129	13.876	2.03
AVERAGE 2005	19.219	12.502	14.019	1.12
AVERAGE 2004	20.102	12.057	13.498	
Site 4 Spot 2 Engraving				
AVERAGE 2006	14.474	10.110	13.720	2.25
AVERAGE 2005	14.546	11.918	15.053	1.26
AVERAGE 2004	14.560	10.857	14.375	
Site 4 Spot 2 Background				
AVERAGE 2006	27.783	13.465	15.515	1.65
AVERAGE 2005	26.268	13.657	16.129	0.35
AVERAGE 2004	26.523	13.902	16.106	
Site 4 Spot 3 Engraving				
AVERAGE 2006	24.307	12.431	18.130	2.61
AVERAGE 2005	23.421	14.489	19.478	1.83
AVERAGE 2004	22.407	13.675	18.185	
Site 4 Spot 3 Background				
AVERAGE 2006	28.758	13.100	14.793	4.00
AVERAGE 2005	25.298	13.833	16.654	1.99
AVERAGE 2004	26.325	13.300	15.035	

## Site 5: Burrup Rd



Sample	Colour scale			Colour difference*
	L*	a*	b*	ΔE
Site 5 Spot 1 Engraving				
AVERAGE 2006	21.817	13.581	19.187	2.327
AVERAGE 2005	22.227	15.496	20.444	4.383
AVERAGE 2004	18.897	14.243	17.883	
Site 5 Spot 1 Background				
AVERAGE 2006	29.526	10.882	12.221	6.280
AVERAGE 2005	27.381	14.453	16.920	5.132
AVERAGE 2004	22.937	12.893	14.883	
Site 5 Spot 2 Engraving				
AVERAGE 2006	27.517	16.197	21.235	4.858
AVERAGE 2005	22.761	16.798	22.020	1.682
AVERAGE 2004	22.987	16.777	20.353	
Site 5 Spot 2 Background				
AVERAGE 2006	27.191	13.759	15.230	3.609
AVERAGE 2005	29.526	15.277	17.526	
AVERAGE 2004	No 2004 measurements			
Site 5 Spot 3 Engraving				
AVERAGE 2006	35.584	17.401	23.667	7.253
AVERAGE 2005	28.452	17.505	22.352	9.243
AVERAGE 2004	36.880	20.007	25.207	
Site 5 Spot 3 Background				
AVERAGE 2006	32.635	13.272	14.071	6.717
AVERAGE 2005	26.136	14.016	15.598	1.000
AVERAGE 2004	25.305	13.748	15.110	

## Site 6: Water Tanks



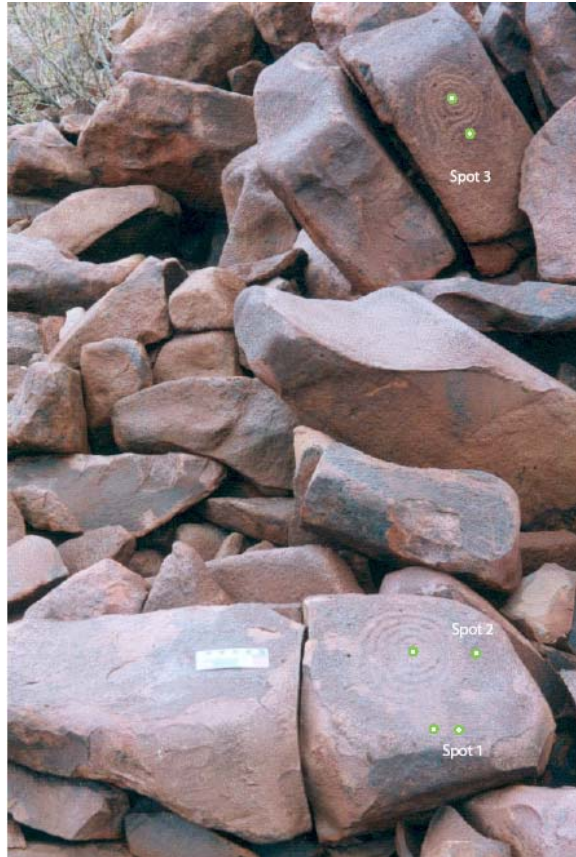
Sample	Colour scale			Colour difference*
	L*	a*	b*	$\Delta E$
Site 6 Spot 1 Engraving				
AVERAGE 2006	36.833	11.279	17.686	1.281
AVERAGE 2005	35.712	11.564	18.236	5.557
AVERAGE 2004	30.200	12.270	18.250	
Site 6 Spot 1 Background				
AVERAGE 2006	36.891	13.761	18.506	3.020
AVERAGE 2005	34.044	12.800	18.204	2.852
AVERAGE 2004	36.865	13.220	18.245	
Site 6 Spot 2 Engraving				
AVERAGE 2006	33.471	11.103	16.806	2.282
AVERAGE 2005	31.249	11.241	17.305	2.534
AVERAGE 2004	33.733	11.010	16.867	
Site 6 Spot 2 Background				
AVERAGE 2006	35.899	11.981	15.826	1.085
AVERAGE 2005	34.858	11.901	16.122	1.724
AVERAGE 2004	35.273	13.077	17.313	
Site 6 Spot 3 Engraving				
AVERAGE 2006	33.494	10.260	15.616	2.564
AVERAGE 2005	34.969	11.453	17.340	1.536
AVERAGE 2004	36.387	11.087	16.877	
Site 6 Spot 3 Background				
AVERAGE 2006	36.029	11.186	15.506	3.311
AVERAGE 2005	35.594	13.396	17.932	1.455
AVERAGE 2004	36.883	12.767	17.693	

## Site 7: Deep Gorge



Sample	Colour scale			Colour difference*
	L*	a*	b*	$\Delta E$
Site 7 Spot 1 Engraving				
AVERAGE 2006	12.887	8.466	11.741	
AVERAGE 2005	28.131	14.485	18.789	23.706
AVERAGE 2004	7.100	8.550	9.600	
Site 7 Spot 1 Background				
AVERAGE 2006	19.853	12.009	14.061	2.998
AVERAGE 2005	17.038	12.990	13.743	1.409
AVERAGE 2004	17.075	13.260	15.125	
Site 7 Spot 2 Engraving				
AVERAGE 2006	5.497	5.663	6.360	6.800
AVERAGE 2005	11.021	8.560	9.069	8.746
AVERAGE 2004	3.510	6.440	5.120	
Site 7 Spot 2 Background				
AVERAGE 2006	17.849	11.886	13.475	3.490
AVERAGE 2005	14.556	12.925	12.967	10.143
AVERAGE 2004	24.650	12.010	13.360	
Site 7 Spot 3 Engraving				
AVERAGE 2006	12.774	9.354	11.517	
AVERAGE 2005	2.004	2.419	2.168	
AVERAGE 2004	no 2004 measurements			
Site 7 Spot 3 Background				
AVERAGE 2006	19.218	11.734	13.457	8.593
AVERAGE 2005	11.268	10.207	10.576	8.875
AVERAGE 2004	18.440	13.300	14.790	

## Site 8: King Bay South



Sample	Colour scale			Colour difference* ΔE
	L*	a*	b*	
Site 8 Spot 1 Engraving				
AVERAGE 2006	28.282	13.426	16.376	2.529
AVERAGE 2005	25.770	13.711	16.325	5.591
AVERAGE 2004	31.260	14.748	16.120	
Site 8 Spot 1 Background				
AVERAGE 2006	26.481	10.545	12.129	2.538
AVERAGE 2005	27.101	12.558	13.544	1.305
AVERAGE 2004	27.412	11.905	12.457	
Site 8 Spot 2 Engraved				
AVERAGE 2006	17.800	9.770	12.591	10.323
AVERAGE 2005	27.283	13.235	14.744	6.389
AVERAGE 2004	20.940	12.580	14.337	
Site 8 Spot 2 Background				
AVERAGE 2006	25.809	10.272	11.829	2.566
AVERAGE 2005	23.693	11.525	12.561	2.213
AVERAGE 2004	25.867	11.687	12.180	
Site 8 Spot 3 Engraved				
AVERAGE 2006	22.845	12.463	17.591	6.205
AVERAGE 2005	16.794	12.227	16.237	5.260
AVERAGE 2004	21.715	13.400	17.680	
Site 8 Spot 3 Background				
AVERAGE 2006	22.568	12.529	15.330	1.618
AVERAGE 2005	24.033	13.194	15.497	3.192
AVERAGE 2004	26.977	13.087	14.267	

### 3.3.1 Reflectance Spectra

The measurements collected by the portable spectrophotometer can also be displayed as spectral curves. Figures 33–38 represent an example set, for Site 8, in 2004. Each of the sample spectra correspond to the average of seven L\*a\*b\* measurements for each sampling spot.

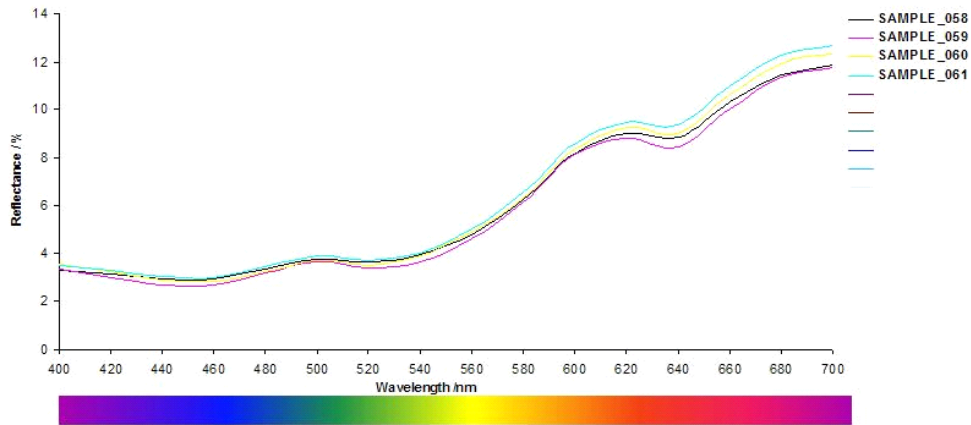


Figure 37: Site 8 spot 1 background.

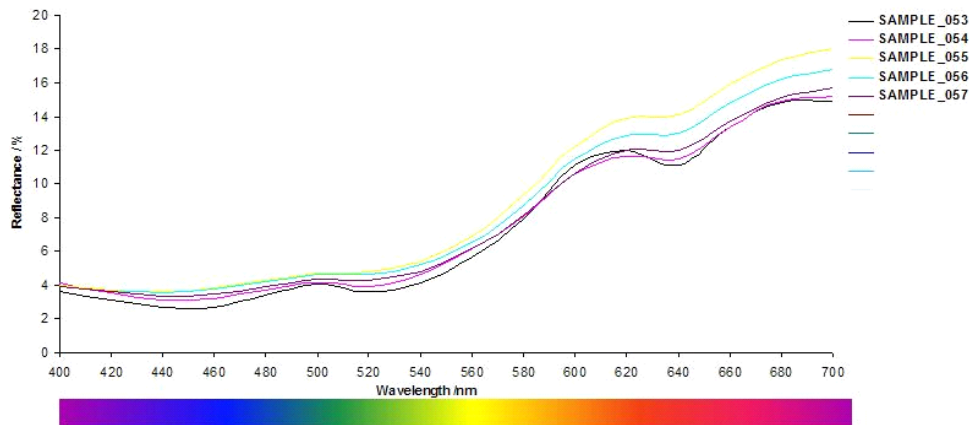


Figure 38: Site 8 spot 1 engraving.

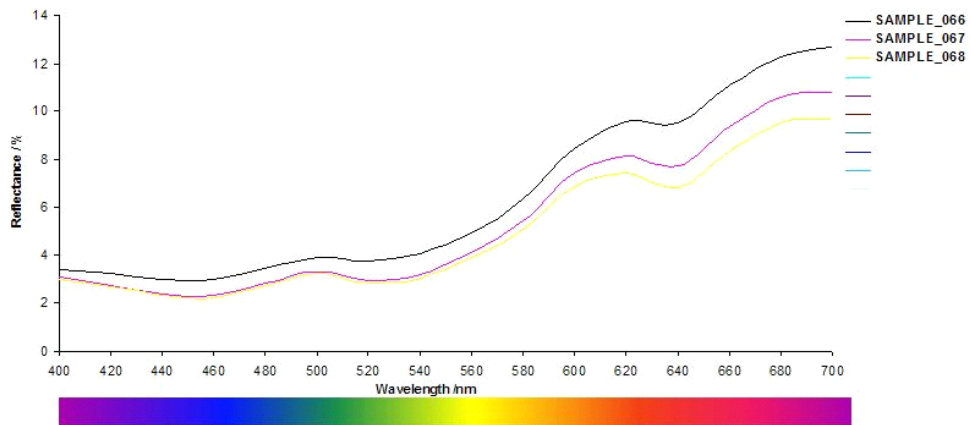
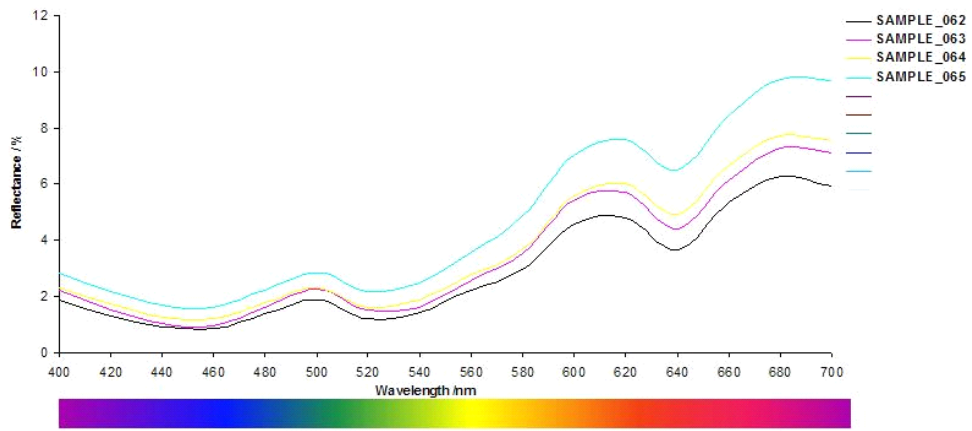
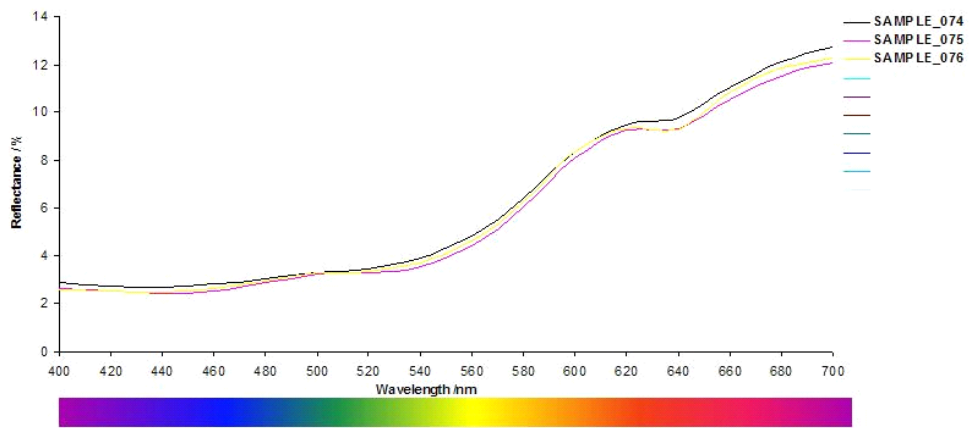


Figure 39: Site 8 spot 2 background.



**Figure 40: Site 8 spot 2 engraving.**



**Figure 41: Site 8 spot 3 background.**

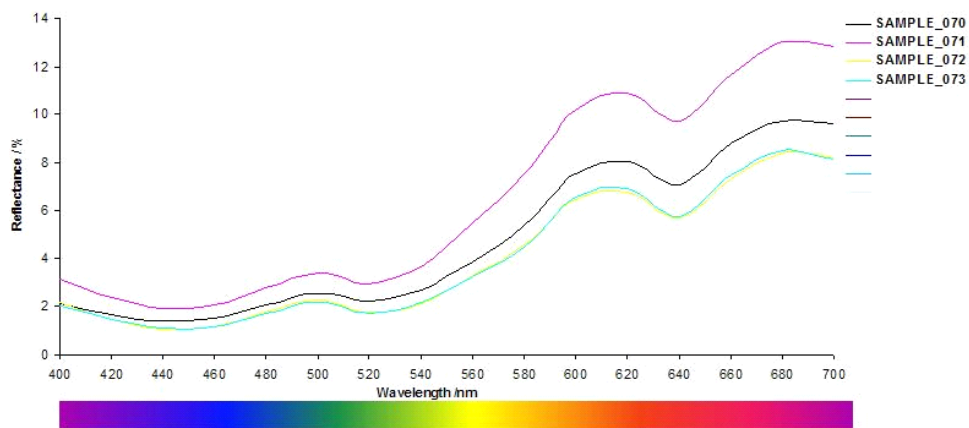


**Figure 42: Site 8 spot 3 engraving.**

**Table 22: Averaged colour change for each site**

Site	Averaged site-specific colour change		
	$\Delta E$ 05-06	$\Delta E$ 04-05	$\Delta E$ 04-06
SITE 4 Delta E average	1.89	1.29	1.86
SITE 5 Delta E average	4.77	4.29	5.20
SITE 6 Delta E average	2.43	2.61	2.61
SITE 7 Delta E average	6.10	10.58	4.17
SITE 8 Delta E average	4.14	3.99	2.83
<b>Southern Sites Average</b>	<b>3.87</b>	<b>4.55</b>	<b>3.34</b>
SITE 1 Delta E average	3.12	2.97	2.64
SITE 2 Delta E average	3.01	3.56	2.83
<b>Northern Sites Average</b>	<b>3.07</b>	<b>3.26</b>	<b>2.74</b>

The averaged colour change for each site is presented in Table 22, which is an average of each of the 6 spots measured in the petroglyph. The colour change average for Southern sites for the first period (04-05) is higher than the second period (05-06), and is believed to be a consequence of improved experimental practice during measurement taking over successive years.

Considering each site average individually for the 04-05 and 05-06 period,  $\Delta E$  has increased slightly for Southern sites 4, 5 and 8 and decreased for sites 6 and 7. In comparison, the Northern site 1 has increased in colour change and site 2 has decreased.

It is probably more informative to consider the 04-06  $\Delta E$  which measures the colour change over a two year interval. Sites 5 and 7 display the most colour change. Sites 4, 6 and 8 (Southern) colour change values are quite similar to the Northern sites 1 and 2.

Where the colour difference appears to have larger values overall, this may be in some way contributed to by surface roughness of the rock, which influences the placement of the microspectrophotometer. The site with the smoothest rock face is Site 6, however this did not record the lowest colour change values. Site 4 has the lowest colour change value and has relatively moderate surface roughness.

When considered collectively, the remote Northern Sites (1 and 2) have a comparatively slightly lower average colour change index than the Southern industrial Sites (4–8) which is consistent for the measurement periods 04-05, 05-06 and 04-06. Overall, the colour change measurements at this stage do not indicate any perceptible colour change.

### **3.4 Conclusions and Future Work**

The collection of the final set of colour measurement data is planned for August 2007 and will provide an opportunity to observe whether a trend has emerged in the annual colour change measurements. With only two annual  $\Delta E$  measurements taken so far it is difficult to establish whether a real trend exists, even though this year's measurements currently indicate there is no increase in colour change over the 04-06 period. However even after next year's  $\Delta E$  is calculated, suitable caution must be applied to the interpretation of a trend from only three

measurements of annual colour change. Confidence in the direction of the trend could be improved with additional data points provided by collection in following years.

The colour measurements collected thus far may be used as a baseline measurement against which to compare future measurements in the short or long term, and are a valuable and independent evaluation of changes in rock surface colouration on the Burrup Peninsula.

A final colour change report will be presented at the end of 2007, after the final colour change measurement.

## Part 4: Spectral Mineralogy

---

### 4.1 Introduction

Reflectance spectroscopy is now available as a field tool for geologists through the development of portable instruments like the analytical spectral device (ASD) FieldSpec Pro field spectrometer. These systems measure diagnostic mineral spectral features that are particularly suitable for quantitative analysis of many geological materials. Some of the advantages of the technique include little sample preparation (if any) and rapid measurement (around 1 s), although the measurement is restricted to the sample's surface (<50  $\mu\text{m}$ ).

CSIRO has been involved in the development of reflectance spectroscopy techniques for characterisation of iron ores, gold, bauxites, mineral sands, talc, lateritic nickel and asbestos during the past 12 years [12–23]. Using field reflectance spectrometry, the mineralogy of the samples can be characterised on the basis of key spectral features.

Reflectance spectroscopy – the analysis of reflected light – between 400 and 2500 nm is now a proven technique for mineral analysis in both the laboratory and in the field. Reflectance spectroscopy has been used intensely to characterise weathering minerals such as iron oxides and clay minerals. The most common iron oxide minerals (hematite, maghemite and goethite) have broad absorptions between 400 and 1000 nm (visible and near infra-red, or VNIR), whereas OH-bearing minerals such as phyllosilicates and inosilicates, as well as carbonates and sulphates, show narrow absorption features of between 1000 and 2500 nm (short wave infra-red, or SWIR). The combination of these wavelength ranges provides a step forward towards quick and accurate mineral characterisation.

The ASD FieldSpec Pro (Figure 43) covers the spectral range 400–2500 nm with a spectral resolution of 3 nm at 700 nm, thanks to three detectors: a 512-element Si photodiode array for the 400–1000 nm range, and two separate TE-cooled, graded index InGaAs photodiodes for the 1000–2500 nm range. The input is through a 1.4 m fibre optic. The average scanning time to acquire a spectrum is 1 second. There are two ways of operating the ASD, consisting of either using (a) an external source of light (sun or artificial), or (b) an internal source of light. Absolute measurements are obtained using a white reference plate that reflects 100% of the light in the 400–2500 nm wavelength range. For this study, the second lighting option was used as it eliminates any external light interference.

This study has the overall objective to assess the mineralogy and to monitor the mineralogical changes (if any) of seven rock art sites in the Burrup Peninsula (Western Australia) over a four-year period (2004–2007).

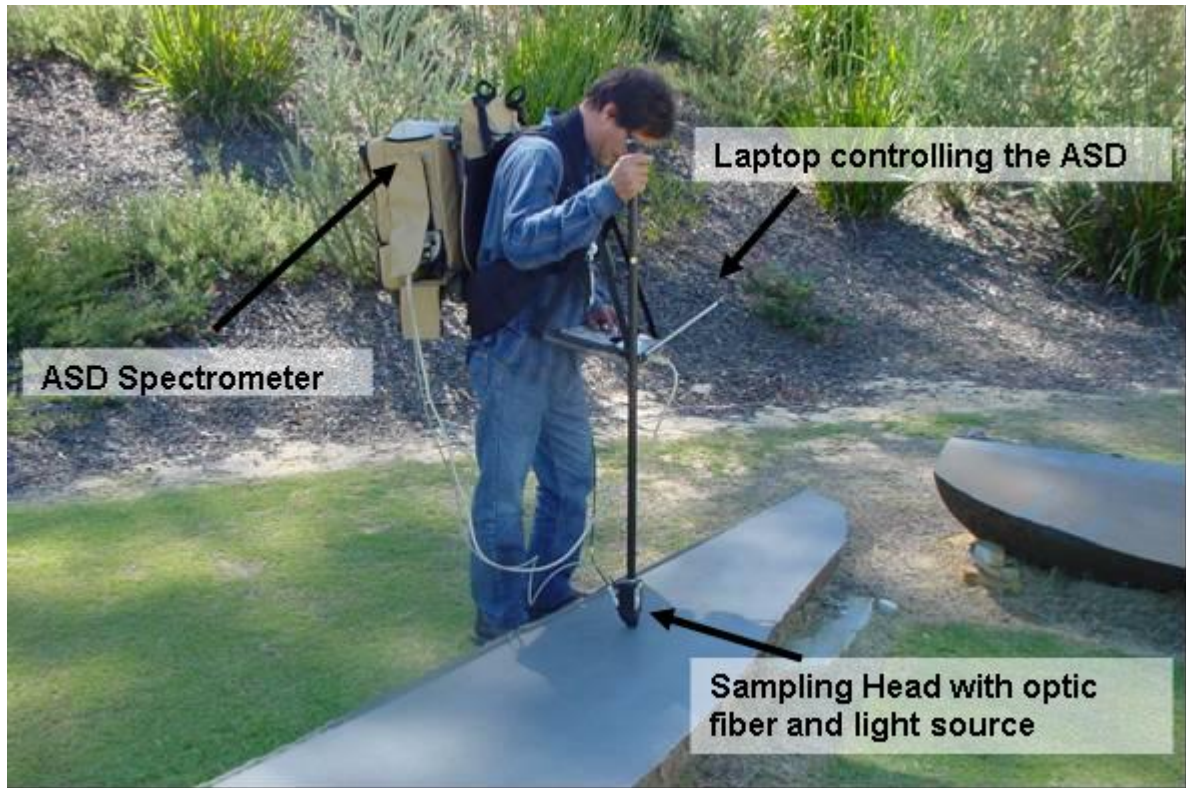


**Figure 43: ASD FieldSpec Pro operating on a rock surface.**

The work program includes:

- Acquiring 42 (7 measurements per spot with 3 spots and their associated background) spectral measurements for each site with the ASD (own light source) in the same sampling locations used for colour measurements, i.e. both on the engravings and the surrounding undisturbed background rocks.
- Cross-checking the colour value calculated by CMMT to the colour value calculated by the ASD.
- Characterising and comparing the mineralogy of the surface of the rock art and the surrounding undisturbed background rocks.
- Monitoring the potential change for a four-year period (2004–2007).

## **4.2 Experimental**

The (Landsat) satellite image of the Burrup Peninsula provided in Figure 1 indicates the seven locations being measured during the course of this study. The exact coordinates are shown in Table 1. Figure 44 is a photo of Deborah Lau taking a measurement with the visible spectrometer. The colour value calculated was cross-checked with the colour value calculated by the ASD spectrometer. As an example, results for Site 6 spot 2 for engravings and background are shown in Figure 45. The general shape of the spectra is consistent in both instruments and the difference in absolute reflectance only varies from 0.6% to 5%.



Figure 44: ASD FieldSpec Pro operating on petroglyphs on the Burrup Peninsula.

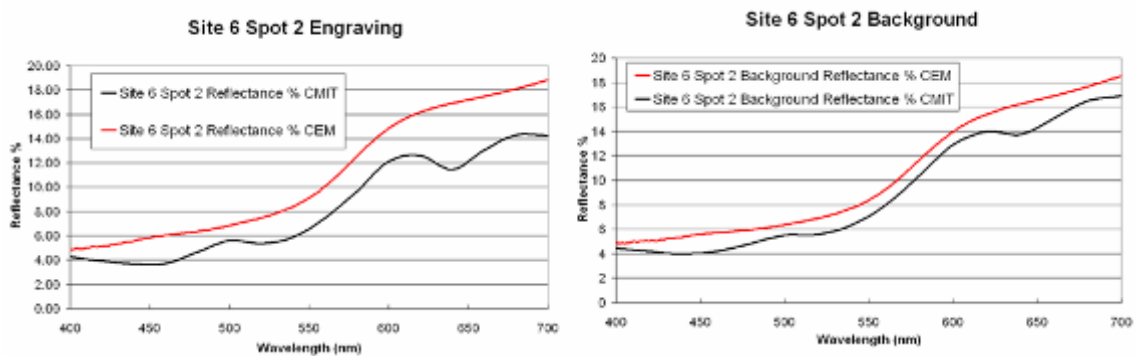


Figure 45: Comparison between field spectrometers for engravings and background.

### 4.3 Results and Discussion

For each site, the description and interpretation include:

- A digital image of the engraving with the location of the measurement spots (Site 1 shown in in Figure 46).
- Average spectra for the engravings and background for each of the spots (Site 1, Figure 47).
- Mineralogical interpretation of the spectra (Site 1, Table 23).
- Spectral variability for engravings and background for each of the measurement spots (Site 1, Figure 48).

Only Site 1 data is shown here to prevent repetition.



Figure 46: Digital image of the Site 1 engravings and locations of the measurement spots.

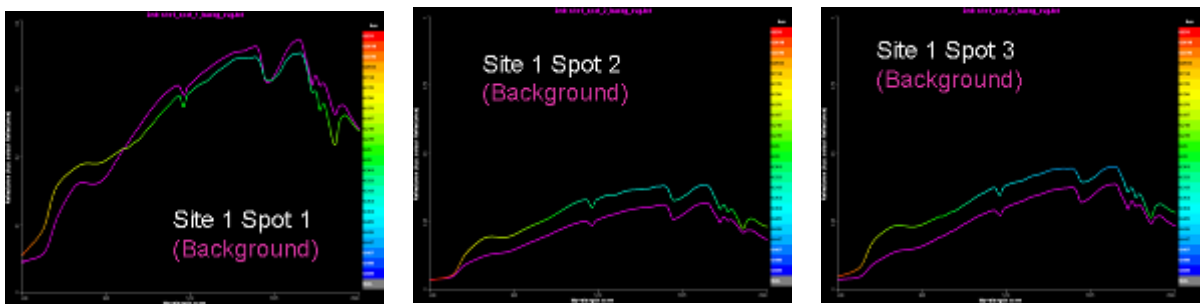
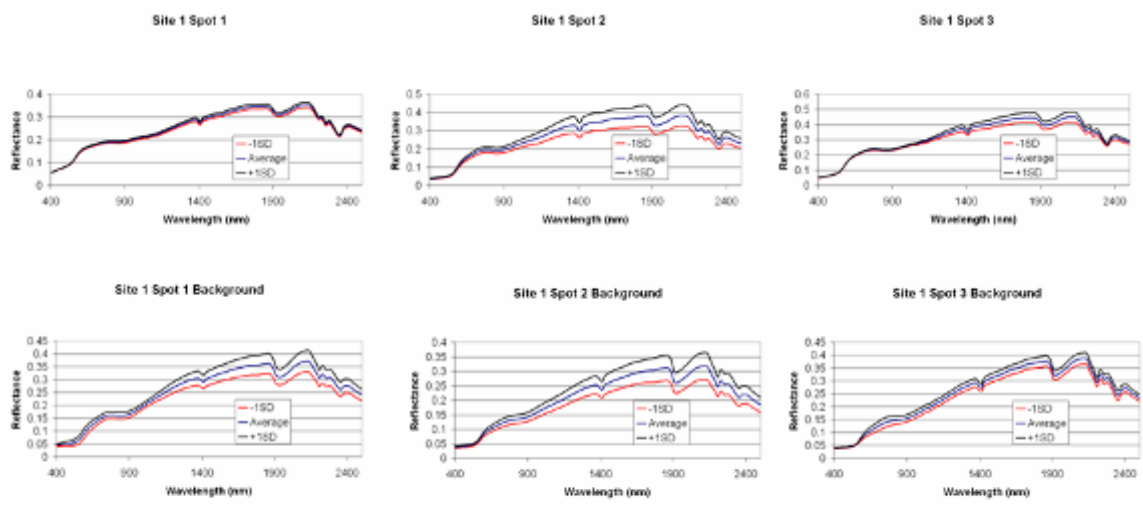


Figure 47: Average spectra for the Site 1 engravings and the background.

Table 23: Spectral mineralogy of the Site 1 engravings and the background

Engravings	Background
<ul style="list-style-type: none"> <li>▪ Small amount of hematite</li> <li>▪ Poorly ordered kaolinite</li> <li>▪ Intermediary Chlorite</li> </ul>	<ul style="list-style-type: none"> <li>▪ Spot 1: More hematite than engraving and naturally darker in the visible</li> <li>▪ Spot 2 &amp; 3: less hematite than engraving but darker in the visible probably manganese oxides or organic matter</li> </ul>

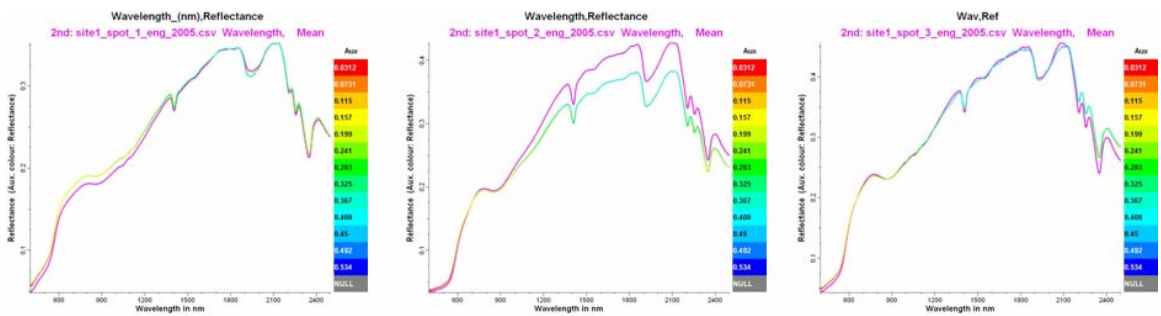


SD: 1 standard deviation

Figure 48: Spectral variability for engravings and background for Site 1.

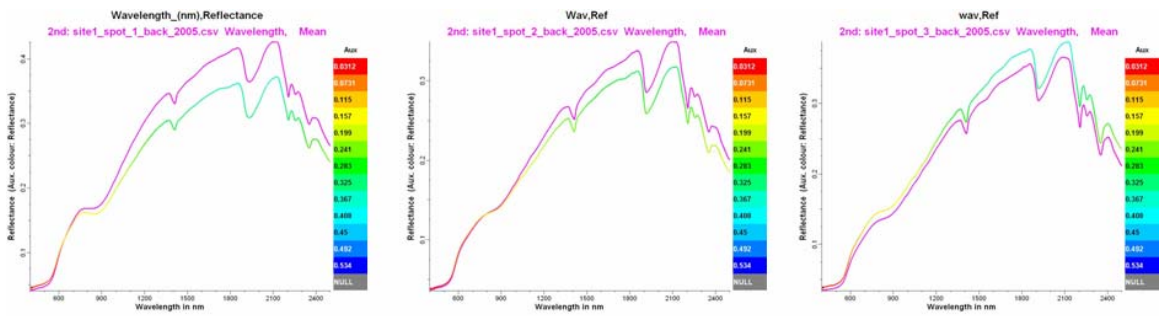


Figure 49: Digital image of the Site 1 engravings and locations of the measurement spots.



The purple spectrum was acquired in 2005

Figure 50: Comparison of the average spectra for the engravings between 2004 and 2005 for Site 1.



The purple spectrum was acquired in 2005

Figure 51: Comparison of the average spectra for the backgrounds between 2004 and 2005 for Site 1.

**Table 24: Spectral interpretation for spots 1, 2 and 3 for Site 1**

---

<b>Engravings</b>	<b>Background</b>
<ul style="list-style-type: none"><li>▪ Spot 1 &amp; 3: No significant change</li><li>▪ Spot 2: 2005 spectrum brighter after 1000 nm</li></ul>	<ul style="list-style-type: none"><li>▪ Spot 1 &amp; 2: No significant change in the visible, 2005 spectrum brighter after 1000 nm</li><li>▪ Spot 3: 2005 spectrum darker over entire wavelength range</li></ul>

---

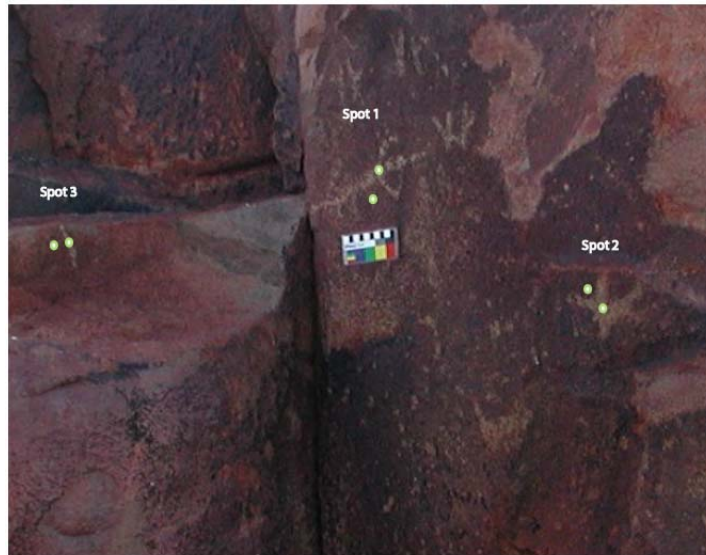
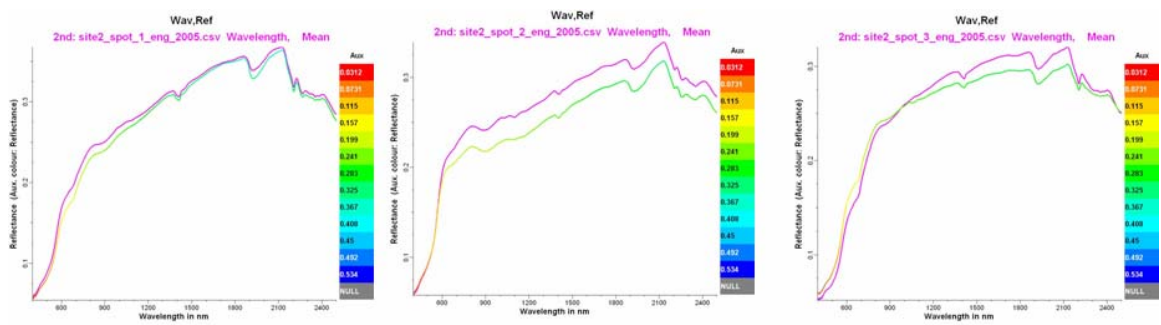
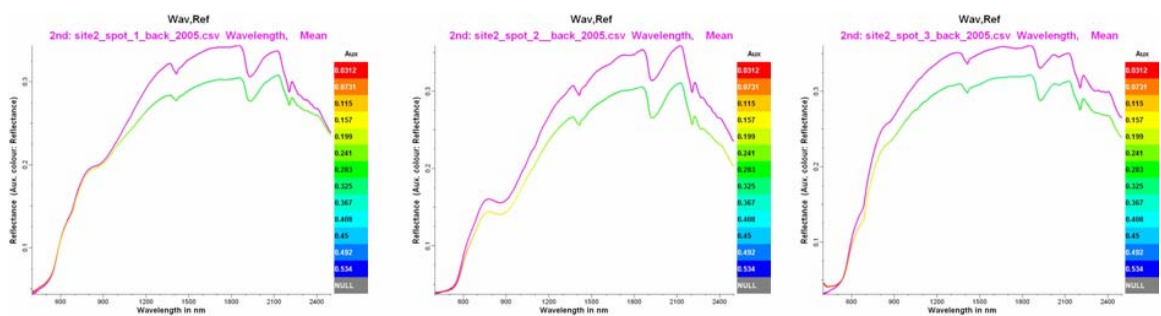


Figure 52: Digital image of the Site 2 engravings and locations of the measurement spots.



The purple spectrum was acquired in 2005

Figure 53: Comparison of the average spectra for the engravings between 2004 and 2005 for Site 2.



The purple spectrum was acquired in 2005

Figure 54: Comparison of the average spectra for the backgrounds between 2004 and 2005 for Site 2.

Table 25: Spectral interpretation for spots 1, 2 and 3 for Site 2

Engravings	Background
<ul style="list-style-type: none"><li>▪ Spot 1: No significant change</li><li>▪ Spot 2: 2005 spectrum brighter after 900 nm</li><li>▪ Spot 2: 2005 spectrum darker before 900 nm and lighter after 900 nm</li></ul>	<ul style="list-style-type: none"><li>▪ Spot 1: No significant change in the visible. 2005 spectrum brighter after 900 nm</li><li>▪ Spot 2 &amp; 3: 2005 spectra brighter after 500 nm</li></ul>

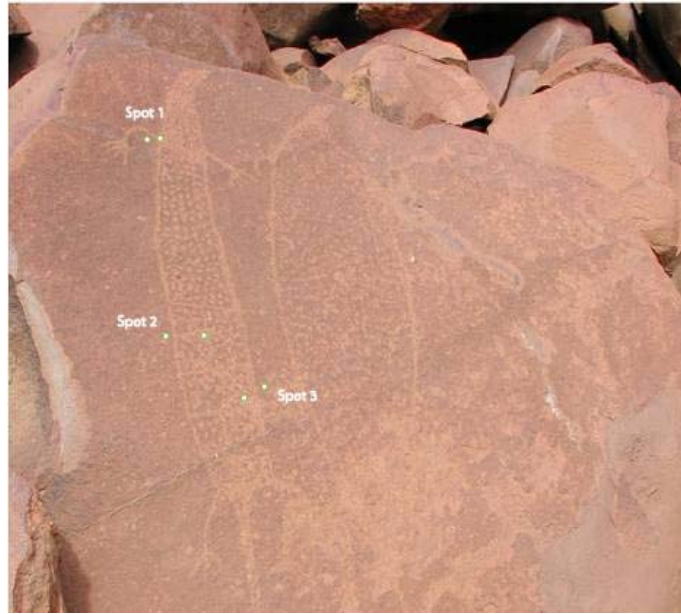
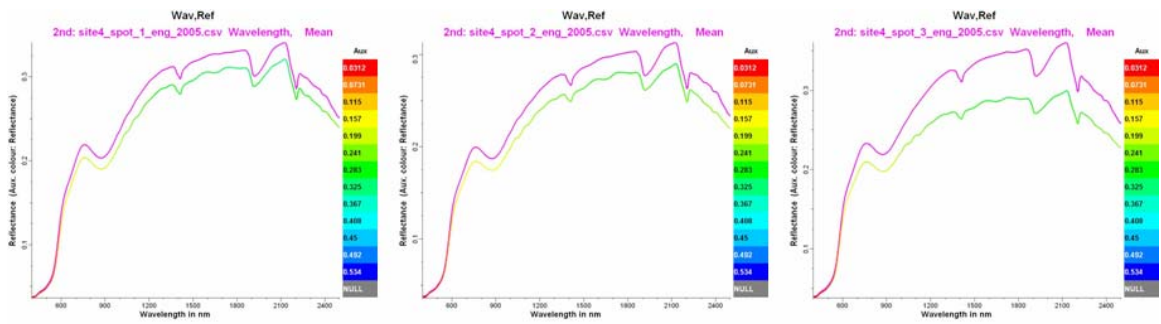
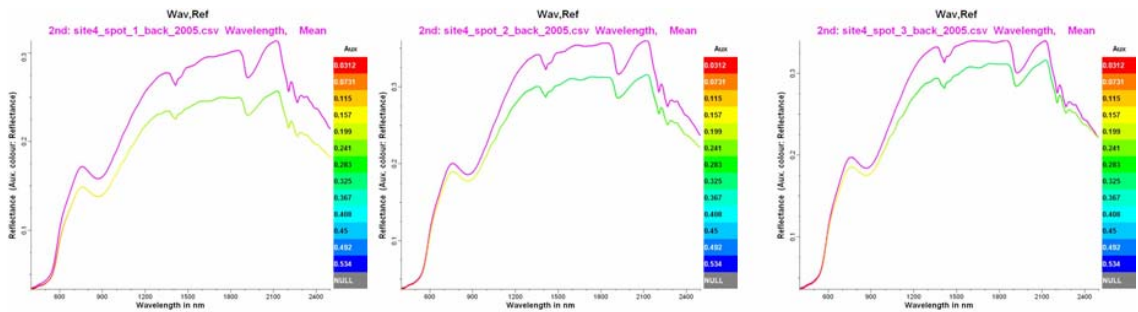


Figure 55: Digital image of the Site 4 engravings and locations of the measurement spots.



The purple spectrum was acquired in 2005

Figure 56: Comparison of the average spectra for the engravings between 2004 and 2005 for Site 4.



The purple spectrum was acquired in 2005

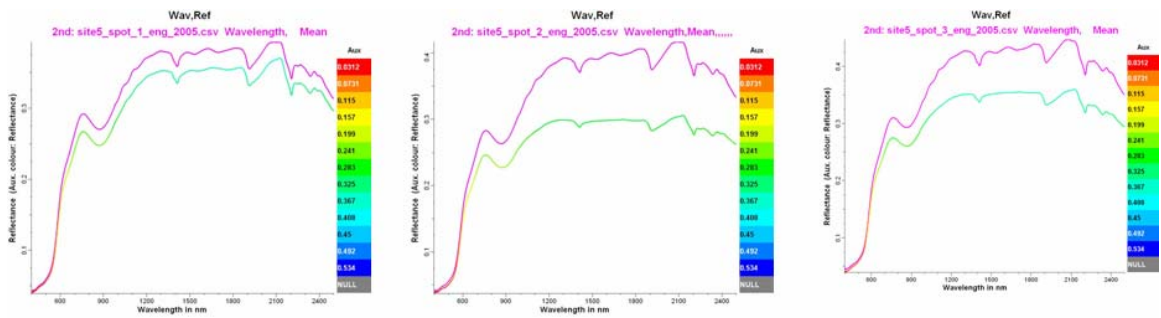
Figure 57: Comparison of the average spectra for the backgrounds between 2004 and 2005 for Site 4.

Table 26: Spectral interpretation for spots 1, 2 and 3 for Site 4

Engravings	Background
<ul style="list-style-type: none"><li>Spot 1, 2 &amp; 3: No significant change in the visible. 2005 spectrum brighter after 900 nm</li></ul>	<ul style="list-style-type: none"><li>Spot 1, 2 &amp; 3: No significant change in the visible. 2005 spectrum brighter after 700 nm</li></ul>

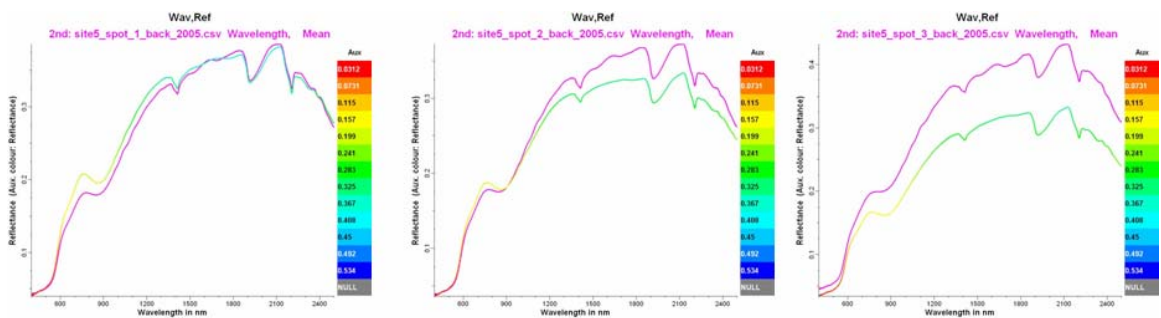


Figure 58: Digital image of the Site 5 engravings and locations of the measurement spots.



The purple spectrum was acquired in 2005

Figure 59: Comparison of the average spectra for the engravings between 2004 and 2005 for Site 5.



The purple spectrum was acquired in 2005

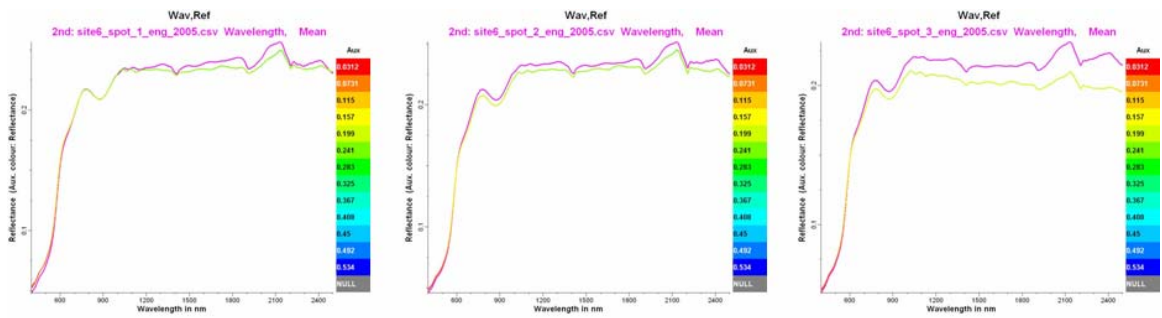
Figure 60: Comparison of the average spectra for the backgrounds between 2004 and 2005 for Site 5.

Table 27: Spectral interpretation for spots 1, 2 and 3 for site 5.

<b>Engravings</b>	<b>Background</b>
<ul style="list-style-type: none"><li>Spot 1, 2 &amp; 3: No significant change in the visible. 2005 spectra brighter after 700 nm</li></ul>	<ul style="list-style-type: none"><li>Spot 1: No significant change in the visible. 2005 spectrum darker after 600 nm until 1500 nm and then no change</li><li>Spot 2: No significant change in the visible. 2005 spectrum brighter after 900 nm</li><li>Spot 3: 2005 spectrum brighter</li></ul>

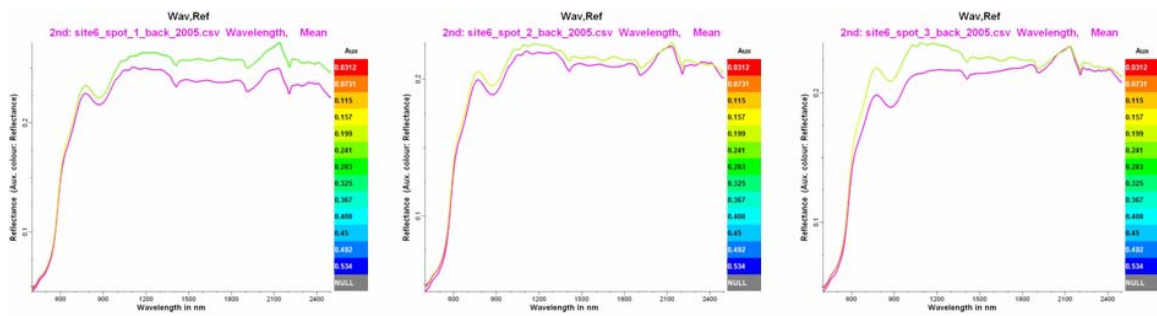


Figure 61: Digital image of the Site 6 engravings and locations of the measurement spots.



The purple spectrum was acquired in 2005

Figure 62: Comparison of the average spectra for the engravings between 2004 and 2005 for Site 6.



The purple spectrum was acquired in 2005

Figure 63: Comparison of the average spectra for the backgrounds between 2004 and 2005 for Site 6.

Table 28: Spectral interpretation for spots 1, 2 and 3 for Site 6

Engravings	Background
<ul style="list-style-type: none"><li>Spot 1, 2 &amp; 3: No significant change in the visible. 2005 spectra brighter after 1000 nm</li></ul>	<ul style="list-style-type: none"><li>Spot 1, 2 &amp; 3: No significant change in the visible. 2005 spectra darker after 1000 nm</li></ul>

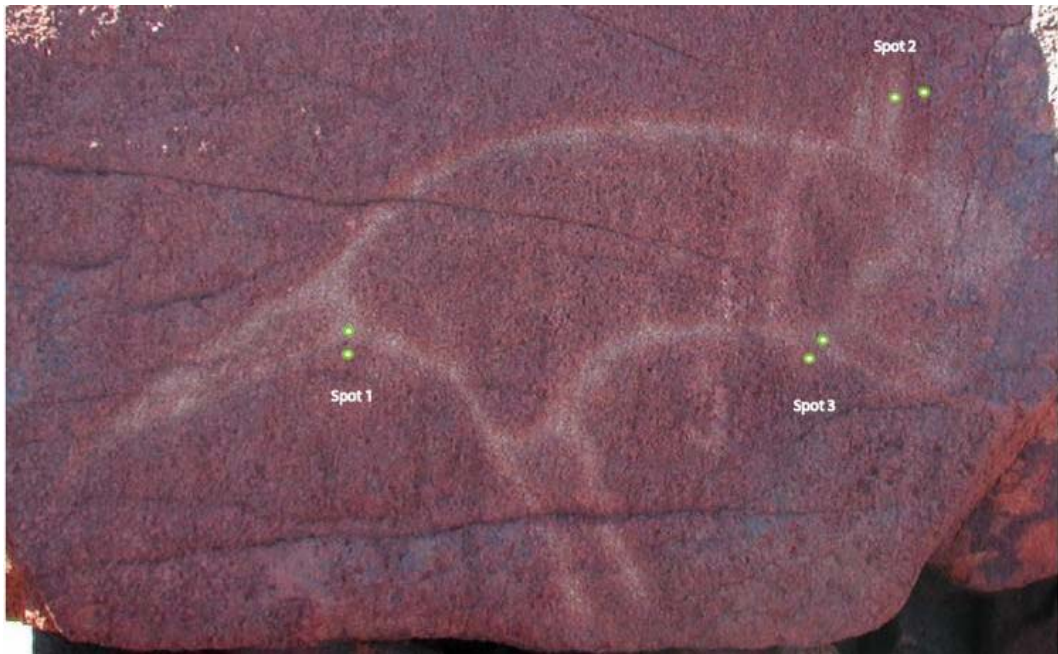
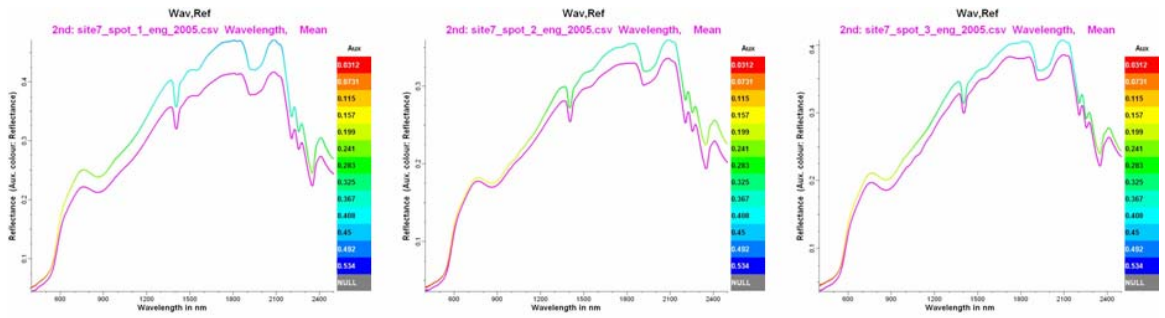
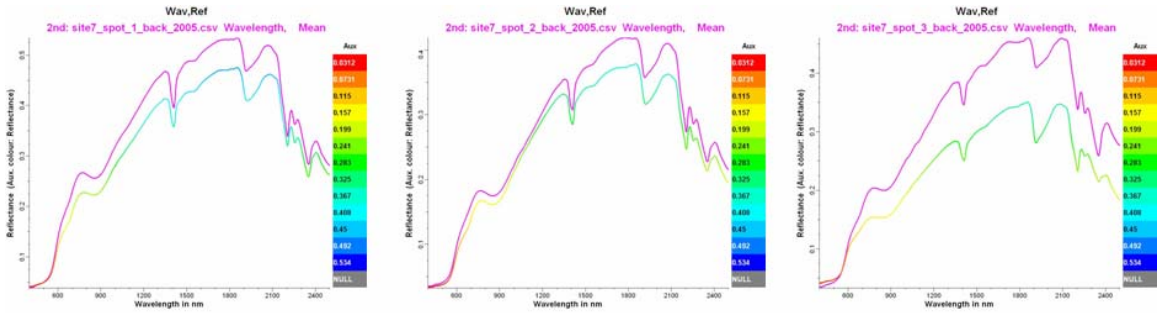


Figure 64: Digital image of the Site 7 engravings and locations of the measurement spots.



The purple spectrum was acquired in 2005

Figure 65: Comparison of the average spectra for the engravings between 2004 and 2005 for Site 7.



The purple spectrum was acquired in 2005

Figure 66. Comparison of the average spectra for the backgrounds between 2004 and 2005 for Site 7.

Table 29. Spectral interpretation for spots 1, 2 and 3 for Site 7

<b>Engravings</b>	<b>Background</b>
<ul style="list-style-type: none"><li>▪ Spot 1, 2 &amp; 3: 2005 spectra darker over entire wavelength range</li></ul>	<ul style="list-style-type: none"><li>▪ Spot 1, 2 &amp; 3: 2005 spectra are brighter over entire wavelength range</li></ul>

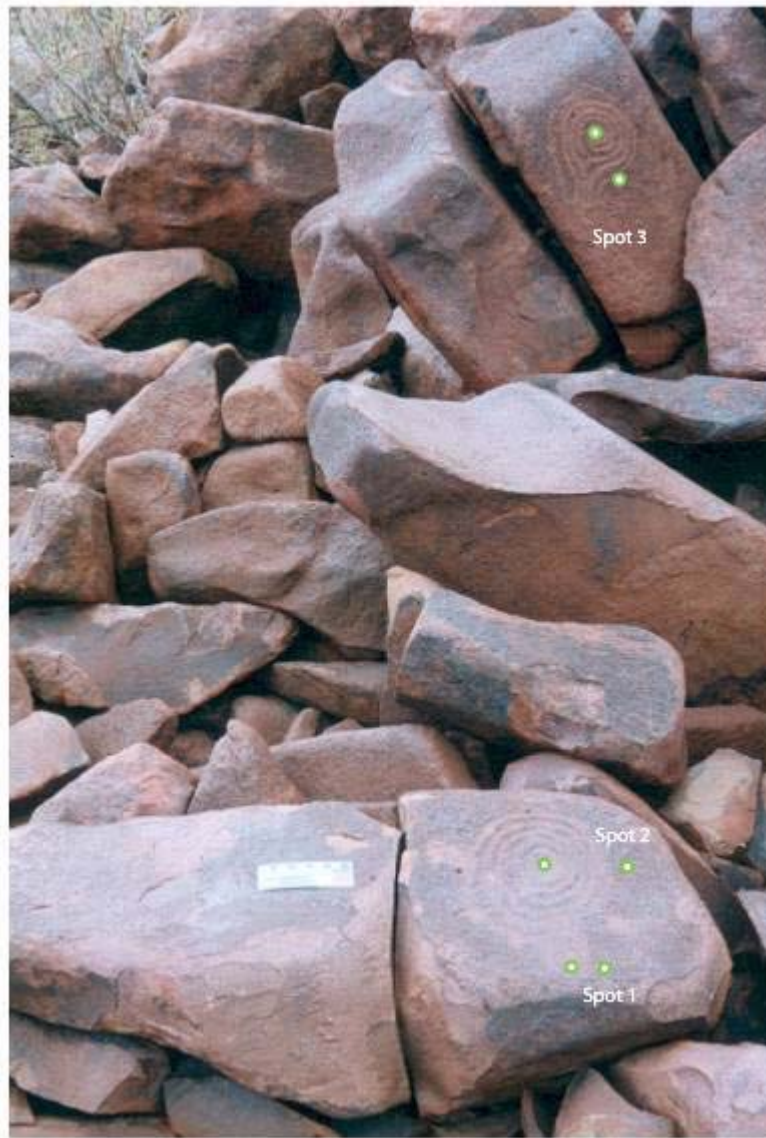
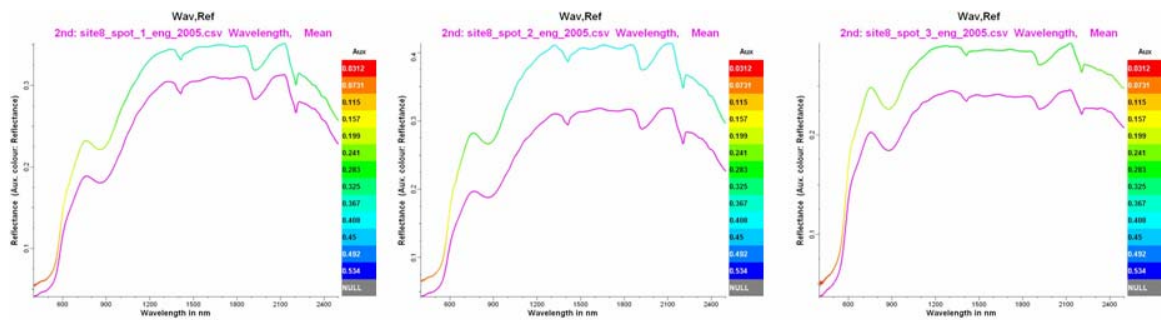
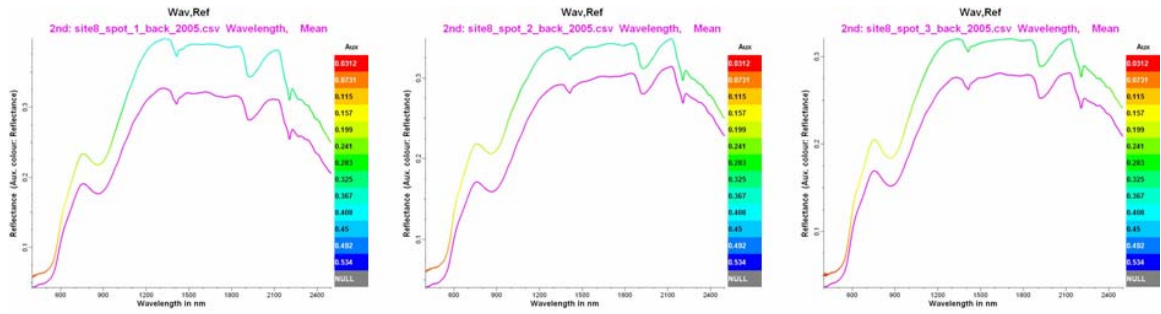


Figure 67: Digital image of the Site 8 engravings and locations of the measurement spots.



The purple spectrum was acquired in 2005

Figure 68: Comparison of the average spectra for the engravings between 2004 and 2005 for Site 8.



The purple spectrum was acquired in 2005

Figure 69: Comparison of the average spectra for the backgrounds between 2004 and 2005 for Site 8.

Table 30. Spectral interpretation for spots 1, 2 and 3 for Site 8

Engravings	Background
<ul style="list-style-type: none"> <li>Spot 1, 2 &amp; 3: 2005 spectra darker over the entire wavelength range</li> </ul>	<ul style="list-style-type: none"> <li>Spot 1, 2 &amp; 3: 2005 spectra darker over the entire wavelength range</li> </ul>

## **4.4 Conclusions and Future Work**

The petroglyphs at seven sites in the Burrup Peninsula were measured using reflectance spectroscopy covering the visible to short wave infra-red wavelength range (400–2500 nm). Both the engravings and background rocks were measured in situ. Forty-two spectral measurements were acquired for each site with the ASD spectrometer (own light source) at the same sampling locations measured in 2004, for both the engravings and the surrounding undisturbed background rocks. The seven spectra acquired for each spot were averaged.

The mineralogy of the rock has not changed, and the absorption features are similar to those found in 2004. The minerals include:

- Hematite.
- Poorly ordered kaolinite.
- Chlorite.
- Minor goethite.
- Minor manganese oxides.

The amount of reflected light detected has changed – sometimes it is brighter, sometimes darker. This behaviour was observed in the visible (380–750 nm) and in the near infra-red (>750 nm) ranges. These changes could be explained by:

- Surface variation (relative change in mineral abundance, organic growth, moisture content, mineral heterogeneity at the rock surface).
- Probe not positioned at exactly the same sample locations as measured in 2004.

Additional spectra will be acquired in the following years to provide enough data to draw definite conclusions for the final report for this initial spectral mineralogy contract.

## Concluding Remarks

---

In summary, of the four parts of the project two are still progressing, viz.:

- Colour measurement and spectral mineralogy are being recorded annually, with the next visit scheduled for August 2007. This will be the final visit for the current study.

This report documents the final results of fumigation and dust characterisation. The field and laboratory results for colour measurement and mineralogy are consistent, with a defined mineralogy being collected for the background and engraved type rock surfaces and the dust in remote locations and closer to industrial activity.

### *Dust Deposition*

The rates of dust deposition and retention of dust on the rock surfaces are barely detectable in the remote sites. There is evidence of greater deposition rates in the Southern sites from both evidence on the synthetic tile surface, and separate collection by CSIRO Division of Atmospheric Research dust deposition measurements. However, the dust that settles on the rock surfaces in the Southern sites was observed to reach a maximum level that is controlled by environmental factors such as wind and washing by rain that act to remove deposited material. The maximum build up observed in the rough rock type used in this study is in the order of 1 – 2 microns in thickness at the bottom of depressions measuring 4 mm deep.

### *Fumigation*

There is a significant challenge in replicating the conditions that contribute to ageing and weathering of rock surfaces in the natural world. It is also acknowledged that the conditions used to simulate the effect of accelerated ageing do not take into account all the possible parameters that are involved in the natural situation. With regard to these considerations, the fumigation cycles involved exposure to elevated levels of pollutants and cycles of heating, wetting and drying designed to emulate natural diurnal cycles.

The mineralogy and chemistry of the rock surfaces exposed to these conditions was compared with unexposed (control) samples and there was no significant difference observed between the two. This was substantiated by exposure of rock surface minerals to concentrated solutions of the pollutants, and only in the case of sulphuric acid in combination with elevated heat was any mineralogical change observed.

## References

---

- [1] Warke, P.A., Micro-environmental conditions and rock weathering in hot, arid regions, *Zeitschrift für Geomorphologie (Annals of Geomorphology)*, 2000, **120**, 83–95.
- [2] Geological Survey of Western Australia, *Dampier–Barrow Island*, Sheet SF50-2 and part of Sheet SF50-1, Second Edition, Department of Industry and Resources, 2001.
- [3] Schroeder, P.A.; Melear, N.D.; West, L.T.; Hamilton, D.A., Meta-gabbro weathering in the Georgia Piedmont, USA: implications for global silicate weathering rates, *Chemical Geology*, 2000, **163**(1–4), 235–245.
- [4] Dragovich, D., Microchemistry of small desert varnish samples, western New South Wales, Australia, *Earth Surface Processes and Landforms*, 1998, **23**(5), 445–453.
- [5] Thiagarajan, N.; Aeolus Lee, C.–T., Trace-element evidence for the origin of desert varnish by direct aqueous atmospheric deposition, *Earth and Planetary Science Letters*, 2004, **224**(1–2), 131–141.
- [6] Edwards, H.G.M.; Moody, C.A.; Jorge Villar, S.E.; Mancinelli, R., Raman spectroscopy of desert varnishes and their rock substrata, *Journal of Raman Spectroscopy*, 2004, **35**(6), 475–479.
- [7] McKeown, D.; Post, J. Characterization of manganese oxide mineralogy in rock varnish and dendrites using X-ray absorption spectroscopy, *American Mineralogist*, 2001, **86**, 701–713.
- [8] Wang, A.; Haskin, L.A.; Jolliff, B.L., *Characterization of Mineral Products of Oxidation and Hydration by Laser Raman Spectroscopy – Implications for In-Situ Petrologic Investigation of the Surface of Mars*, Department Earth & Planetary Sciences and the McDonnell Center for Space Sciences, 1998.
- [9] Mirmehdi, M.; *et al.*, Automated analysis of environmental degradation of paint residues, *Journal of Archaeological Science*, 2001, **28**(12), 1329–1338.
- [10] Mirti, P.; Davit, P., New developments in the study of ancient pottery by colour measurement, *Journal of Archaeological Science*, 2004, **31**(6), 741–751.
- [11] Hunter, R.S.; Harold, R.W., *The Measurement of Appearance*, John Wiley and Sons, Canada, 1987.
- [12] Ramanaidou, E.R.; Cudahy, T.J., Determination of the hematite/goethite ratio by field VNIR spectroscopy, Proc. 1st Australian Conference on Vibrational Spectroscopy, University of Sydney, 1995, p. 92.
- [13] Ramanaidou, E.R.; Cudahy, T.J., Application of field spectrometry to the characterisation of iron oxides: hematite and goethite, Proc. 5th International Congress on Applied Mineralogy in the Minerals Industry, Warsaw, Poland, 1996, pp. 80–84.
- [14] Ramanaidou, E.R.; Nahon, D.; Decarreau, A.; Melfi, A., Hematite and goethite from duricrusts developed by lateritic chemical weathering of Precambrian banded iron formations, Minas Gerais, Brazil, *Clays and Clay Minerals*, 1996, **44**(1), 22–31.
- [15] Ramanaidou, E.R.; Tapley, V.; Van Bronswijk, W., Determination of aluminium substitution in hematite and goethite by vibrational spectroscopy, Proc. 2nd Australian Conference on Vibrational Spectroscopy, Queensland University of Technology, pp. 35–36, 1996.
- [16] Cudahy, T.J.; Ramanaidou, E.R., Measurement of the hematite: goethite ratio using field spectrometry in the Channel iron deposits, Western Australia, *Australian Journal of Earth Science*, 1997, **44**, 411–420.
- [17] Ramanaidou, E.R.; Cudahy, T.J., Mineralogical and chemical characterisation of ooidal iron ore (Channel iron deposits) using field spectroscopy, presented to Regolith 98 Conference: New Approaches to an Old Continent.

- [18] Ramanaidou, E.R.; Cudahy, T.J., Application of field reflectance spectroscopy to iron ore characterisation, *Exploration and Mining News*, 1998, **9**, 8–9.
- [19] Ramanaidou, E.; Pal, P., Detection of asbestos minerals using a field portable spectrometer, Proc. 3rd Australian Conference on Vibrational Spectroscopy, University of Melbourne, 29 September to 2 October 1998, pp. 184–185.
- [20] Medd, J.; Ramanaidou, E.; Van Bronswijk, W., In situ analysis of aluminous hematites and goethites by Raman spectroscopy, Proc. 3rd Australian Conference on Vibrational Spectroscopy, University of Melbourne, 29 September to 2 October 1998, pp. 198–199.
- [21] Ramanaidou, E.; Pal, P., Detection of asbestos minerals using a field portable spectrometer, *Exploration and Mining News*, 2000, **12**, 9–10.
- [22] Ramanaidou, E.R.; Connor, P.; Cornelius, A.; Fraser, S., Imaging spectroscopy for iron ore mine faces, Proc. Iron Ore 2002 Conference, Perth, 9–11 September 2002, AusIMM Publication Series No. 7/2002, pp. 155–157.
- [23] Ramanaidou, E.R., *Burrup Peninsula Aboriginal Petroglyphs: Spectral Mineralogy for 2004*, CEM Report P2005/.

1. <http://www.geo.mtu.edu/svl/pioneer/ftir/ftirfig2.htm>.
2. **Bikiaris D, Daniilia S, Sotiropoulou S, Katsimbiri O, Pavlidou E, Moutsatsou AP, and Chryssoulakis Y.** Ochre-differentiation through micro-Raman and micro-FTIR spectroscopies: application on wall paintings at Meteora and Mount Athos, Greece. *Spectrochimica Acta Part A: Molecular and Biomolecular Spectroscopy* 56: 3-18, 2000.